

POLISH POLAR RESEARCH	18	3-4	171-225	1997
-----------------------	----	-----	---------	------

Tomasz JANIK

Institute of Geophysics
 Polish Academy of Sciences
 Ks. Janusza 64
 01-452 Warszawa, POLAND
 e-mail: janik@igf.edu.pl

Seismic crustal structure of the Bransfield Strait, West Antarctica

ABSTRACT: Four Geodynamical Expeditions of the Polish Academy of Sciences carried through wide research seismic program in West Antarctica in 1979–1991. Three of these expeditions operated in the Bransfield Strait. The experiment of deep refraction and wide-angle reflection in West Antarctica focused on deep structure of the lithosphere, mainly of the Earth's crust. The network of deep seismic soundings (DSS) profiles covered all the Bransfield Strait. Five land stations on the South Shetland Islands, three stations on the Antarctic Peninsula and nine ocean bottom seismographs (OBS) recorded seismic waves, generated by explosions in a sea. The Bransfield Rift and the Bransfield Platform form a marginal basin against a volcanic arc of the South Shetland Islands. The paper presents new results of 2-D seismic modeling for network of five selected profiles. Four of them, ranging in length from 150 to 190 km, crossed main structures of the Bransfield Strait and the fifth, which connected the other ones and was 310 km long, ran along the Bransfield Rift. Two or three seismic models were presented for each profile. Finally, mutually corrected and controlled 2-D models of described profiles were constructed. They all presented spatial complex structure of the Earth's crust in a young rift of the Bransfield Strait, including extent of its main element *i.e.* anomalous high velocity body (HVB) ($V_p > 7.4$ km/s), detected in 10–30 km depth range except profile DSS-4 (southwest part of the Bransfield Strait). This inhomogeneity is interpreted as intrusion of the upper mantle (?asthenosphere) during stretching of the continental crust. The Moho discontinuity was found at depth 30–35 km, with velocities equal to about 8.1 km/s.

Key words: Antarctica, Bransfield Rift, crustal structure, seismic modelling.

Introduction

Role of West Antarctica in disintegration of the Gondwanaland is of primary significance for evaluation of physical and geological processes, acting in regional but also, in global scale. It is undoubtedly dependent on progress of geodynamic research of mutual relations of the South Shetland Islands micro-

plate and the Antarctic plate (or precisely, its part named the Drake's, Aluk or Phoenix microplate) which subducts from underneath. The Bransfield Rift, together with the Bransfield Platform form a marginal basin against a volcanic island arc of the South Shetland Islands.

Four Geodynamical Expeditions of the Polish Academy of Sciences carried through wide research program in West Antarctica in 1979–1991, including seismic, geologic, sedimentologic and paleontologic investigations. Three of these expeditions operated in the Bransfield Strait. The experiment of deep refraction and wide-angle reflection focused on deep structure of the lithosphere, mainly the Earth's crust. In the Bransfield Strait, network of deep seismic soundings (DSS) profiles was carried out and very rich research material was collected. It has been already many a time presented in publications, mainly with 1-D modelling, and occasionally also 2-D modelling (Guterch *et al.* 1985, 1990, 1991; Grad *et al.* 1992, 1993a, b).

Complex seismic wave field, resulting from investigation of the Earth's crust by explosive seismology, reflects complex geological structure and tectonics, and therefore strong variation of physical properties of the Earth's crust, and in the case of marine studies – specific effects connected with this environment. Wave field at seismic record sections from the Bransfield Strait is particularly complex as mutually interdependent on different relations which are unfavourable for measurements.

Evolution of regional tectonic system

Tectonic history of West Antarctica is strictly connected with tectonic evolution of the neighbouring areas, particularly of the Scotia Sea, southern margins of South America and the South Pacific (Antarctic) plate. As stated by Dott (1976), understanding of mechanism which resulted in development of the present tectonic pattern in the Scotia arc area, is a key to reconstruction of disintegration history of the whole southwestern Gondwanaland. Many such reconstructions have been created, two of which are presented (Figs 1–2). The Antarctic Peninsula, one of the five continental blocks of West Antarctica, is a narrow long (over 1500 km) silver of continental crust, surrounded by ocean crust of the Drake Passage (Barker and Burrell 1977), South Pacific (Heron and Tucholke 1976, Cande *et al.* 1982), Scotia Sea (Barker and Hill 1981) and Weddell Sea (LaBreque and Barker 1981). Geology of the Antarctic Peninsula indicates many similarities to the southernmost part of South America (Arctowski 1895, 1896, 1897; Saunders and Tarney 1982; Dott *et al.* 1982; Thomson *et al.* 1983; Dalziel 1984). Both these regions are suggested to have been connected with each other in the Early Mesozoic (Dalziel and Elliot 1973, Barker and Griffiths 1977). Reconstruction of regional evolution of tectonic pattern (Barker

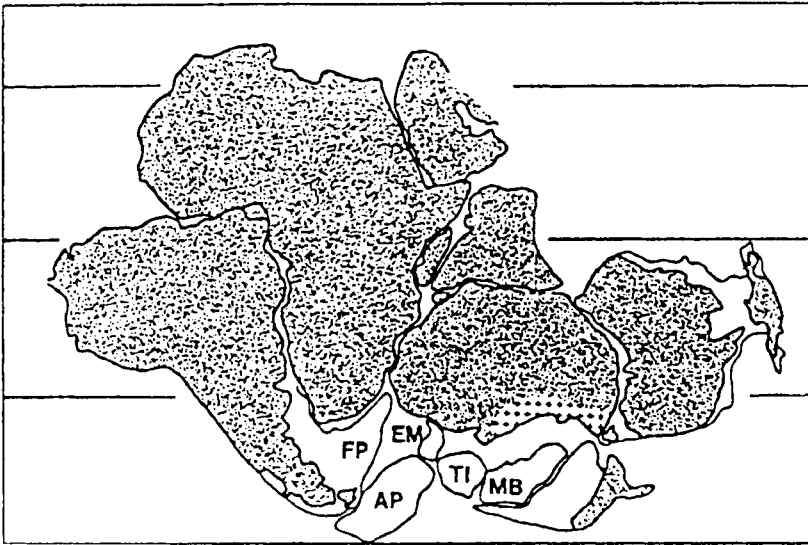


Fig. 1. Reconstruction of the Gondwana at 180 Ma (after Lawver and Scotese, 1987) showing the microplates of West Antarctica. AP – Antarctic Peninsula, EM – Ellsworth Mountains, MB – Marie Byrd Land, TI – Thurston Island, FP – Falklands Plateau, and dotted area – Transantarctic Mountains.

1976; De Wit 1977; Lawver *et al.* 1981, 1985; Dalziel 1983; Lawver and Scotese 1987; Elliot 1991; Lawver and Gahagan 1991) indicated that active volcanic arc formed a continuous zone from the Andes to the Antarctic Peninsula. This arc created western marginal zone of the Gondwanaland that, since the Triassic, has been active all the time (Smellie and Clarkson 1975, Thomson *et al.* 1983, Storey and Garrett 1985). Opening of the Drake Passage and development of the Scotia arc occurred after the Oligocene (Barker and Burrell 1977). Through a complex system of plate boundaries, the Scotia arc connects(?) arc of the Andes in South America with the Antarctic Peninsula (Barker and Lawver 1988). In a much similar way, the Caribbean arc connects plates of North and South America. According to Dott (1976), strong asymmetry of the present Pacific floor suggests that vast area of the Mesozoic sea floor (complementary to those of the north-western Pacific) could be consumed under South America, Antarctic Peninsula and West Antarctica during the Mesozoic and Early Tertiary (Weaver *et al.* 1979). Development of continental crust of the peninsula and its tectonic evolution during the Triassic were connected with the east-oriented proto-Pacific subduction of ocean lithosphere. Accretion and magmatic processes during the Mesozoic and Cainozoic thickened and enlarged fragment of ancient crystalline crust of the peninsula (Storey and Garrett 1985). Evolution history of the western marginal part of the peninsula was reconstructed mainly from surface distribution of synchronic magnetic anomalies of the neighbouring sea floor (Herron

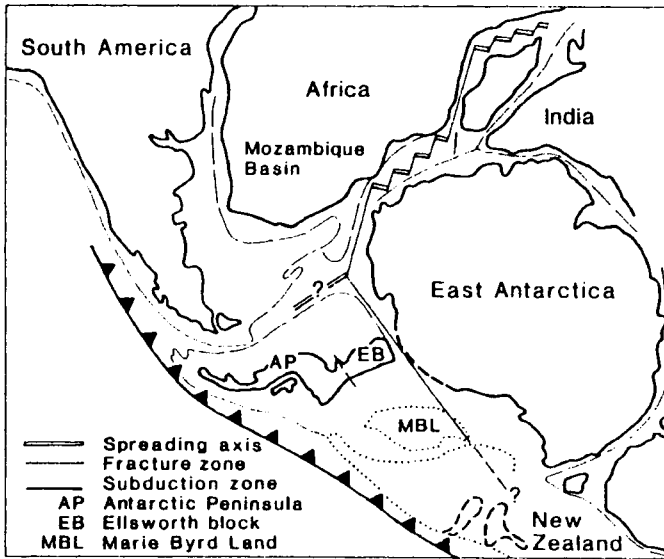


Fig. 2. Schematic reconstruction of the early stages in the evolution of the south-west Indian Ocean and Weddell Sea regions (after Elliot 1991).

and Tucholke 1976, Herron *et al.* 1981, Barker 1982, Garrett *et al.* 1986/87, Royer *et al.* 1990). Starting from about 65 million years ago, the ocean crust at the Aluk Ridge must have also disappeared under the peninsula, until the ridge itself had been consumed as long as subduction was stopped. Collisions of the ridge crest with a trench started about 50 million years ago in the southern part of the peninsula, at margin of the Ellsworth Land. Subduction and spreading ceased at definite segments of plates, trench topography disappeared and the zone became a passive boundary. These processes repeated in successive segments of the subducting plate, cut by numerous transformation faults. According to Larter and Barker (1991), this process had occurred until about 6.5–4 million years ago when the last segment of the ridge crest reached a trench to the south of the Hero Fracture Zone (HFZ). Between the latter and the Shackleton Fracture Zone (SFZ), there is the last preserved although disrupted fragment of the spreading axis Aluk-Antarctic. These several ridge fragments stopped spreading about 4 million years ago (Barker 1982). In this very place only a rift topography is distinct – floor depth reaches 5000 m. Segment of the Drake microplate between HFZ i SFZ is also the last relic of the subducting Aluk plate. During 30–35 million years since the opening of the Drake Passage, a northern part of the continental block of the Antarctic Peninsula has been subjected to numerous rifting episodes. Except for the opening of the Bransfield Basin about 20–30 million years ago, moving of the South Orkneys block to its present location, opened the Powell Basin. It has presumably resulted from back-arc spreading,

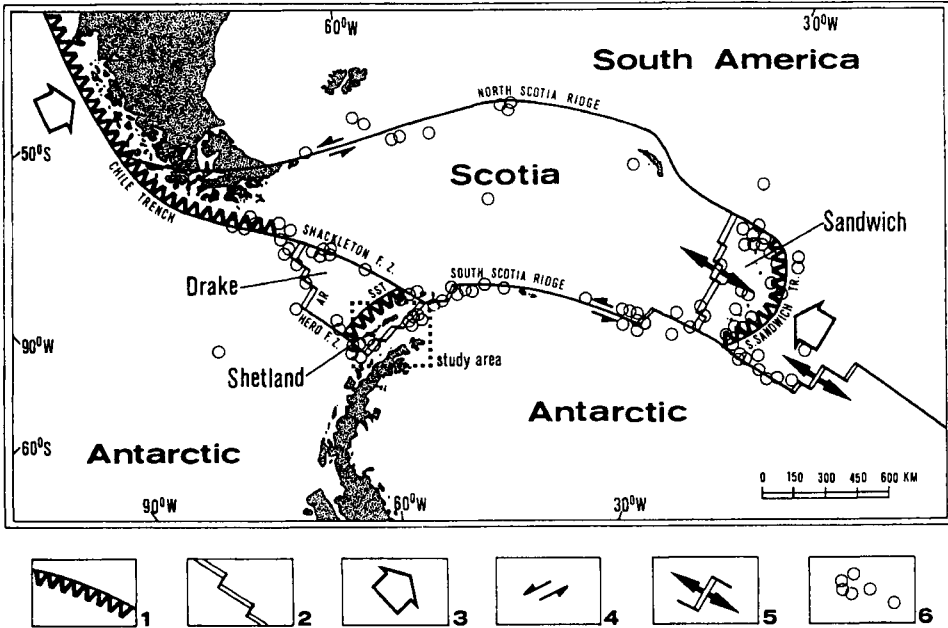


Fig. 3. Plate tectonic element around the Scotia region from the Tectonic Map of the Scotia Arc (1985), and Pelayo and Wiens (1989) and Birkenmajer *et al.* (1990). SST: South Shetland Trench; AR: Aluk Ridge. (1) Subduction trench; (2) divergent plate boundary, ridge and transform faults; (3) direction of subduction; (4) relative motion at the plate boundary; (5) direction of the relative motion at spreading ridges; (6) epicenters of the 1963–185 earthquakes (for earthquakes with $m_b > 5.0$; east of 30°W only for earthquakes with $m_b 6.0$). The dotted box shows the location of the study area (after Grad *et al.* 1993).

caused by westward subduction at eastern side of the South Orkneys (King and Barker 1988). The present, very complex tectonic pattern of this region is presented (Fig. 3).

Previous studies of the Bransfield Basin

The back-arc of the Bransfield Basin with the Bransfield Platform is a Cainozoic marginal basin, located in forefield of the South Shetland Islands and the Shetland Trench (Birkenmajer 1992). Geological and geophysical evidence proves that before development of the Bransfield Basin, the South Shetland Islands formed a part of the Antarctic Peninsula (Barker 1970, Ashcroft 1972, Davey 1972, Thomson *et al.* 1983). The volcanic arc has existed there since the Jurassic. Before development of the Bransfield Basin, the arc occurred on the Antarctic Peninsula. The Bransfield Basin separated the South Shetland Islands (present location of the volcanic arc) from the Antarctic Peninsula. Age

of opening of the Bransfield Basin is unclear. Birkenmajer (1983, 1989) as well as Birkenmajer and Keller (1990) suggest that rifting could be initiated at the turn of the Oligocene and the Miocene. It has been isotope-dated at 20–21 mln years, on the basis of diabase dikes on the King George Island, whereas opening of the rift itself could occur about 14 mln years ago. Trouw (1992) suggests that opening of the basin could be slightly older. According to Barker (1982) and also others (Storey and Garrett 1985, González-Ferrán 1985), who based on age analysis of magnetic anomalies, present evidence indicates that the basin was formed less than 4 mln ago. Some normal faults and subsidence at margins of the basin, point out the Late Pliocene (Barton 1965, Weaver *et al.* 1979). Extension chronology of the Bransfield Strait seems to have been connected with collision model of the ridge crest – trench type. According to Jeffers *et al.* (1991), rifting could have been started during the Early Pliocene, before opening of the basin about 2 mln lat ago (Weaver *et al.* 1982, González-Ferrán 1991). When discussing age of magnetic anomalies, Roach (1978) speculates that sea floor spreading has occurred for the last about 1.3 mln lat, and Parra *et al.* (1988) fixes age of the rift at 1.8 mln years. These considerable discrepancies suggest that application of magnetic anomalies is not precise if considering them for index of sea floor spreading history of such a young basin as the Bransfield Basin.

Opening of the Bransfield Strait formed a new microplate, the South Shetlands plate, delimited by postulated axis of back-arc spreading in the Bransfield Basin, the South Shetland trench as well as Shackleton and Hero fractures. HFZ separates volcanic arc of the South Shetland Islands and the Bransfield Basin from a continental, passive zone further to the south (Herron and Tucholke 1976) (Fig. 3). Strong argument that supports connection of subduction with back-arc extension is that active extensive rift of the Bransfield Strait occupies the same length of the Antarctic Peninsula as the preserved trench of the South Shetland Islands, against free relic spreading segments of the Aluk Ridge. Barker (1982) has proposed that Bransfield Strait opened because of the cessation of spreading, as a result of the continuing sinking of the remnant plate at the trench. Simultaneously, active extension occurred in the Bransfield Strait. A crust subjected to slow extension has been subjected to intensive fracturing what enabled entering of the upper mantle material and resulted in opening of the Bransfield Rift.

The South Shetland Islands form the island arc with volcanism history back to about 140 mln years ago (Weaver *et al.* 1982). Mesozoic volcanism in the South Shetland Islands predominated in eruptions of low-potassium, calcareous-alkaline basalts and basaltic andesites. Age of calcareous-alkaline magmatic rocks on the Antarctic Peninsula is estimated at about 180 mln years and is close to subduction of the lithospheric Pacific plate along the western side of the peninsula. Mesozoic volcanic rocks have varying composition, from basalts predominant in a western part of the peninsula to rhyolites, occurring in the east.

Tectonic environment and chemism of volcanic rocks at the eastern shore are similar to volcanic rocks of the southernmost part of South America (Tobifera silicic rocks).

Bathymetry. — The Bransfield Strait has strongly asymmetric transversal section. It consists of two large morphologic units *i.e.* broad shelf of the Antarctic Peninsula, defined occasionally as the Bransfield Platform, and a deepwater back-arc basin, named the Bransfield Basin or the Bransfield Trough, 15–20 km and locally to 100 km wide. In the Bransfield Basin, three subbasins are commonly distinguished (Jeffers and Anderson 1990, Szeliga *et al.* 1994): the largest – central, deepest – eastern (maximum depth 2784 m see Bochu *et al.* 1995), and the smallest and most shallow one – the western subbasin (Fig. 4). There are also other subdivision proposals but they are only occasionally used. In spite of earlier expeditions, detailed measurements with use of multi-beam echo sounder enabled finally preparation of a detailed map of sea floor for central and eastern subbasins (Gràcia *et al.* 1996). These maps are important for better understanding the present evolution of the Bransfield Basin.



Fig. 4. Bathymetry of the Bransfield Basin, showing location of western (W.S.), central and eastern (E.S.) subbasins (compiled and simplified from Jeffers and Anderson 1990, Szeliga *et al.* 1994, Cunningham *et al.* 1995, Gràcia *et al.* 1996). Black stars show positions of large underwater volcanoes; open stars show positions of stratovolcanoes.

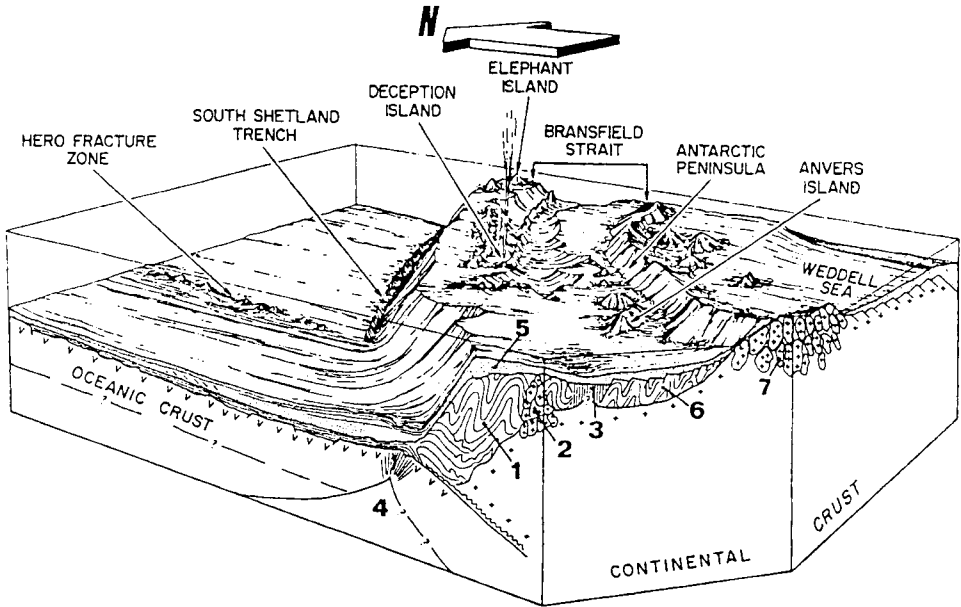


Fig. 5. Perspective block diagram of the study area. Note the major change in the margin tectonic style across the Hero Fracture Zone (HFZ) from "passive" margin in the south to "active" margin in the north. (1) fore arc material; (2) eroded arc; (3) closed back arc basin; (4) fossil spreading centre; (5) sedimentary wedge; (6) metamorphic rocks; (7) intrusive and extrusive acid rocks (after Gambôa and Maldonado 1990).

Submarine volcanic ridges. — The islands Deception (Barker *et al.* 1976) and Penguin (González-Ferrán and Katsui 1970) are defined, together with the Bridgeman Island, as stratovolcanoes formed after the Pleistocene due to opening of the Bransfield Strait (Weaver *et al.* 1982, González-Ferrán 1985). They represent the only visible part out of several volcanoes of a large submarine ridge, about 300 km long, that runs between the islands Deception and Bridgeman (Figs 5–6). Lawver *et al.* (1995) distinguished four volcanic lines, parallel to the basin axis, the latter generally defined as the line between the islands Deception and Bridgeman. All volcano rows occur between the South Shetland Islands and the basin axis.

Volcanic activity is assumed to be a continuous process in this region. Its both types *i.e.* land and submarine ones are to be noted in future in every volcanic centre or in other rift-affected areas (González-Ferrán 1985). Active tectonic movements occur in numerous fractures that cut present marine sediments (Gambôa and Maldonado 1990). Recent volcanism (Sauders and Tarney 1984) and seismicity (Forsyth 1975, Pelayo and Wiens 1989) along the axis of the Bransfield Basin, indicate that extension is common also recently. Volcanic products of the zone Deception–Bridgeman describe geochemical and isotopic features,

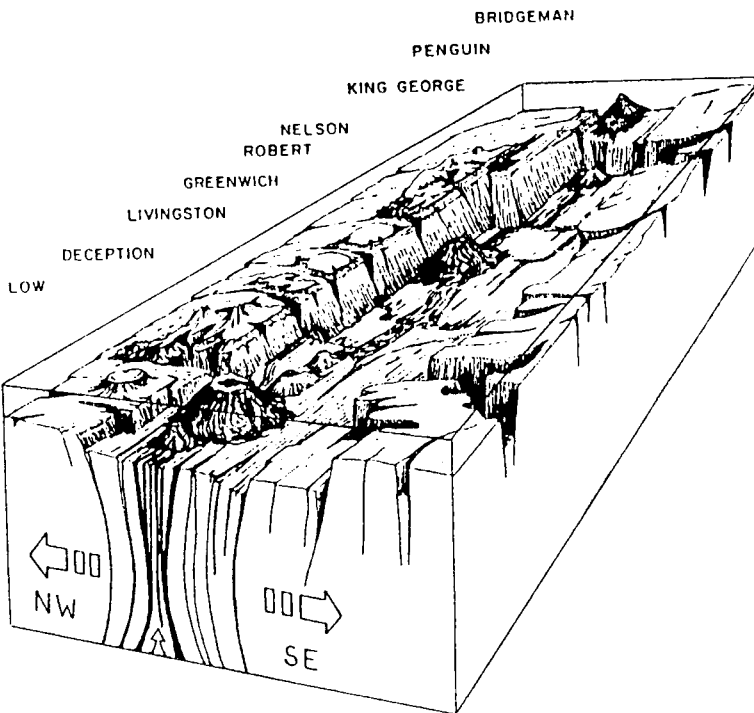


Fig. 6. Block diagram of the Bransfield rift and its volcanic ridge (after González-Ferrán 1991).

changing along its axis (Keller *et al.* 1987, 1988, 1991). They are transitional between magmas from a mid-ocean ridge and calcareous-alkaline ones (Weaver *et al.* 1979), which are to occur in early evolution stage of back-arc spreading. Lawver *et al.* (1995) assumed that volcano products have been more and more similar to the Mid-Ocean Ridge Basalt (MORB) during rift development in the Bransfield Basin. Occurrence of the ridge is accepted as mature stage of rift development.

Heat flow and hydrothermal activity. — Estimation of heat flow in 1989 (Lawver and Nagihara 1991, Lawver *et al.* 1995) at 54 measuring sites in the King George (Central) Basin, proved it to be from 50 to 626 mW m^{-2} *i.e.* generally high and significantly varying. One fourth of results exceeded 220 mW m^{-2} . The highest values were noted for central part of the basin as well as along southern and northern margins of its eastern part, from 150 to 250 mW m^{-2} and 370 mW m^{-2} , respectively. In western and north-western parts of the basin, values were commonly below 100 mW m^{-2} . After analysis of heat flow and echo sounding data, the authors suggest occurrence of extension, similar to the one in central and northern part of the Californian Bay rather than extension of a back-arc basin.

Hydrothermal activity in the Bransfield Strait confirms presence of submarine volcanic activity (Han and Suess 1987, Suess *et al.* 1987).

Magnetics and gravimetry. — Complex geological structure and tectonics of West Antarctica in the Bransfield Strait region are reflected by gravimetric and magnetic anomalies. At the most recent map, published by the British Antarctic Survey (BAS) GEOMAP (Maslanyj *et al.* 1991) (see Fig. 7), aeromagnetic anomalies are negative (to -700 nT) for the South Shetland Islands, the Bransfield Basin and the Antarctic Peninsula, and they are positive (to 1000 nT) in the Drake Passage (Garrett *et al.* 1986/87, 1987; Garrett 1990). They are opposite to positive anomalies (to 200 nT) at the Bransfield Platform. Negative anomalies (to -300 nT) occur at the Antarctic Peninsula.

Magnetic measurements have been also carried out in the Bransfield Strait with use of research vessels, associated with simultaneous bathymetric measurements (Kim *et al.* 1992). At 8 profiles that transect the strait, positive anomalies were noted (from 200 nT to 2000 nT) and interpreted as coming from intrusions of basalt dikes along a ridge axis (anomaly decreases with increasing water depth). Gràcia *et al.* (1996) correlate positive anomalies (300–400 nT) to large volcanoes. Small amplitudes of positive anomalies in the eastern subbasin occur at the basin axis. Magnetic anomalies determined on the basis of the most dense measurement network (Bochu 1994, Bochu *et al.* 1995), were subdivided into three areas in the Bransfield Strait: block of the South Shetland Islands, the Bransfield Rift and the Bransfield Platform. High-value positive anomalies were noted at the platform (100–400 nT), and negative anomalies to -300 nT in the Bransfield Rift, although accompanied by positive anomalies equal to 200–900 nT. Such phenomenon is interpreted by the authors as contrast of the younger component rock of volcanoes from the surrounding older crystalline bedrock. Block of the South Shetland Islands is the area of positive anomalies to 300–1000 nT.

Regional magnetic field over the Antarctic Peninsula is predominated by the West Coast Magnetic Anomaly (WCMA), recognized by Renner *et al.* (1982, 1985). According to them, magnetic anomalies suggest presence of a batholite that encircles the peninsula from the west and a splitting in the Bransfield Strait region. The western body, 30–50 km wide, is combined with positive anomalies 500–1500 nT. The eastern body, 50–70 km wide, is connected with a complex of positive anomalies 500–900 nT. WCMA, modelled as series of large and simple bodies with uniform magnetisation, is a great simplification (Garrett 1990). The batholite can contain in fact many mafic and medium-mafic plutons of various types and age, as well as intrusions formed during crustal extension. Occurrence of the batholite is not reflected in surface geology (Johnson and Smith 1992). WCMA is similar to a great magnetic anomaly, observed in continental fragments of the Scotia arc and used in reconstructions of plate history.

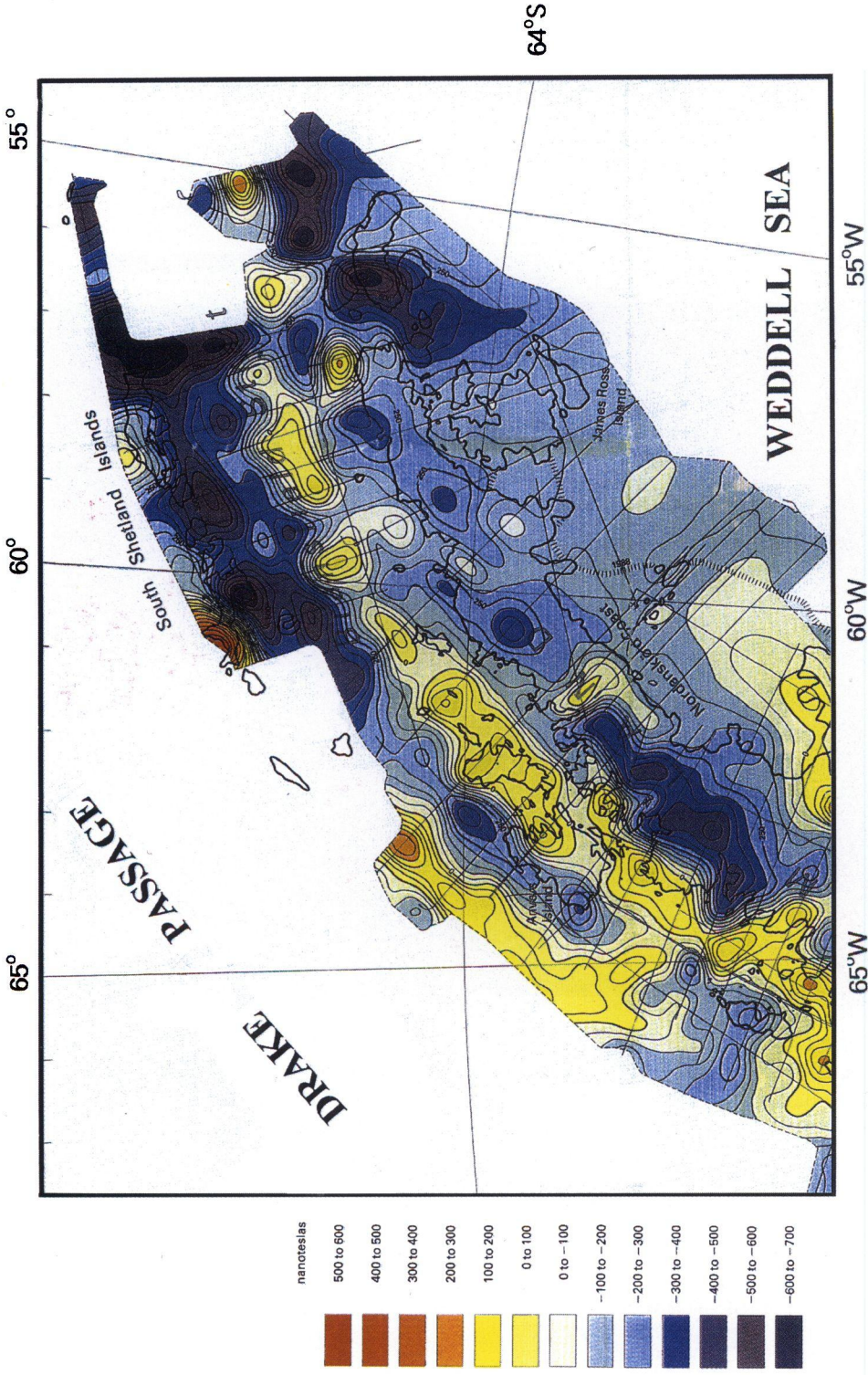


Fig. 7. Fragment of the Aeromagnetic Anomaly Map of West Antarctica (Weddell Sea Sector), after Maslanyj *et al.* 1991.

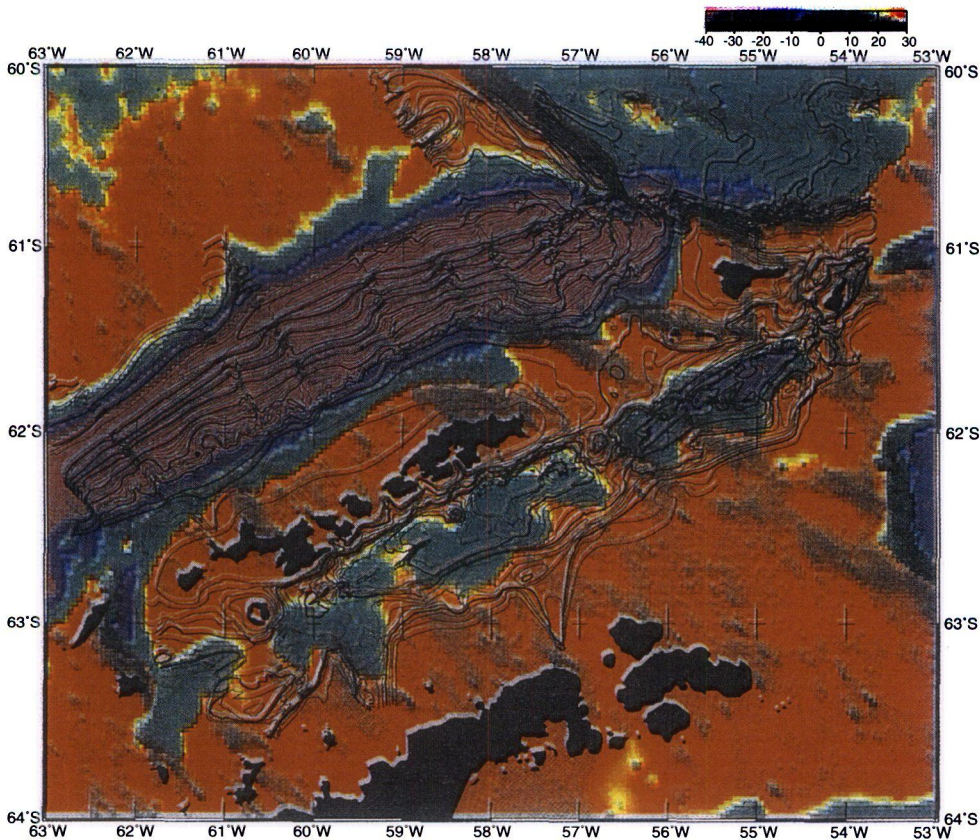


Fig. 8. Geosat/ERS-1 gravity data from Sandwell and Smith (1992), with superimposed digital bathymetric data after Klejpes and Lawver (1994). The gravity data colour bar indicates gravity values from -40 mgal to +30 mgal. Bold black bathymetric contours are shown every 500 m, while thin black contours are observed bathymetry contoured every 100 m. Thin blue contours are interpolated bathymetric data contoured every 100 m.

Parra *et al.* (1984, 1988) and González-Ferrán (1983, 1985) received similar distribution of magnetic anomalies in the basin, using interpretation of air measurements for the area between the Antarctic Peninsula and a centre of the Drake Passage, for denser measurement network than the network BAS.

BAS has been carrying through recognition of land gravimetric data on the Antarctic Peninsula since 1959. Data were collected from about 1500 stations, founded in lithic rock, and from marine and glacial profiles (Renner *et al.* 1985). In the described area, Bouguer anomalies are concordant with structures of the island arc and peninsula, with positive values 20–140 mgal – maximum in the Bransfield Strait, according to the authors caused by thin Earth's crust in a marginal basin. However, measurements on glaciers if their thickness is unknown, can be charged with error from 10 to 100 mgal (Garrett 1990).

Measurements of free-air gravity anomalies, carried through from a vessel for a relatively dense network of the profiles in the Bransfield Strait (Bochu *et al.* 1995), enabled determination of the anomalies parallel to the South Shetland Islands and the Antarctic Peninsula. The South Shetland trench has negative anomalies -20 to -120 mgal, and the South Shetland Islands – positive ones equal to 60–90 mgal. In the Bransfield Strait, anomalies indicate varying values from -31 to 112 mgal. They are equal to 60–90 mgal for the Antarctic shelf and form a zone with low anomalies in the Bransfield Rift.

There are generally four areas if varying gravimetric anomalies are concerned: the South Shetland trench with high negative anomalies, the South Shetland Islands with positive anomalies, the Bransfield Rift with negative anomalies and finally, the Antarctic shelf with high positive anomalies. This subdivision, taking map scale into account, is generally concordant with picture of gravimetric anomalies by Sandwell (1992) for West Antarctica (see Fig. 8) and the Bransfield Strait (Barker 1995), based on satellite measurements (satellite GEOSAT/ERS1). Accuracy is equal to 1 mgal (measuring profiles at every 4 km).

Seismic reflection data. — In whole West Antarctica and particularly, in the Bransfield Strait many marine seismic reflection investigations were carried out (Guterch *et al.* 1985; Jeffers *et al.* 1986, 1990, 1991; Jeffers 1987; Macdonald *et al.* 1988, 1990; Meissner *et al.* 1988; Gambôa *et al.* 1990, 1994; GRAPE Team 1990; Henriot *et al.* 1990, 1992; Acosta *et al.* 1992; Larter 1991; Banfield *et al.* 1994; Bochu 1994; Canals *et al.* 1994; Camerlenghi *et al.* 1994; Bochu *et al.* 1995; Gizejewski 1995). These data are available in a common data base of the Antarctic Offshore Acoustic Stratigraphy Project ANTOSTRAT (Behrendt 1990, Cunningham *et al.* 1995) (Fig. 9). Received sections enable analysis of a sedimentary cover, particularly in sedimentary basins, and to detect crystalline bedrock at some sections. Due to strong reverberation, useful penetration of seismic ray into sea floor structures, is equal to from 0.1 s on shelves to 2.5 s of double time for deepest fragments of the basin (Fig. 10A). There is distinct

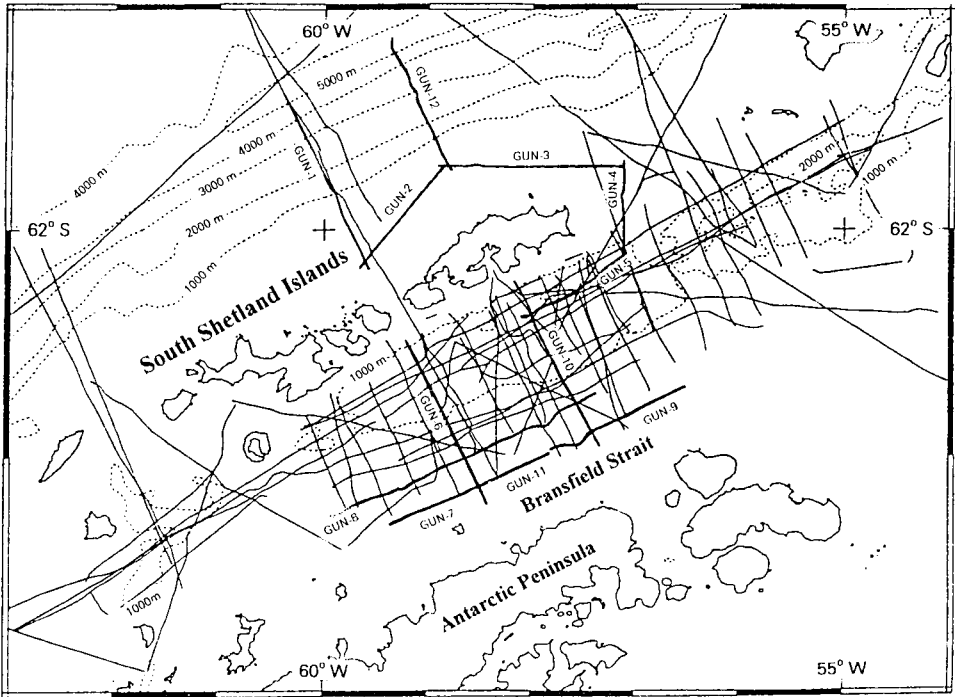


Fig. 9. The ANTOSTRAT digital navigation compilation. This data shown distribution of seismic reflection data in the region of South Shetland Islands (after Cuninghame *et al.* 1995). Digital navigation contributions by the Polish Academy of Sciences are presented by sicked lines with names.

separation of margins of volcanic domes at profiles transversal to a rift axis. It is exemplified by the section that cuts a volcanic dome (Fig. 10B) and was presented by the expedition of the Polish Academy of Sciences (Grad *et al.* 1993a, b).

Sediments. — Two elements determine occurrence of sediments in the central basin: varying supply with sediments and occurrence of volcanic domes. Jeffers and Anderson (1990) found deposition in the Bransfield Basin to have been predominated by glaciomarine sediments, transported to a higher degree from the Antarctic Peninsula than from the South Shetland Islands. According to their suggestion, a submarine volcanic zone can act as local dam for sediments but in fact, a neo-volcanic ridge is not a continuous structure (Gràcia *et al.* 1996).

Interpretation of data of the seismic reflection (Barker *et al.* 1988) indicates that lavas and sediments are innerly stratified, magmatic activity favours iniection of dikes and sills within the sediments, thus creating thin beds within lavas and terrigenous sediments. Magnetic minerals are much more dissipated in such surroundings and more weakly magnetized than a normal ocean crust (Lawver

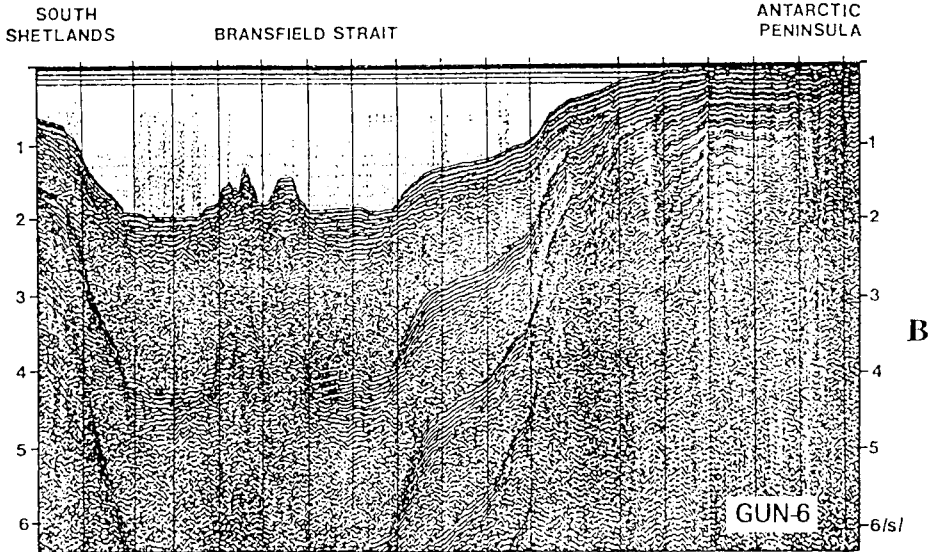
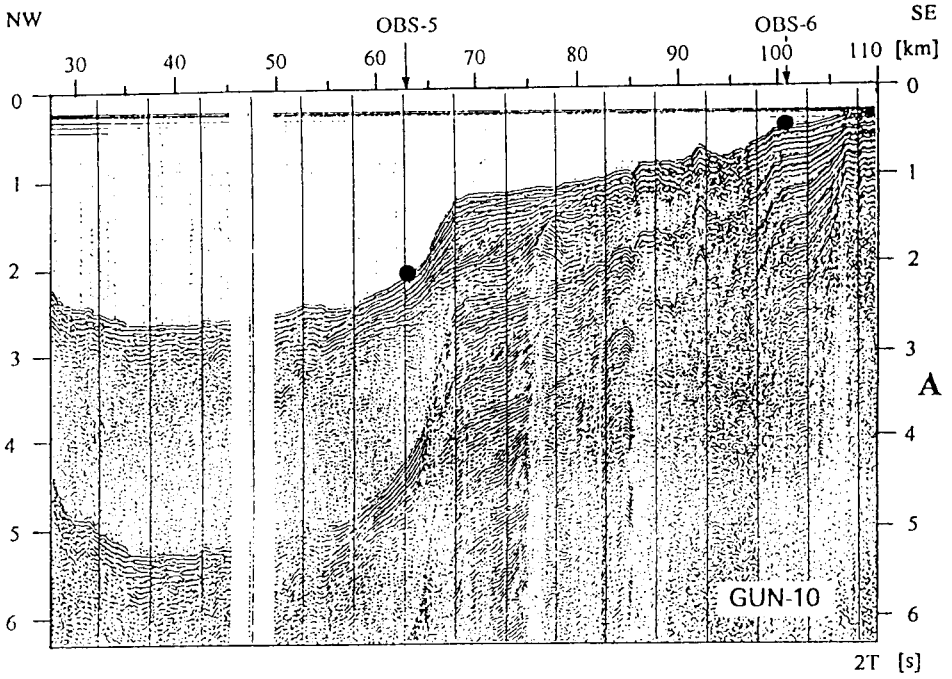


Fig. 10. Examples of seismic reflection sections across the Bransfield Strait. A – GUN-10, B – GUN-6.

and Hawkins 1978). Therefore, typical anomalies for the ocean floor spreading cannot be formed.

Seismic refraction. — British Antarctic Survey has carried through seismic refraction measurements at the beginning of the sixties. They were elaborated by Ashcroft (1972), being important argument in discussion of tectonic models of the region. A discontinuity, located by Ashcroft at depth of 15–20 km with velocity $V_p = 7.7$ km/s, was interpreted as the Moho discontinuity with anomalously low velocity.

Seismicity. — Analysis of seismic events in active marginal zones brings abundant and extremely important information to studies of present mutual relations of lithospheric plates in subduction zone. Depth of event generation, their magnitude and mechanisms, are principal information when dynamics and type of mutual movements of plates are considered. Analysis of 50 selected events with magnitude about 5.0 mb and more, coming from the Antarctic in 1925–1980 at the World-Wide Standard Seismograph Network (WWSSN) stations, was done by Forsyth (1975), Okal (1981) as well as Pelayo and Wiens (1989).

Forsyth (1975) analyzed events from the South Atlantic and the Scotia Sea, and took into account also two events from the Bransfield Strait region. Analysis of mechanism of the first event (1971, 6.3 mb) from the Shackleton fracture zone (left lateral strike-slip) presumably confirms that, in relation to North America the Antarctic plate rotates eastwards quicker than the Scotia plate. The Drake microplate is proved also to move slowly towards the South Shetland Islands. The second event from the western basin (1969, 5.9 mb) occurred in a normal fracture and suggests back-arc extension.

Most complete analysis of events in the Drake Passage and the Bransfield region was done by Pelayo and Wiens (1989). The South Shetland Islands region presents temperate seismic activity, the weakest ones if compared with other active marginal zones. Lack of deep sources of events is typical for this zone as only two quakes were noted at depths 35 and 55 km, while the others come from depth 8–27 km. Two shallow events near the Elephant Island, close to transect of the South Shetland trench with the SFZ, indicate lateral strike-slip fractures and fractures at contact of two plates in a subduction zone (thrust faulting). Two events in the Bransfield Strait indicate tension at directions NW-SE. The greatest event, 45 km to the southwest of the Deception Island in 1971, with well determined depth (15 km), indicates that the event has not been directly connected with volcanic activity. The authors suggest that it is a clear tectonic event, resulting from active rifting in the Bransfield Strait.

Other events in this region can be directly connected to the volcano Deception or to tectonic activity of a rift structure of direction NE-SW. During observations in 1987 and 1988 on the Deception Island, local events from sources at distances from 40 to 80 km were noted. Observations of seismic activity, collected by Villa

et al. (1992) on the Deception Island also indicate a large number of insignificant local events.

Large normal events occur along the South Scotia Ridge and in the region of active back-arc rifting in the Bransfield Strait. These events are deeper and have larger seismic moment than events connected with spreading of a mid-ocean ridge (Pelayo and Wiens 1989).

Depths of two mentioned events (35 and 55 km) are considerably larger than the ones noted elsewhere in the described area and deeper than could be expected for inner-plate seismicity in the present volcanism area (Pelayo and Wiens 1989). They also suggest that events can occur in relic material of the plate that remained in the same place, where active subduction was stopped 4 mln years ago and they also indicate active subduction. Considering the fact that both events are of tensile type, it seems obvious that slow subduction persists along the South Shetland trench. Other shallow event centres, coming from fractures at contacts of plates in a subduction zone (thrust focal mechanism) and connected with subduction also, indicate its activity. Low seismic velocity along the South Shetland trench can be explained by small age of the subducting lithosphere (12–22 mln years), presumable slow convergence and decoupled contact between the plates. If spreading along the Aluk Ridge is dead as known from examination of a sea floor, the convergence rate can be similar to the extension rate in the Bransfield Strait, which is not exactly known but probably low. At low convergence, young ocean lithosphere can be submelted due to high heat transport and therefore, deeper event sources should not be expected. Additionally, a subduction zone which indicates back-arc extension, generally shows absence of events at plate contacts in the subduction zone (thrust interface earthquakes) that can be interpreted as lack of contact between the plates.

Stresses. — Tokarski (1991) analyzed directions of fractures and dikes from the King George Island, and suggested that stress propagation from the Scotia Sea to the Bransfield Strait, with decreasing influence of stress generated by the subducting Aluk microplate, could play significant role in a primary rifting stage. On the King George Island he observed transition from transpressive deformation zone of strike-slip type in the Upper Miocene to extension at present. He noted also right-hand rotation of the main axial stress from the east-southeast to the west-southwest. González-Ferrán (1985) presented extensive volcanism of the Bransfield Basin within larger network of young volcanism of the northern Grahama Land (northeastern part of the Antarctic Peninsula). Tokarski (1991) considers them for fragments of a larger, inner-plate 'fan-shaped' rift system. These zones can be interpreted as symptoms of inner deformations of the Antarctic plate that were generated by stress regime, caused by surrounding spreading centres. Jeffers *et al.* (1991) suggest possible interrelations between segments of the Bransfield Basin and its early spreading, whereas the southwestern

subbasin is still at primary rifting stage. Different sinking time of segments of the subducted plate, older and denser fragment of a plate beneath the north-eastern subbasin can subside quicker, making extension stronger than to the southwest. Left-handed rotation of the Scotia plate that obliquely penetrates under northern margins of the South Shetland Islands and the Drake microplate, can result in westward (limited in time) rotation of the South Shetland microplate.

Seismic measurements suggest too that segmentation is of tectonic origin. Eastern and western subbasins are subjected to relatively frequent seismic events, contrary to the central subbasin which is distinctly a non-seismic one (BAS Tectonic Map of the Scotia Arc 1985, Pelayo and Wiens 1989).

Detailed maps of a sea floor enabled morphostructural analysis of central and eastern subbasins. They made authors (Gràcia *et al.* 1996) draw opposite conclusions than Jeffers *et al.* (1991). The central subbasin is considerably different from the eastern one if its structure, dynamics, size of volcanoes and sedimentary cover are concerned. Analysis of shapes of large volcanoes in the central subbasin indicates possible extension northwest-southeastwards. Occurrence in the central subbasin of linear extensive fractures with a primary activity of the volcanism of the type similar to MORB, is interpreted as a very early stage of sea floor spreading. On the contrary, the eastern subbasin, being still at rifting stage, is mainly predominated by diffused spreading with scattered volcanism and semicircular volcanoes. Possible occurrence of strike-slip movements along the eastern subbasin is suggested by rhomboid-shaped basins and probable influence of stress from left-hand movement of the South Scotia Ridge. Similar small basins are noted along this ridge. They are interpreted as pull-apart basins (Acosta *et al.* 1994).

Occurrence of scattered extension in the eastern subbasin is concordant with general description of the so-called scattered development, present in the back-arc basins *e.g.* in the Japan Sea (eastern subbasin) (Dadlez and Jaroszewski 1994, Tatsumi *et al.* 1989) or between the southern and northern Okinawa rifts (Sibuet *et al.* 1987). Spreading axes are short and disrupted if they really occur, and linear magnetic anomalies cannot be easily identified.

Geodynamical expeditions of the Polish Academy of Sciences

In 1979–1991 four geodynamical expeditions, organized by the Institute of Geophysics of the Polish Academy of Sciences, examined the region of West Antarctica (Fig. 11). During these expeditions, explosive deep soundings of the Earth's crust have been done. Seismic energy was generated by explosion of TNT charges from 16 to 144 kg, usually 50 or 100 kg, detonated with electric impulse at depth about 60 m. Shots sites were commonly about 5–7 km apart. Their location

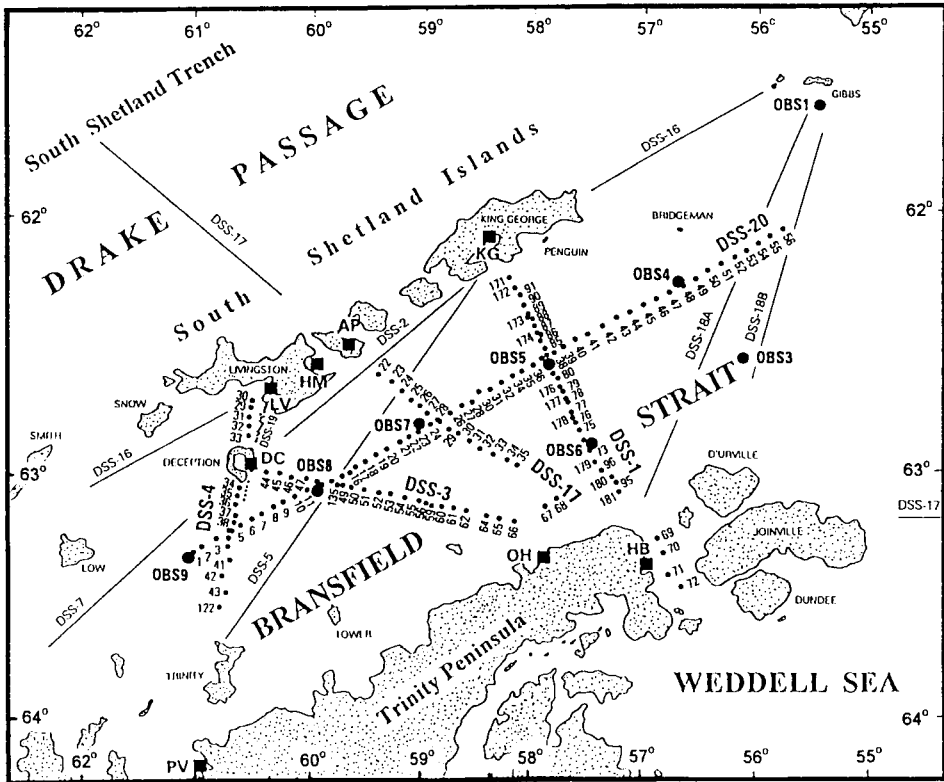


Fig. 11. Location of selected deep seismic sounding profiles (DSS) in the region of Bransfield Strait. Dots – shot points and their consecutive numbers along profiles discussed in the text, open circles – ocean bottom seismometers; black squares – seismic stations: AP – Arturo Prat, DC – Deception, HM – Half Moon, HB – Hope Bay, KG – King George, OH – O'Higgins, LV – Livingston, PV – Primavera.

was determined by satellite navigation and also radar bearings were done. Each explosion was associated with measurements of sea floor depth with use of a typical vessel echo sounder. Records at land stations were done with use of 3 to 6 seismometers (including 2 horizontal, during the last expedition), specific frequency of which was equal to 1.3 Hz and they were commonly located at distances 100–200 m. Except for a traditional paper record, magnetic record (primary analog and then digital) was done at the same time at most stations. During the last expedition, land record was accompanied with the one using ocean bottom seismographs (OBS) of the Hokkaido University. The applied OBSs were of the type pop-up. The operating depth was up to 6000 m (tested to depth 9500 m) and working at slopes to 30° due to gimbal mechanism (Shimamura 1990). Recorded were three components in analog system, at different amplifier gain and tape speed 0.1 mm/s. The recording frequency range was 1–30 Hz.

Seismic reflection measurements, using a multichannel system DFS-IV with Bolt airguns, were made along profiles with total length of about 1100 km during first expedition (Guterch *et al.* 1985) (Fig. 9). This expedition used the hydrographic vessel ORP *Kopernik*. Next expeditions used the ocean tugs V/S *Jantar* and D/E *Neptunia*.

Geographical coordinates of recording stations are:

	λ	ϕ		λ	ϕ
KG	62°35'72S	59°55'24W	OBS-1	61°32'17S	55°39'52W
DC	62°58'80S	60°34'20W	OBS-3	62°25'74S	56°08'62W
HB	63°24'16S	56°59'34W	OBS-4	62°16'00S	56°50'95W
OH	63°19'32S	57°53'88W	OBS-5	62°35'97S	57°53'40W
HM	62°35'72S	59°55'24W	OBS-6	62°53'59S	57°31'04W
PV	64°09'36S	60°57'36W	OBS-7	62°49'22S	59°04'20W
AP	62°28'90S	59°40'00W	OBS-8	63°04'88S	59°58'63W
LV	62°40'08S	60°23'62W	OBS-9	63°20'24S	61°03'79W

Results of seismic investigation for the stations along profiles are presented (Figs 12–17). All seismic record sections are enlisted in a reduced form, with reduction velocity equal to 7.0 km/s. Record sections were filtered in bands 2–15 or 2–10 Hz. Multi-channel records at land stations enable better determination of successive wave occurrence than single channels. Due to their clarity at seismic sections, it was however necessary to draw apart channels what caused deformation of inclination of correlated impulses in individual records.

Seismic record sections along profile DSS-20. — Measurements along profile DSS-20 (Fig. 11), presenting a most complete measuring scheme, were done in 1991. This profile ran along the Bransfield Strait, close to a rift axis. Its total length was slightly over 300 km. Along the profile, the same (100 kg) 52 shots were detonated. Seismic waves of these shots were recorded by 5 OBSs, located along the profile at distances 50–70 km from one another, and at 5 land stations (KG, HM, HB, OH, PV) and 4 OBSs apart from the profile (Fig. 12). Modelling was based on records from OBSs located on the profile only.

First arrivals of refracted waves are distinct to distance 200 km along profiles for all OBSs. Apparent velocities are equal to from 2.0–5.5 km/s at distances to 20 km from OBS, to 6.5–7.0 km/s at distances to 75–110 km. First arrivals with velocity about 7.7–8.1 km/s are noted from about 110–120 km in a southwestern part of the profile (OBS-9 and OBS-8) and from about 70–80 km in a north-eastern part of the profile (OBS-7, OBS-6 and OBS-5). Except for refracted waves, there are also occasional ones which were reflected from the intra-crustal and the Moho discontinuities, commonly at distances equal to 60–110 km. They are typical for relatively high amplitudes but at short distances, about 30 km.

Only these waves were correlated which were sure enough to be the reflected P waves.

At seismic sections from three southern OBSs (OBS-9, OBS-8 and OBS-7), distinct damping of wave field was noted (records 48–56). Such rapid change can be due to presence of a fracture zone, with strongly damping properties, and can occur at about 250 km of the profile.

Very good seismic record sections along profile DSS-20 enable more detailed modelling of a crust structure, considerably more accurate than on previous profiles in this region. Materials from profile DSS-20 enabled modelling of real amplitudes as all shots were done by the same charges (100 kg TNT). Records were simultaneously done at three amplification levels: high, medium and low. Three pictures of the same seismic record section, received for high, low and hand normalized" amplification are presented for OBS-8 (Fig. 13). The last one was completed with use of varying amplification records, to make its picture most clear for correlation of wave arrivals. Such preparation of sections enabled better correlation of waves and analysis of bubble effect and reverberation.

Seismic record sections along profile DSS-1. — Profile DSS-1, about 168 km long, connects the stations KG and HB that cross the Bransfield Strait almost perpendicularly to its main axis (Fig. 11). Measurements on this profile have been done twice: for the first time in 1979/80, with land record only, generated with 20 shots of charge 50–100 kg TNT each. Measurements were started in 1990/91 again, with recording at the same land stations but also at two OBSs (OBS-5 and OBS-6); 12 shots were fired of charge 50–100 kg TNT each. To distinguish them from the earlier ones, during the expedition 1990/91 the shots have symbols over 100 – with the exception of 37 only – common for profiles DSS-1 and DSS-20. Profile DSS-1 coincided partly with the reflection seismics section GUN-10 (Guterch *et al.* 1985, 1990, 1991; Gizejewski 1995), presented together with OBS-5 and OBS-6 (Fig. 10A). All refracted seismic sections indicate very distinct wave first arrivals and records from the station KG, at distance over 125 km (Fig. 14A), are the only exception. All record sections indicate also great changeability of apparent wave velocities, from 5.6 to 9.7 km/s in the central basin, presumably connected with highly varying water depth from slightly over 100 m on shelves to about 2000 m in the central basin. In these section fragments that transects the antarctic shelf, apparent velocities were equal to 7.8 km/s at the station KG (distance 90–120 km), 6.6 and 7.1 km/s at the station HB (20–55, 55–75 km) (Fig. 14B), and about 7.0 km/s at OBS-5.

Seismic record sections along profile DSS-17. — Measurements along profile DSS-17 were carried out during the third expedition 1984/85. The profile was subdivided into three parts: the northern from the South Shetland Islands to the Drake Passage (Grad *et al.* 1993a, b), the eastern (?Weddell Sea) and the

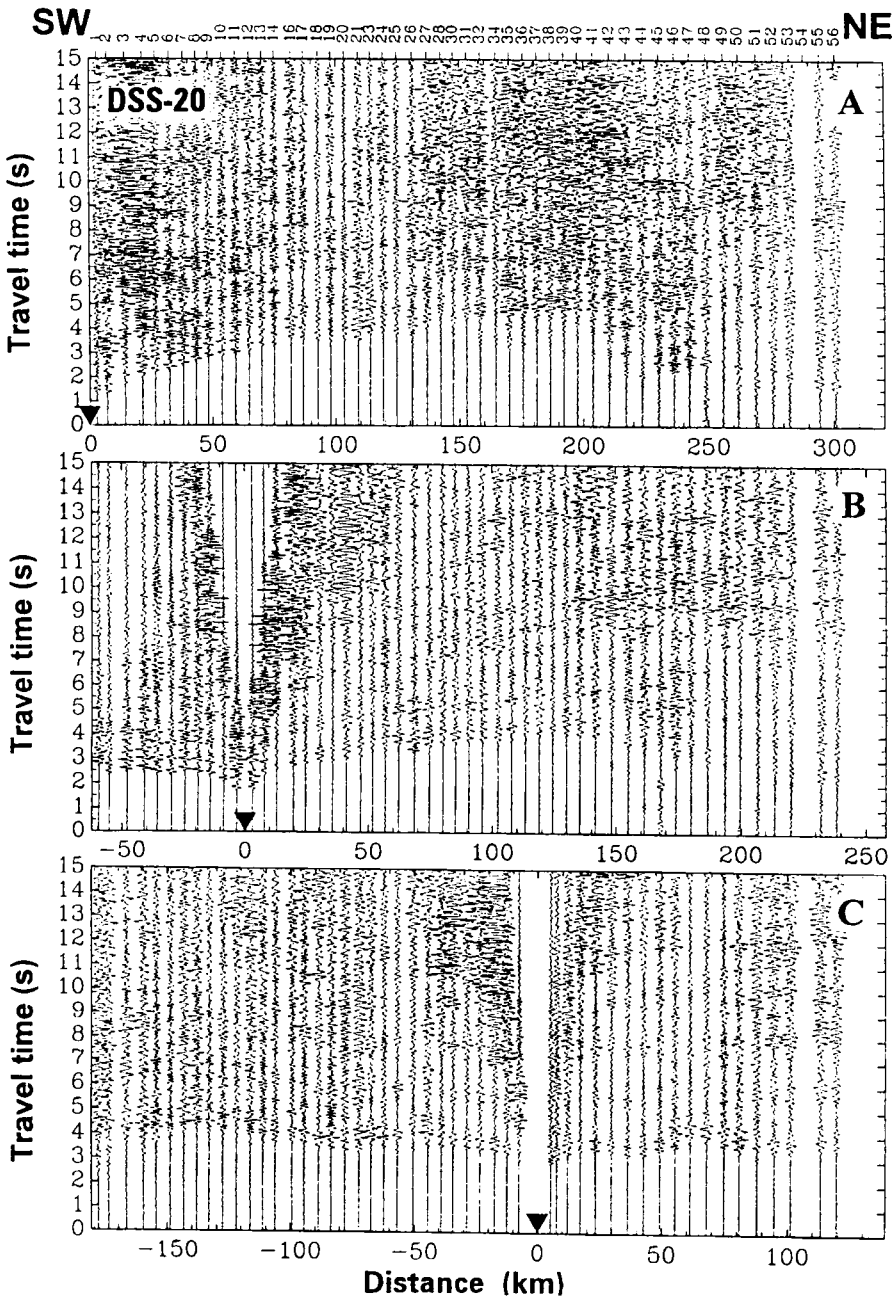


Fig. 12A–C. Examples of seismic record sections for profile DSS-20: A – for OBS-9, B – for OBS-8, C – for OBS-5. All sections with filtration 5–15 Hz or 2–10 Hz and ‘hand normalized’. ‘Hand normalized’ record sections were obtained after choosing an amplification factor for each trace that gave the best visibility of the full wavefield, *i.e.* first arrivals and further phases. ‘Hand normalized’ sections are also shown in Figs 12–20, 22–23, 25–26. Reduction velocity 7.0 km/s.

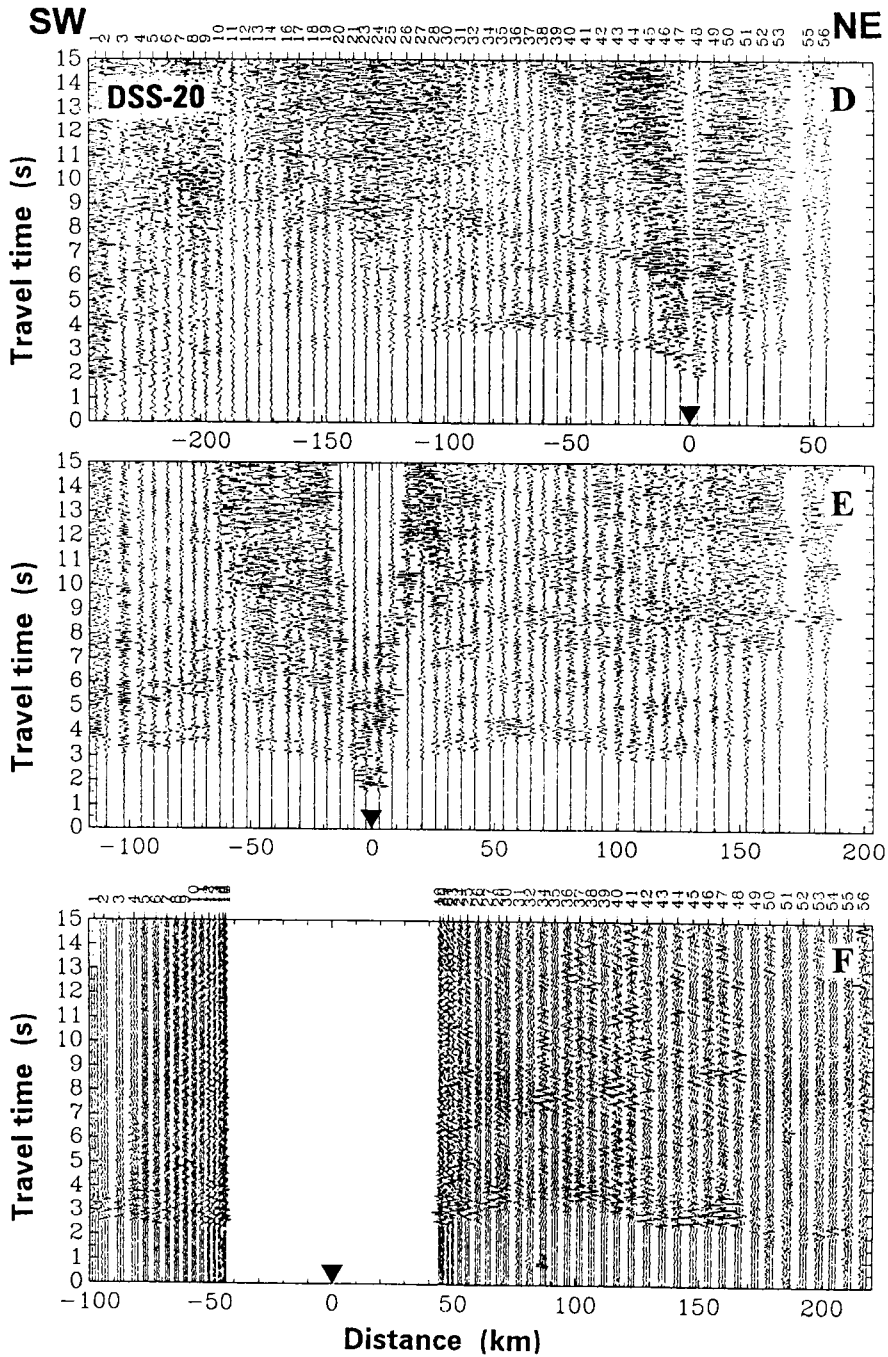


Fig. 12D-F. Examples of seismic record sections for profile DSS-20: D – for OBS-4, E – for OBS-7, F – for land station Half Moon. All sections with filtration 5–15 Hz or 2–10 Hz and 'hand normalized'. Reduction velocity 7.0 km/s.

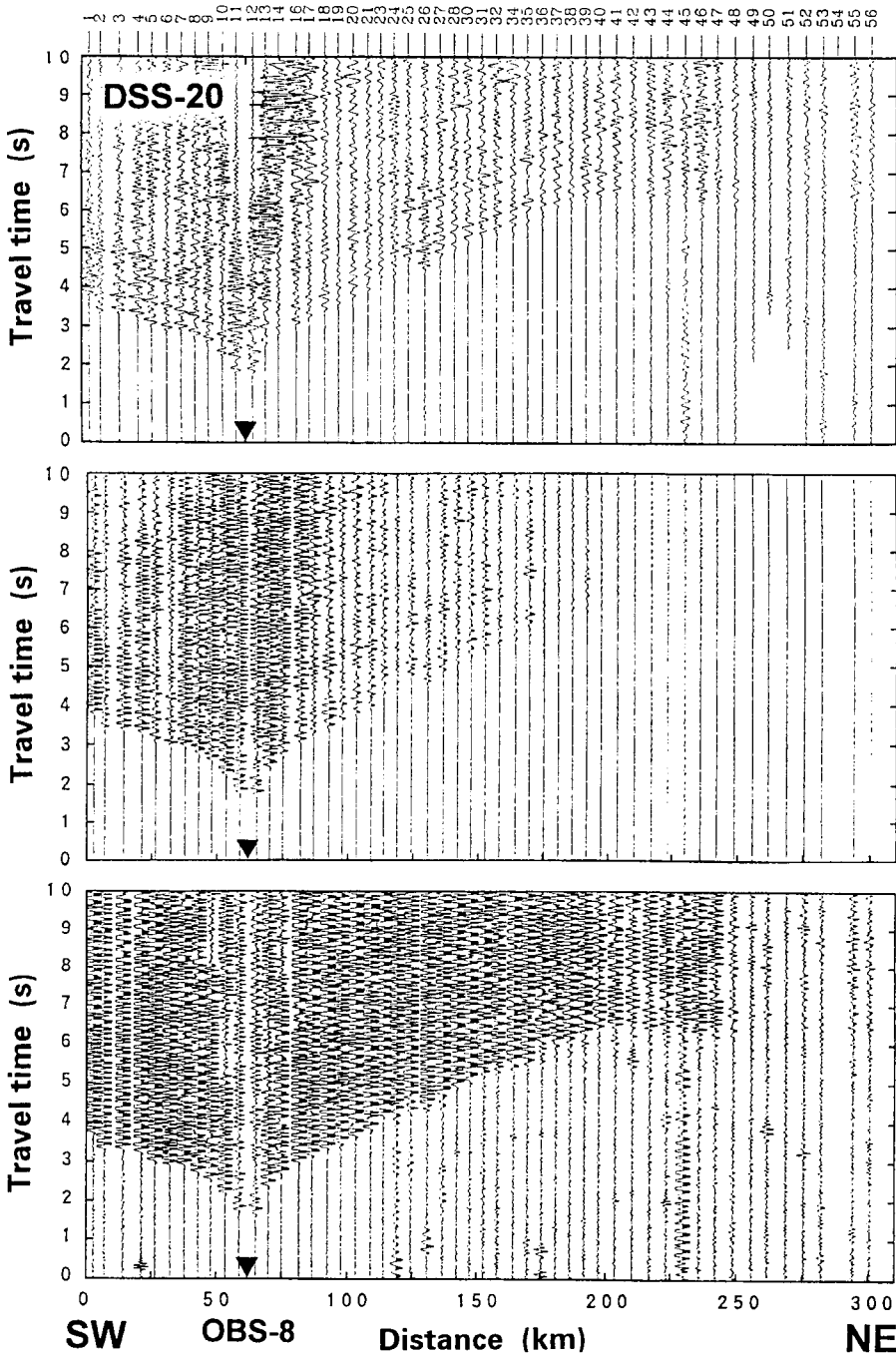


Fig. 13. Examples of seismic record sections for profile DSS-20, OBS-8. 'Hand normalized' (upper diagram), low gain (middle) with filtration 5–15 Hz and high gain (floor), filtration 2–10 Hz. Reduction velocity 8.0 km/s.

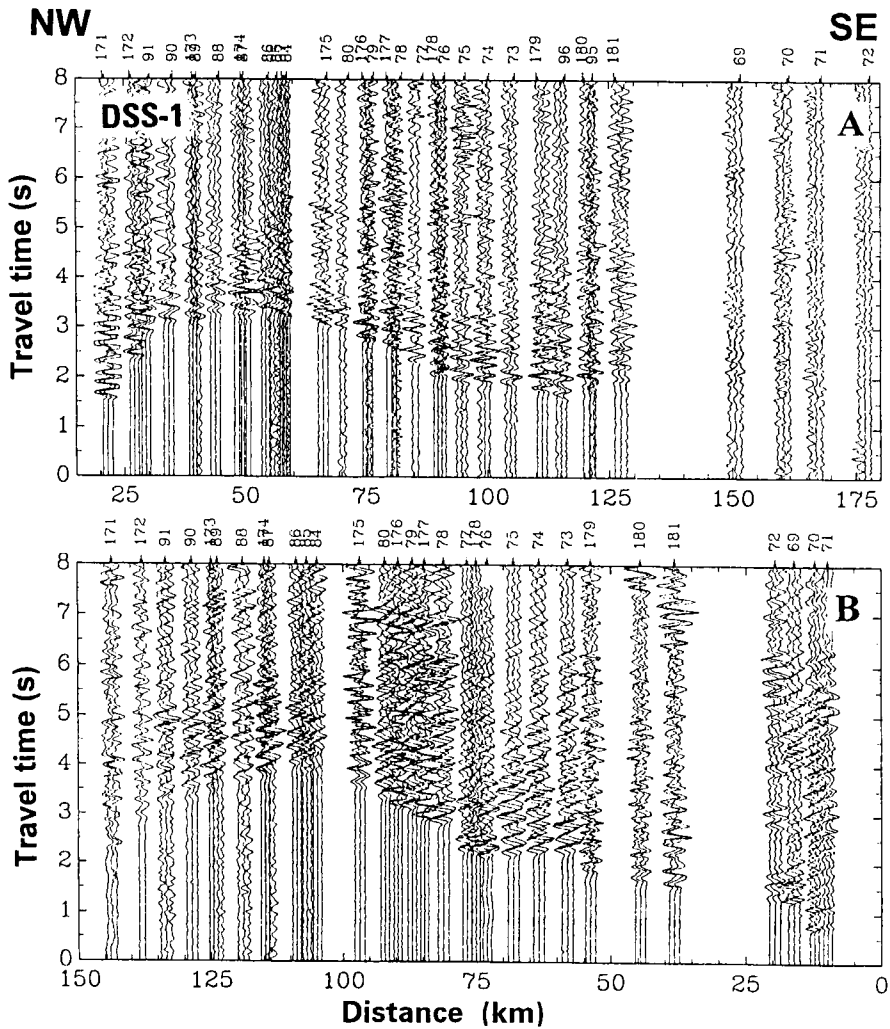


Fig. 14A–B. Examples of seismic record sections for profile DSS-1: A – for King George station, B – for Hope Bay station. ‘Hand normalized’ with filtration 5–15 or 2–10 Hz. Reduction velocity 7.0 km/s.

middle one which transected semi-obliquely the Bransfield Strait between the stations AP and HB, about 170 km apart from each other (Fig. 11). 14 shots, 50 kg TNT each, were detonated at this distance. The section from the station HB was supplemented with records nos 67 and 68 located on the line of the profile but collected during the first expedition. Similar wave field is presented by record sections from the neighbouring stations HM and OH, respectively but, as not located on the profile, they call for individual modelling. Profile DSS-17 begins in the Drake Passage and therefore, distance starts at 135 km in the Bransfield part model.

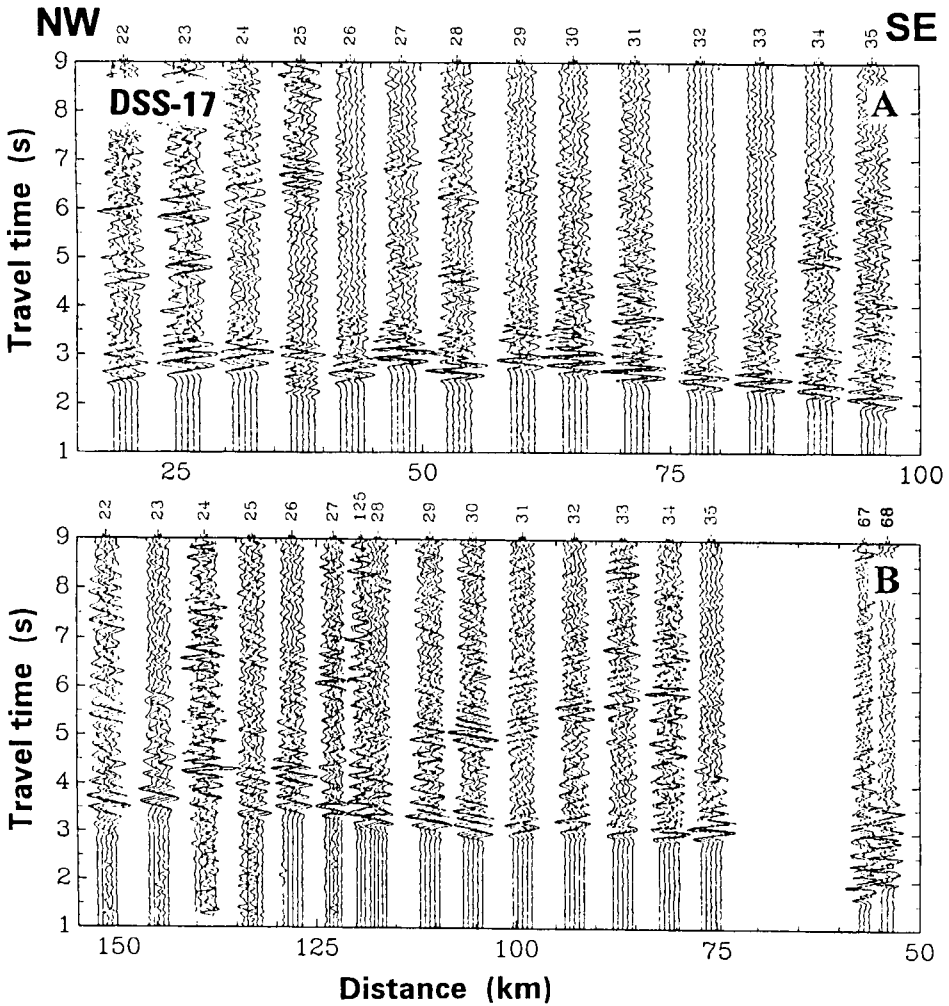


Fig. 15A–B. Examples of seismic record sections for profile DSS-17: A – for Arturo Prat station, B – for Hope Bay station. ‘Hand normalized’ with filtration 5–15 or 2–10 Hz. Reduction velocity 7.0 km/s.

Apparent velocities of main wave rows in the first arrivals were determined. There are relatively high apparent velocities from about 6.8 km/s at distance 20–40 km to about 8.3 km/s at distance 60–100 km at record sections AP and HM in the Bransfield Strait (Fig. 15A, C). There is also a distinct reflected wave at distances 50–100 km, occurring about 1–2 s after the first arrival. Both sections indicate typical strong disturbances of wave correlation in first arrivals at distances 35–50 km. Distinct wave acceleration of about 0.5 s in this area indicates presence of a high velocity seismic wave body in the upper part of the Earth’s crust. It occurs along the section at distance 165–180 km what corresponds to a middle part of the

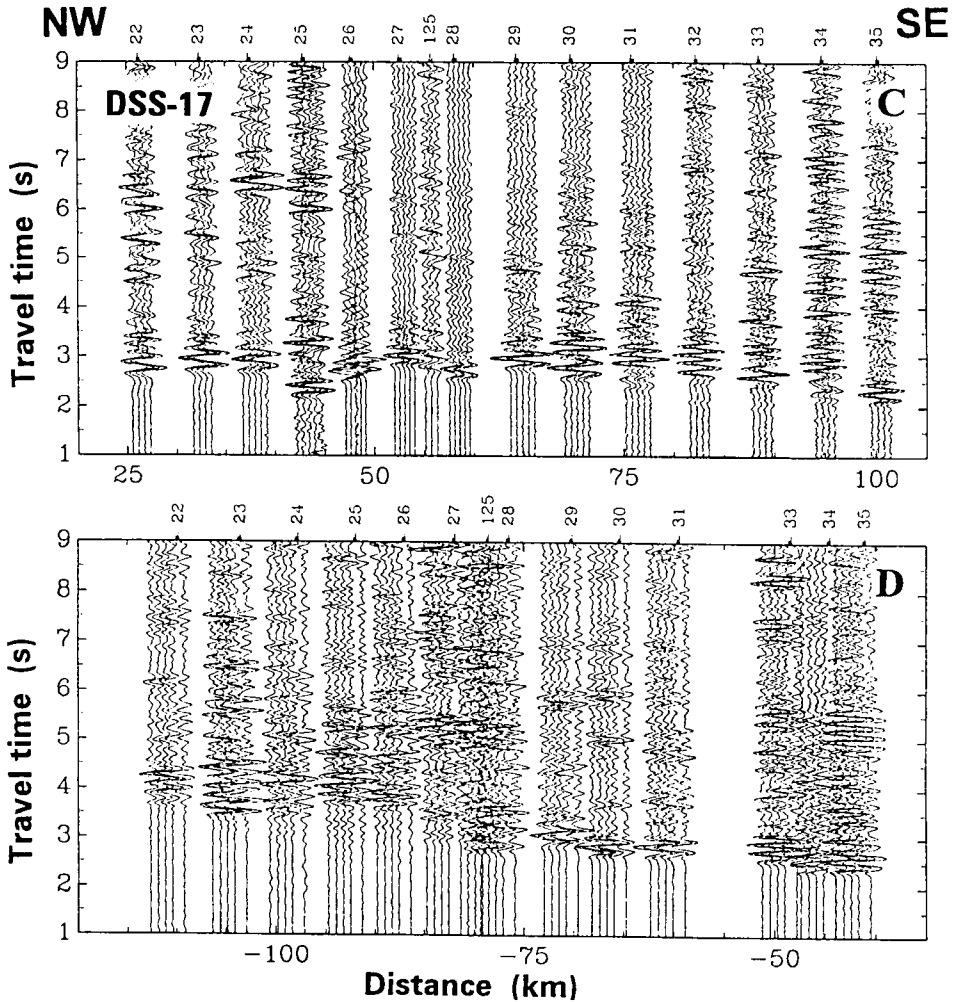


Fig. 15C–D. Examples of seismic record sections for profile DSS-17: C – for Half Moon station, D – for O’Higgins station. ‘Hand normalized’ with filtration 5–15 Hz or 2–10 Hz. Reduction velocity 7.0 km/s.

central basin (Grad *et al.* 1993a, b). Apparent velocities at recorded sections at the stations HB and OH (Fig. 15B, D) are considerably smaller and equal to about 6.9 km/s at distance 75–110 km and about 7.4 km/s at distance 140–155 km, respectively. Such considerably varying apparent velocities are influenced by floor topography (from depths about 100 m on shelves to about 1500 m in the Bransfield Basin) and inclination of seismic discontinuities in the upper crust. Apparent velocities 8.3 km/s and 6.9 km/s for reverses branches indicate high real wave velocities over 7.0 km/s. Strong disturbances of wave correlation at first arrivals in the middle part of the central basin are also observed. Very distinct reflection

wave PmP can be observed at the section from HB at distance 80–150 km, the best noted during the measurements.

The seismic section from OH is partly similar to the sections from the station HB (strong first arrivals of waves and similar apparent velocities) but other features are different, being in turn similar to the ones along profile DSS-3 from the station HB, indicating strong smoothing of the first wave arrivals at distance 85 to 115 km. The following strong pulses of the wave PmP(?) and abundant next arrivals can be hardly clearly correlated.

Seismic record sections along profile DSS-3. — Measurements along profile DSS-3 that cross obliquely (about 45°) the Bransfield Strait between the stations DC and HB, and is about 190 km long, were carried out during the first expedition (Fig. 11). Wave fields for these two stations are considerably different (Fig. 16A–B). Recording conditions at the station DC (volcano) were not good due to high level of noise. Apparent velocities of the first arrivals of waves, distinct to distance of 100 km, change from 4.5 km/s at about 25 km, through 6.3 km/s at 70 km to 7.8 km/s at 100–120(?) km. Except for the first arrivals, there is a wide wave field with high amplitude arrivals that cannot be however correlated. Any waves are hard to be distinguished at larger distances.

Wave field from the seismic record section for the station HB (Fig. 16B) is completely different. Apparent velocities for the first record, at distance 50–105 km from the station, are large and equal about 7.1 km/s, after which there is strong attenuation of seismic energy as far as to 145 km. First arrivals of waves are considerably weaker, indistinct and located about 1 s upwards if compared to the previously presented ones. Besides, there are numerous wave arrivals with high amplitudes and apparent velocities, similar or smaller, with the times to 3 s longer than the ones of the first arrivals of waves. At distance from 125 km to 180 km there are strong wave arrivals, interpreted as the ones reflected from the Moho discontinuity. It is preceded by weaker arrivals of the wave Pn at distance 160 km. Arrivals of the wave PmP initiate a whole set of waves to the following 2–2.5 s, with high amplitudes at the section.

Seismic record sections along profile DDS-4. — Relatively the worst data come from profile DDS-4, along which measurements were done during the first expedition. The profile runs between the stations LV i PV, crossing the station DC (Fig. 11). Fragment of the section between the stations LV and DC corresponded to profile DSS-19 (Grad *et al.* 1992). These materials were used in modelling of profile DDS-4, records along which were done at the stations DC and PV. 14 shots, 25 kg TNT each were fired on northern part of the profile (total length about 165 km) only, except for the Deception Island. Additional records from shots (4,122) on other profiles that transect profile DDS-4, were also included (Fig. 17A–B). The section from the station DC (similar in its wave

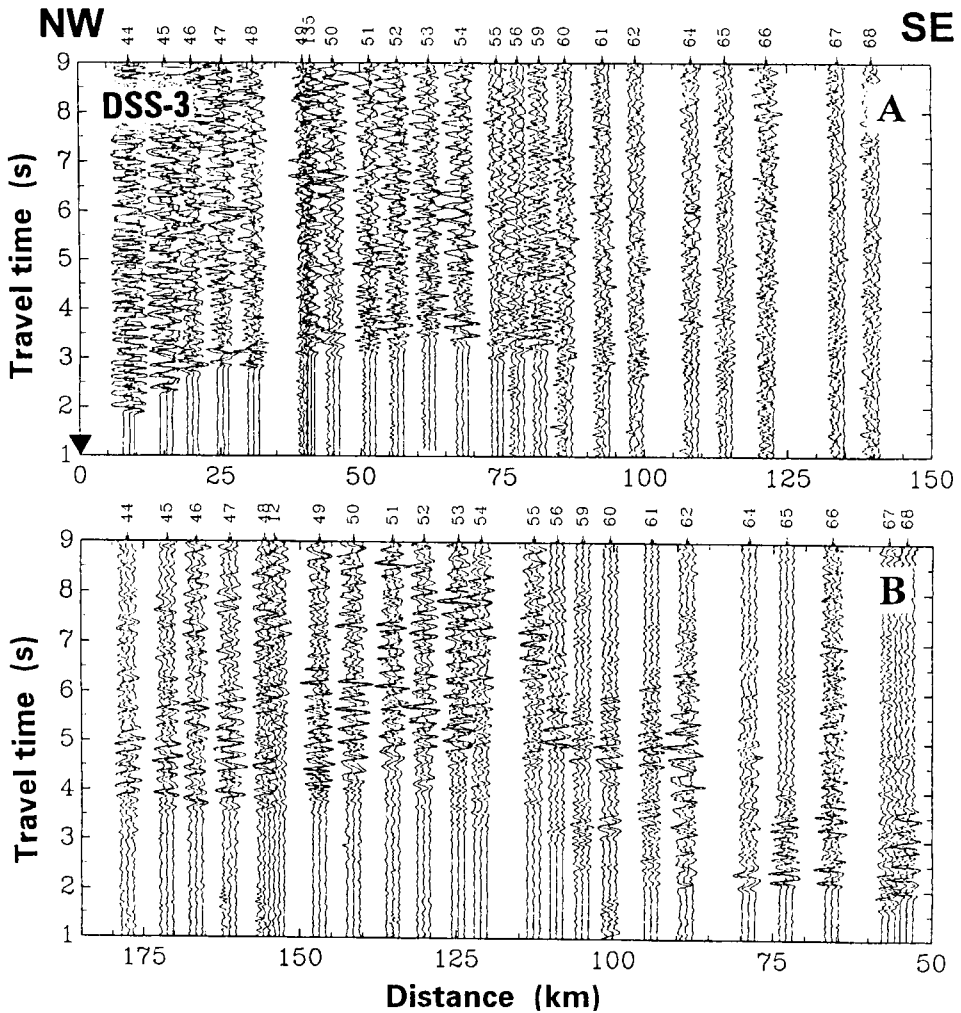


Fig. 16A–B. Examples of seismic record sections for profile DSS-3: A – for Deception station, B – for Hope Bay station. ‘Hand normalized’ with filtration 5–15 Hz or 2–10 Hz. Reduction velocity 7.0 km/s.

field to the one from profile DDS-3) enables correlation of the first arrivals of waves to distance of 35 km as it can be easily distinguished with apparent velocity slightly over 7.0 km/s to the north of the station DC and about 6.7 km/s to the south of it. At further distances (40–60 km to the south), correlation of the first arrivals moves about 0.5 s upwards and apparent velocity increases to 7.0 km/s. Except for first arrivals of waves, there are abundant high amplitude waves which cannot be easily correlated.

Seismic record section from the station PV (six-channel record) is slightly better than the one from the station DC. There are distinct first arrivals of waves

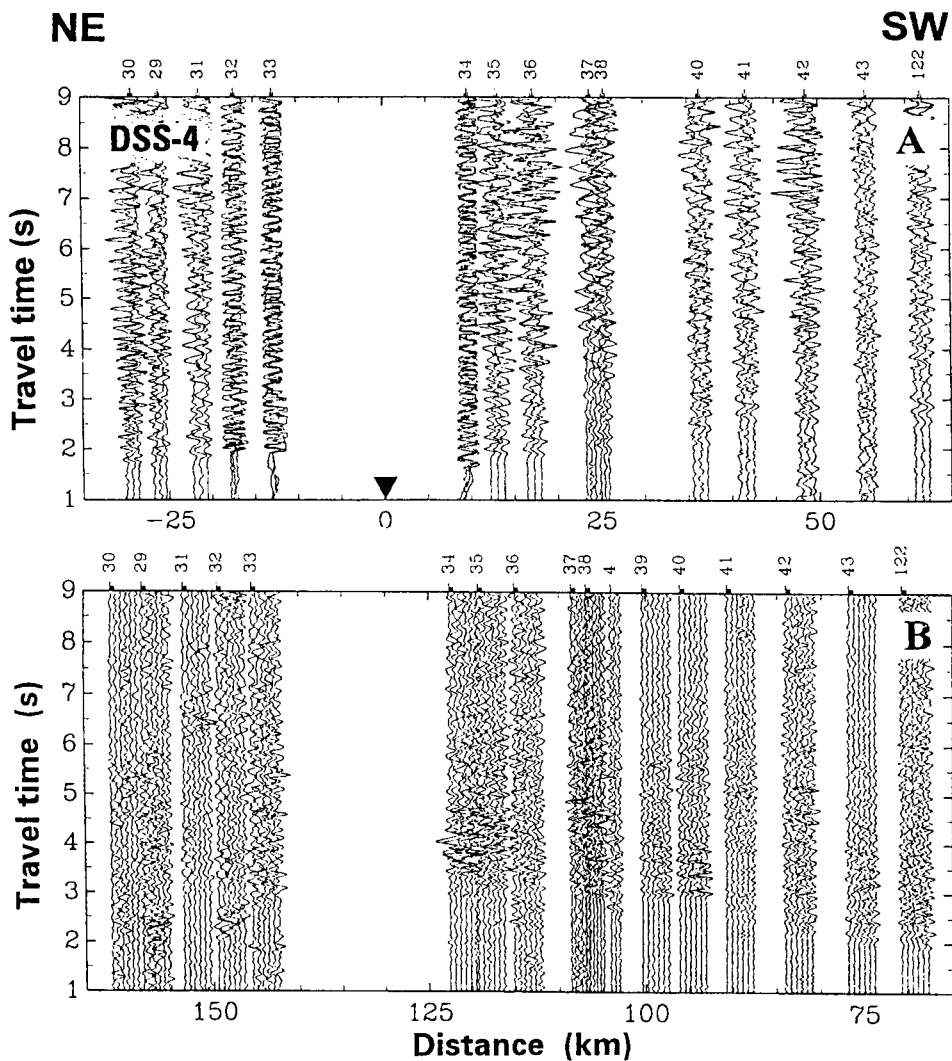


Fig. 17A–B. Examples of seismic record sections for profile DSS-4: A – for Deception station, B – for Primavera Station. ‘Hand normalized’ with filtration 5–15 Hz or 2–10 Hz. Reduction velocity 7.0 km/s.

with apparent velocity 5.7 km/s at distance 70–90 km, and 7.0 km/s (moved 0.5 s upwards) at distance 95–125 km. Correlation of the latter wave is presumably continued after a break in the section (Deception Island) at distance 145–155 km, but these wave arrivals do not need to be the first ones. They are preceded by numerous strong arrivals, among which there is correlation of deeper waves or they can be just disturbances. At distances 70–100 km there are, at the next arrivals, numerous rows of waves with strong amplitudes, running parallel to the correlated first arrivals (similarly as profile DDS-17 at the station OH). 0.5–1.5 s

after the first arrivals there is concentration of waves at distances 105–120 km, and they can be connected with reflection from the Moho discontinuity. These as well as other disturbances at nearer records, can be connected with fracturing at any glacier in the vicinity of the station PV.

Bubble effect and reverberations. — Marine investigation in the Bransfield Strait was carried through in the area with very complex geological structure, in waters with considerably varying depth and difficult navigation. Review of profile DDS-20, in our practice the first section with records done with use of OBSs, enabled to note effects that could not be noted at the earlier refraction sections in this region, prepared on the basis of the land records only. The first noted effect repeated a first strong arrival at intervals 0.3–0.4 s, with amplitude of similar size and very distinct at all sections from profile DDS-20 to about 120–130 km from a shooting site. It was not so regular at further distances but can be occasionally distinct. The second effect repeated first arrivals at intervals from about 0.6 s to almost 2 s, and this happened many a time. Such phenomenon is less or more distinct at all sections from profile DDS-20. There is also the first additional effect to be noted at several multiple repeats *i.e.* double arrival at interval about 0.3–0.4 s.

All these data confirm immense influence of alternating, many a time reflected waves for experiments in a sea, and also reverberations and bubble effect on wave field in a seismic record section. Such conclusions demand great care when correlating the next-by-first arrivals of waves.

Good-quality seismic sections at multiple covering, subjected to 2-D modelling, enable high accuracy model construction (velocity ± 0.10 km/s, depth ± 2 km) for the best documented areas. Reliability of these results increases if there is network of transecting sections. In case of poor or incomplete experimental material, we are obliged to accept certain primary assumptions and it results in more numerous solutions than in case of the most complete and excellent material. Simplicity of a solution is also a criterion that should be taken into account: the more simple model performs a kinematic solution, the better it is.

1-D and 2-D models of the Earth's crust structure in the Bransfield Strait. — First elaborations of the collected experimental materials were based mainly on 1-D modelling as auxiliary tool in examination of the Earth's crust structure (Guterch *et al.* 1985, 1990, 1991). The first 2-D model was prepared for profile DDS-1 (Guterch *et al.* 1985, 1990, 1991). It made interpretation of the wave with apparent velocity of 7.6 km/s (section with KG) possible, as coming from the HVB ($V_p = 7.2$ km/s) at depth of 10 km. 1-D models were taken into account for construction of the section with geological interpretation. The paper of Grad *et al.* (1993a) was the first case when exclusively 2-D modelling was used to describe structure of the Earth's crust (along profile

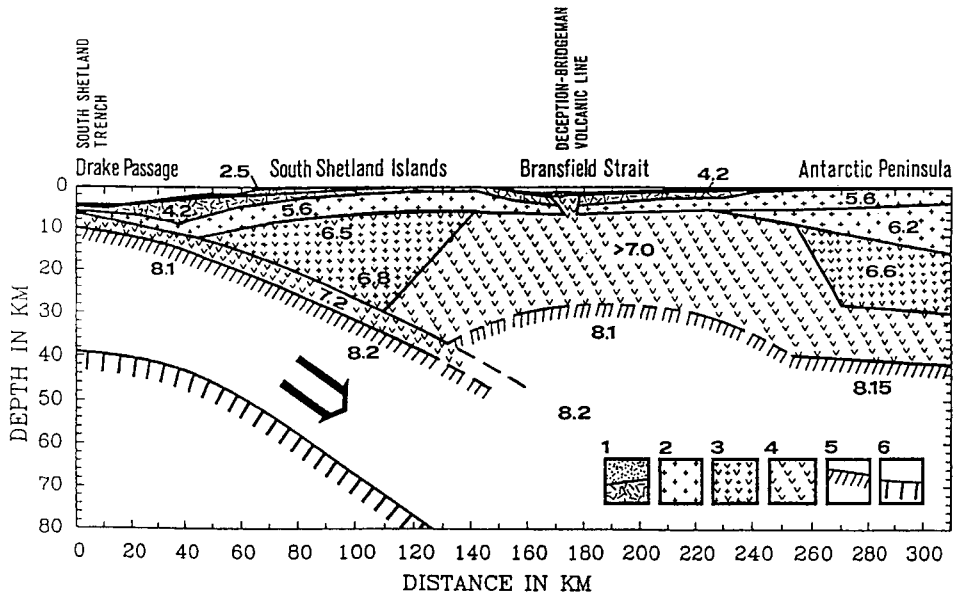


Fig. 18. Seismic model of the lithosphere along profile DSS-17 between Drake Passage and Antarctic Peninsula. (1) sediments $V_p = 2.5\text{--}4.2$ km/s; (2) upper crust, $V_p = 5.4\text{--}6.3$ km/s; (3) middle crust, $V_p = 6.4\text{--}6.8$ km/s; (4) lower crust and high velocity body in Bransfield Strait, $V_p > 7.0$ km/s; (5) Moho boundary, $V_p > 8.0$ km/s; (6) reflection boundary in the lower lithosphere (after Grad *et al.* 1993a, b).

DDS-17). It enabled presentation of a subduction model under the South Shetland Islands, cited later in many papers (see Fig. 18).

New results, very good records along the whole profile DDS-20, collected during the fourth expedition, enabled detailed modelling of the Earth's structure, considerably more precise than at earlier sections. In this paper, 2-D seismic models are presented for five selected sections. Four of them, 150 to 190 km long, cross main structures of the Bransfield Strait and the fifth, connecting the other ones, 310 km long, runs along the Bransfield Rift. Finally, mutually concordant 2-D models for these profiles were received. During modelling, seismic ray tracing in 2-D models with curvilinear boundaries and complex velocity distribution were applied (program SEIS83 – Červený and Pšenčík 1983, Komminaho 1993).

Modelling along profile DDS-20. — Modelling was based on correlations at seismic record sections for five OBSs. A single model was obtained which solves a kinematic task for them all, with accuracy 0.1–0.2 s (Fig. 19; Grad *et al.* 1997a, b). The successive step was to receive synthetic seismograms and to adjust their amplitude relations to experimental seismic record sections (Fig. 19A). Sections with real amplitudes enabled modelling of body parameters, taking into account their influence on amplitude relations of a wave field. Variant

of the program SEIS83, named SEISOBS was used (Hirata and Shinjo 1986) to calculate sections of synthetic seismograms, at which location of a receiver at sea floor was considered. Resulting synthetic seismograms indicate good quality concordance with noted amplitudes of the main rows of refracted and reflected waves.

Calculated variants of model for profile DDS-20 are presented (Fig. 21A–C). Basing on the previously cited papers of the authors: Ashcroft (1972), Jeffers *et al.* (1991), and on seismic refraction data, velocity of the wave P was estimated in a sedimentary bed for the just presented models. Under a water column ($V_p = 1.46$ km/s) that, as we already know, can be from several dozen to over 2000 m deep, there are poorly consolidated, recent sediments with seismic wave velocities equal to 1.9–2.3 km/s. Next bed with velocities 3.5–4.0 km/s contains probably older, better consolidated sediments and pillow lavas. There are two beds with velocities 5.2–5.8 km/s below a sedimentary cover which are typical for metamorphic and acid crystalline rocks. They mantle rocks of a proper crystalline bedrock, with velocities 6.4–6.9 km/s. Below a body with velocity 6.4 km/s, at depth 2–4 km close to the station HB, a zone with lower velocities was detected. It seems to act as continuation of the earlier bed (with $V_p > 5.2$ km/s). The HVB with $V_p > 7.4$ km/s is the main element of the model, discovered between 80 and 250 km of the profile at depth about 14–15 km. It indicates high vertical velocity gradient, at depth equal to 22 km $V_p = 7.7$ km/s. In a southeastern part of the model, at depth 20 km, the second bed of crystalline bedrock was detected with velocity 7.3 km/s. Beneath the HVB, the Moho discontinuity was discovered at depth 30–32 km. Modelling detected a large fracture between 100 and 120 km of the profile, close to its junction with profile DDS-17. After calculation of 2-D models for profiles DDS-1, DSS-17, DSS-3 and DSS-4, their mutual correction could be done at profile junctions (indicated by arrows at the models). Obviously, significance of information from profile DDS-20, as the longest profile with a most complete shot-recording scheme, is considerably greater than information from the other profiles. Models from earlier papers must have been therefore reconstructed when information at junction with profile DDS-20 could be available. Not only data from the model along profile DDS-20 influenced changes at the others but the opposite action was possible too. In case of profile DDS-20, most significant changes occurred at junction with profile DDS-3. Extents of the HVB were enlarged southwestwards what is clear when comparing the presented model (Fig. 21A) with a new one (Fig. 21B). Introduced changes did not disturb coincidence of kinematic solutions and synthetic seismograms for the model. Another possible contact of the HVB with the upper mantle was also tested. Applied was delimitation of the HVB from the bottom and introduction of a thin bed with slightly lower velocity ($V_p = 7.35$ km/s) (Fig. 21C). Such solution is suggested by data from profile DDS-17, and this model correctly executes kinematic solution. Sections of

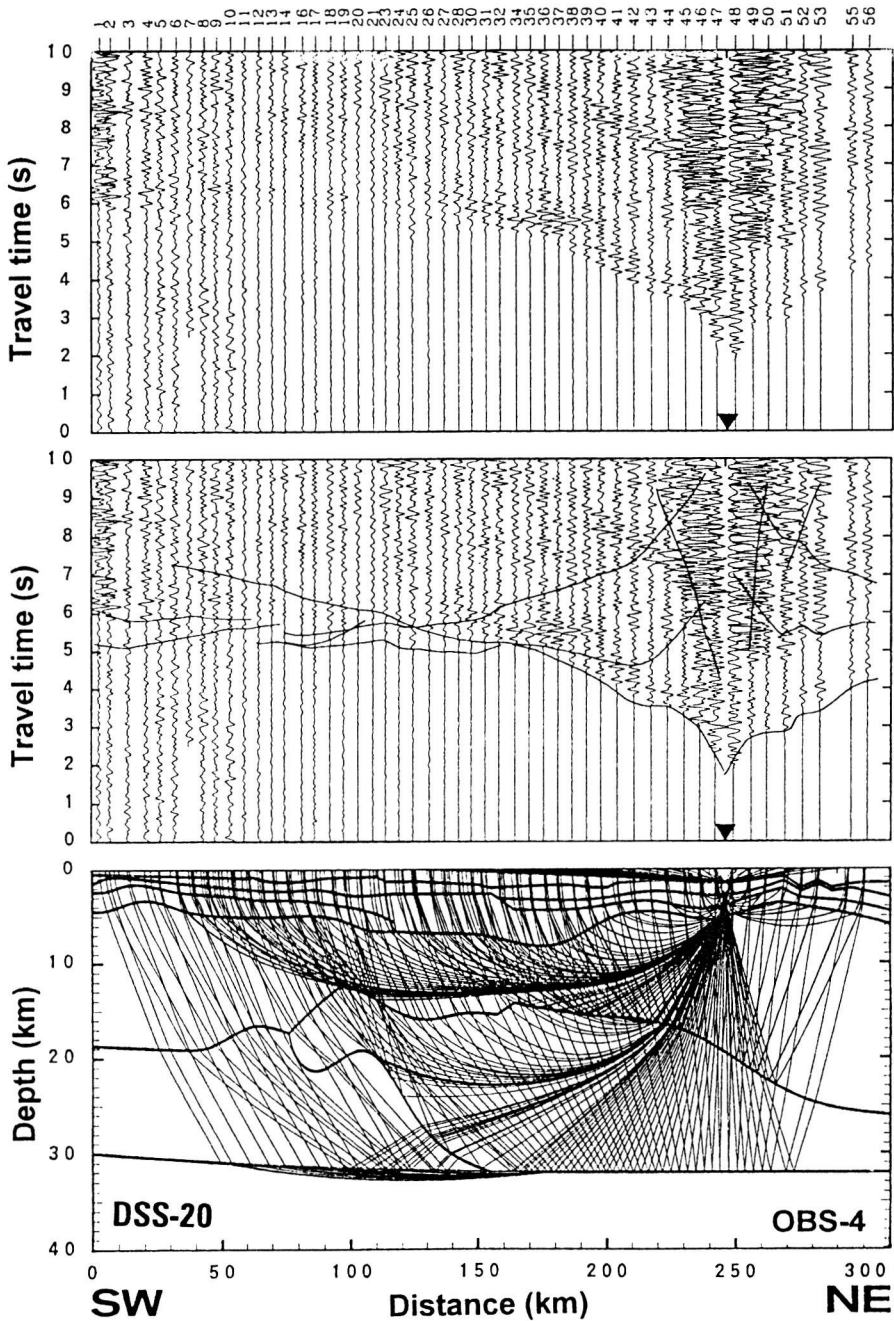


Fig. 19. Kinematic modelling of the crustal structure along profile DSS-20. 'Hand normalized' record section (upper diagram), seismic record section with theoretical traveltimes of the main waves (middle), and model of the structure with selected rays (floor) for OBS-4. Reduction velocity 8.0 km/s (after Grad *et al.* 1997b). See model from Fig. 21A.

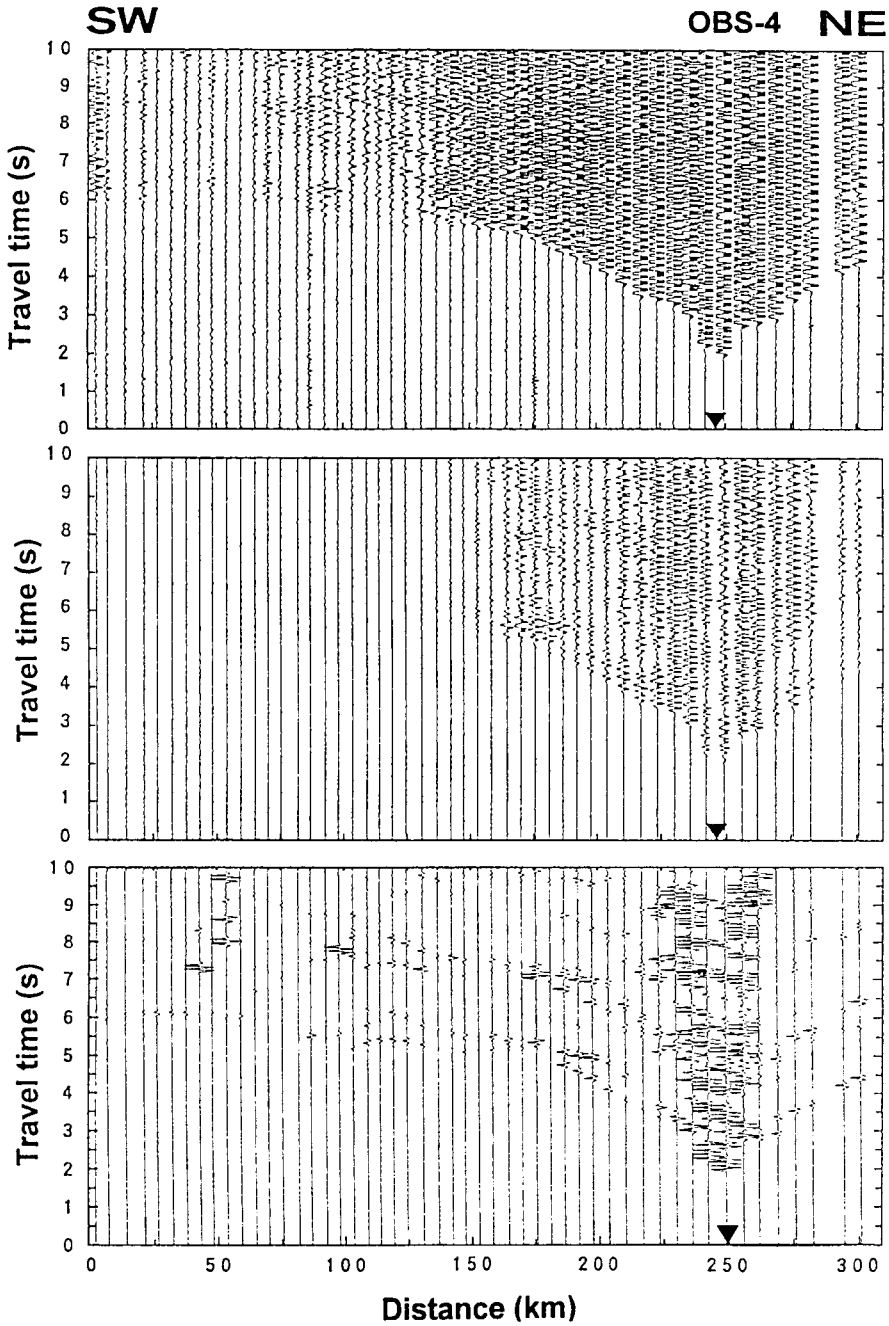


Fig. 19A. Observed seismic section normalized with distance: high gain (upper diagram), low gain (middle) and synthetic seismograms (floor) for profile DSS-20, OBS-4. Synthetic seismograms calculated for P, S and selected converted wave, also with reverberation but without bubble effect. Reduction velocity 8.0 km/s.

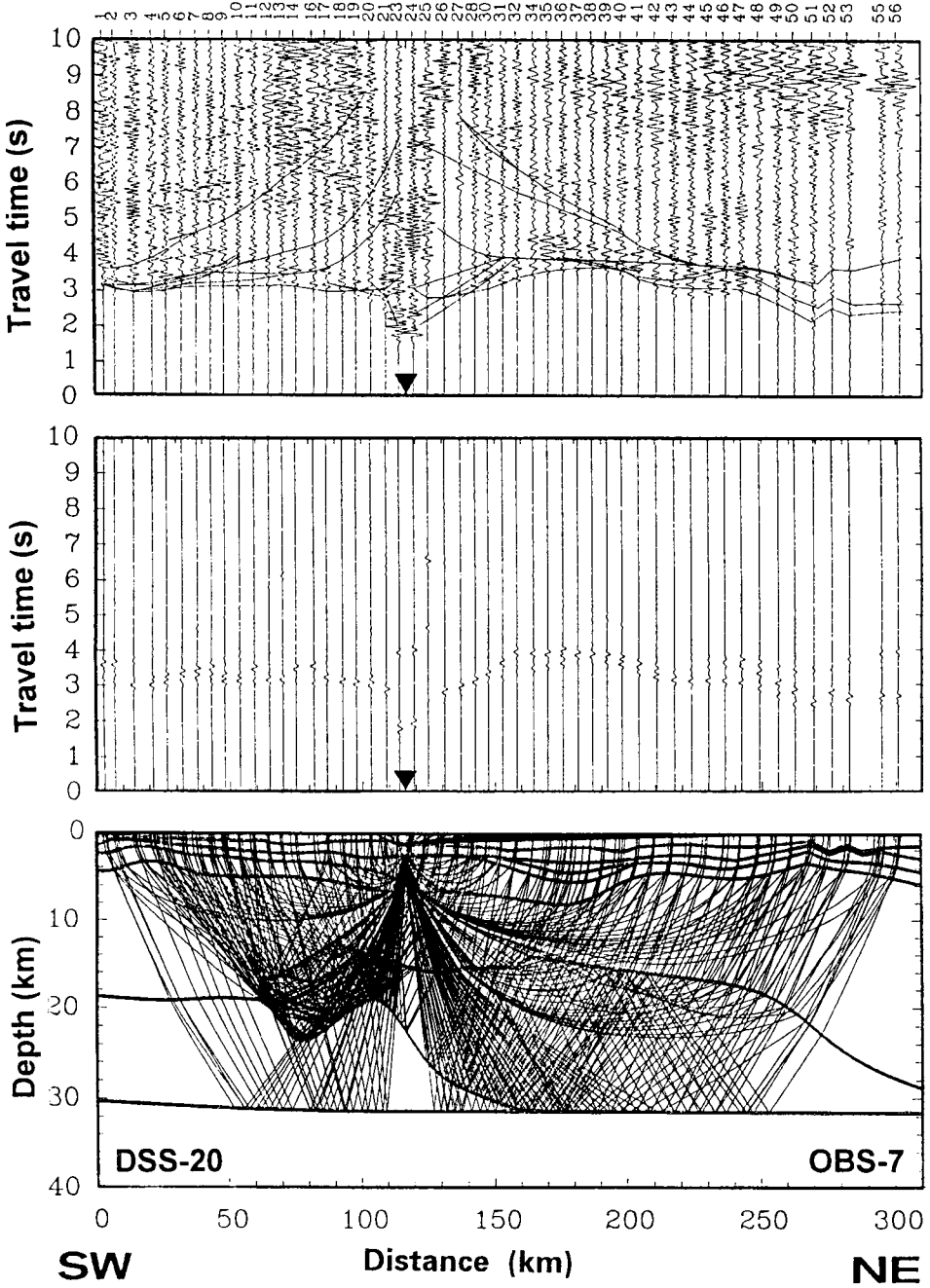


Fig. 20. Final variant of two-dimensional modelling of the crustal structure along profile DSS-20. Seismic record section with theoretical traveltimes of the main waves (upper diagram), synthetic seismograms (middle diagram) and model of the structure with selected rays (floor) for OBS-7. Reduction velocity 7.0 km/s. See model from Fig. 21B.

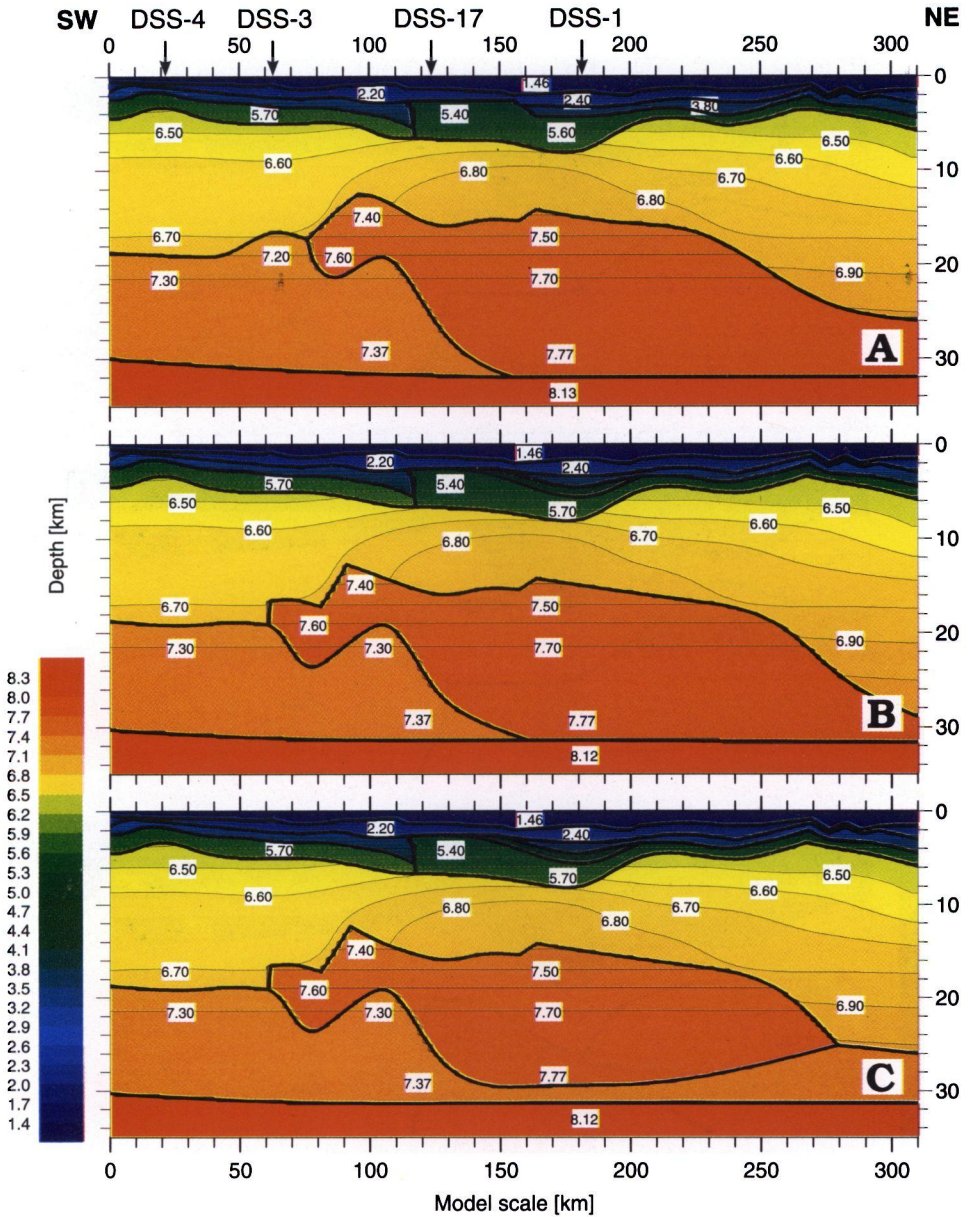


Fig. 21A–C. Variants of crustal velocity model along the Bransfield Rift, profile DSS-20. Thick lines: first order discontinuities; thin lines: P – wave velocity contours (in km/s), arrows indicate junction places with other profiles. Variant A after Grad *et al.* 1997a, b.

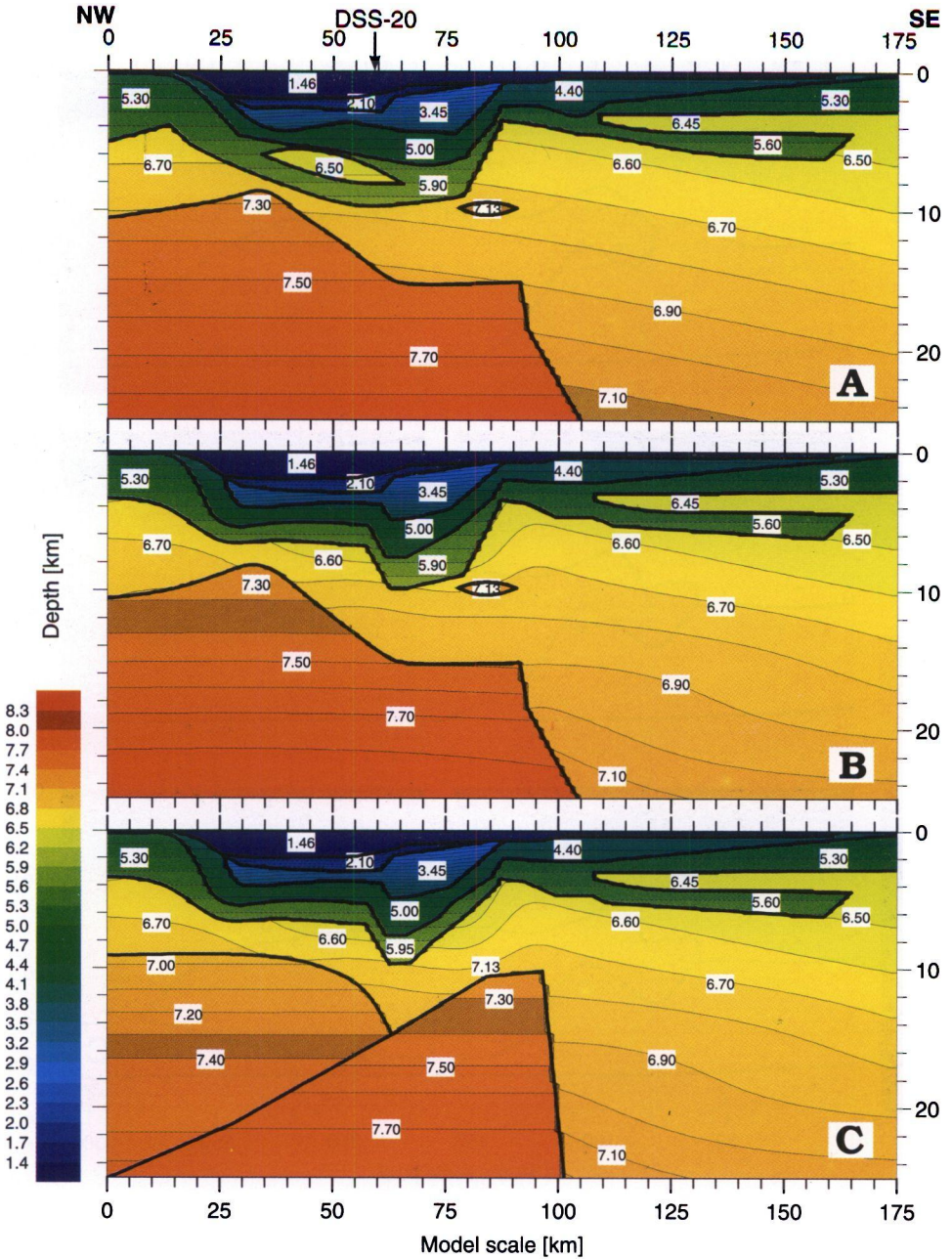


Fig. 24A–C. Variants of crustal velocity model across the Bransfield Rift, profile DSS-1. Thick lines: first order discontinuities; thin lines: P – wave velocity contours (in km/s), arrows indicate junction places with other profiles.

synthetic seismograms are not practically different from the ones of the previous solution, although both solutions (Fig. 21B–C) have been calculated with a use of the program SEIS83 instead of SEISOBS. As a final, the variant from Fig. 21B was taken. Example of 2-D modelling for this variant for OBS-7 is presented (Fig. 20).

Modelling along profile DDS-1. — Modelling at this profile has a longest history. 1-D modelling and the first 2-D model with a use of records from land stations only were presented by Guterch *et al.* 1980, 1990, 1991. A new model could be constructed with new sections from OBS-5 and OBS-6, and a dozen of records from the auxiliary land stations. Several new models were formed that complied requirements of received theoretical and experimental travel times as well as sections of synthetic seismograms (Figs 22–23). If compared with the earlier model, information of new models from OBSs data enabled changes in configuration of the main sedimentary basin and its maximum depth increased from the 6 to 10 km. Besides, a lower velocity zone (LVZ) was determined at depth 4–6 km what is to be also defined as intrusion of a high velocity body ($V_p = 6.4$ km/s) into a lower velocity bed ($V_p = 5.7$ km/s). Two small bodies with higher velocity V_p if referred to the surrounding sediments, were also detected (Fig. 24A). One of them with velocity $V_p = 6.4$ km/s, is located at depth 5 km, between 35 and 65 km of the profile. The second body with velocity $V_p > 7.2$ km/s, at depth 8 km at 85 km of the profile, is originally connected probably with the main high velocity body of the profile, located in its various fragments at 10–15 km and reaches depth of at least 20 km. Large the HVB occupies a distance about 100 km of the profile. Shape of the upper boundary of the HVB was considerably modified. When data from a junction with profile DDS-20 were received, another model could be presented (Fig. 24C). Borders of the main sedimentary basin and the anomalous body were somewhat modified and a small, isolated the HVB disappeared after incorporation into the underlying beds. Velocities in the HVB have also changed and the body was divided into two parts: the first one closer to the South Shetland Islands, with velocity $V_p = 7.0$ – 7.5 km/s, and the second in centre of the rift, with velocity 7.2–7.7 km/s at depth 10–20 km.

The third solution was also calculated (Fig. 24B), as a transitional one between the two described previously. As already mentioned all three solutions, different from one another, are the models that perform kinematic and dynamic task (synthetic seismograms) similarly well. Examples for the models A and C for the stations HB are presented (Fig. 22). Synthetic seismograms for the model A were calculated with a wide pulse, generated from a source and simulating a bubble effect, and for the model C – with a normal arrival (Fig. 23). Basing on modelling along profile DDS-1, development of the model can be observed, starting from a primary stage, being very general (1-D models) to the most

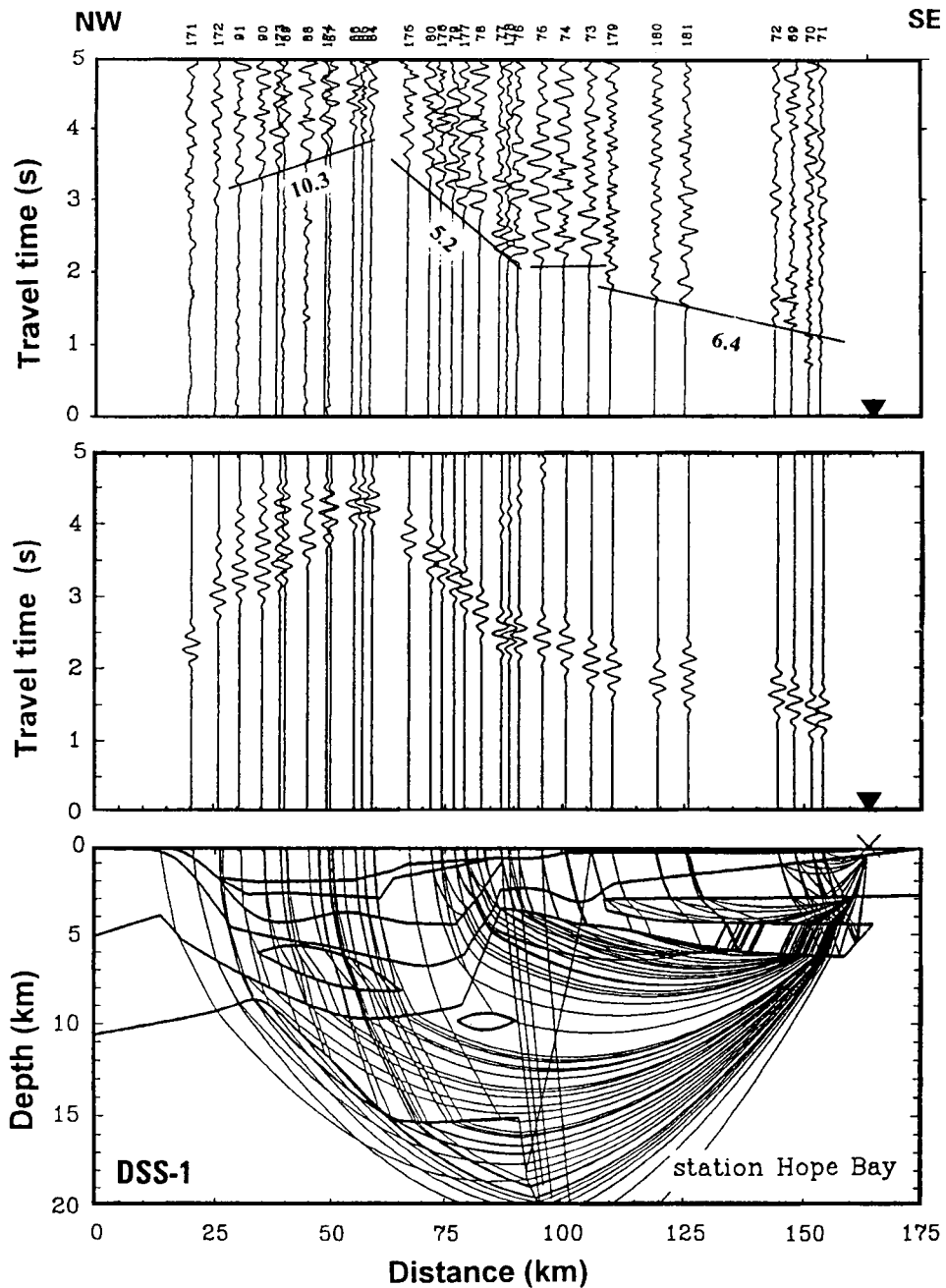


Fig. 22. Variant of two-dimensional modelling of the crustal structure along profile DSS-1. Seismic record section with theoretical travel times of the main waves (upper diagram), synthetic seismograms (middle diagram) and model of the structure with selected rays (floor) for Hope Bay station. Reduction velocity 7.0 km/s. See model from Fig. 24A (Janik 1994).

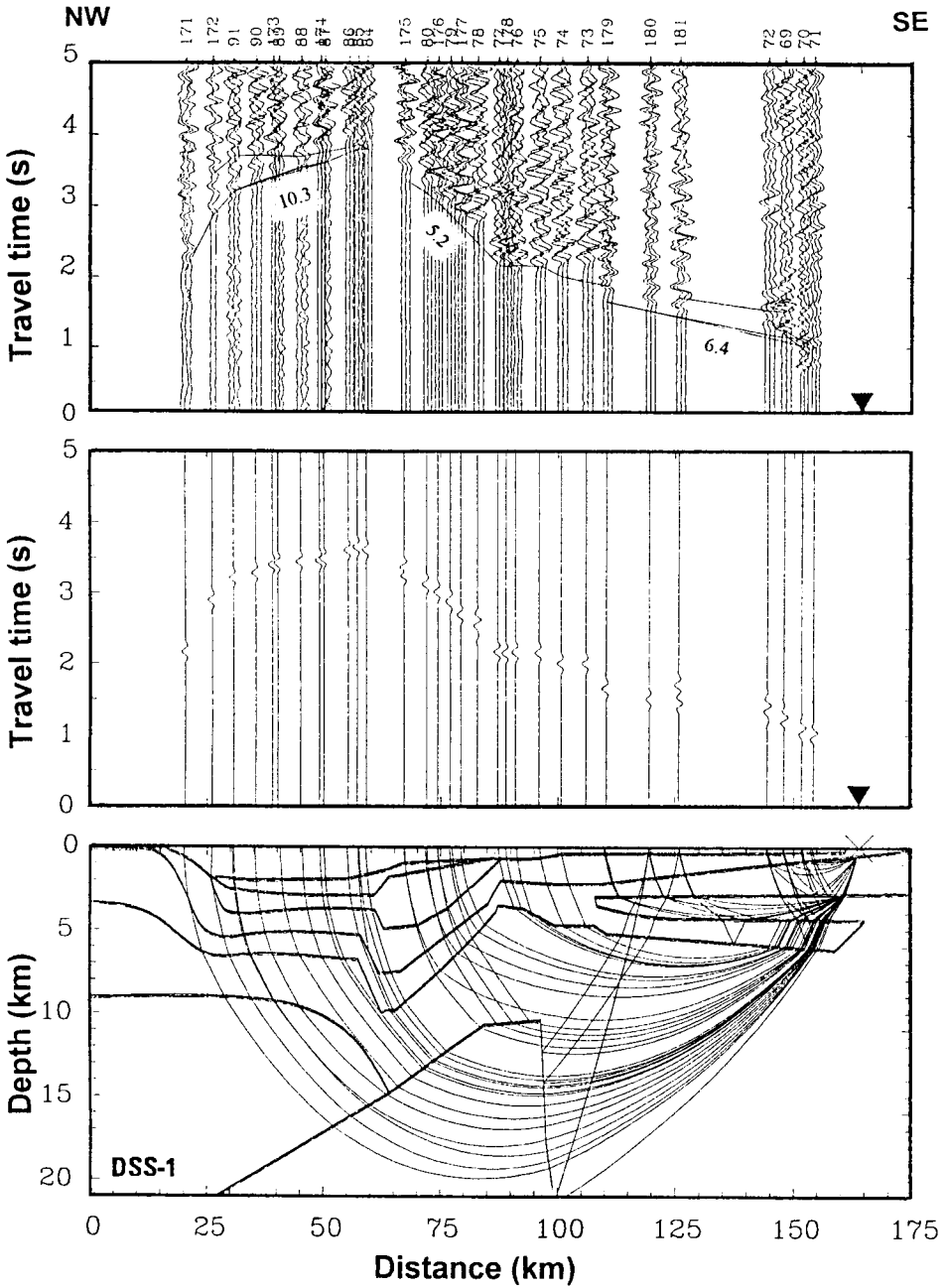


Fig. 23. Variant of two-dimensional modelling of the crustal structure along profile DSS-1. Seismic record section with theoretical travel times of the main waves (upper diagram), synthetic seismograms (middle diagram) and model of the structure with selected rays (floor) for Hope Bay station. Reduction velocity 7.0 km/s. See model from Fig. 24C.

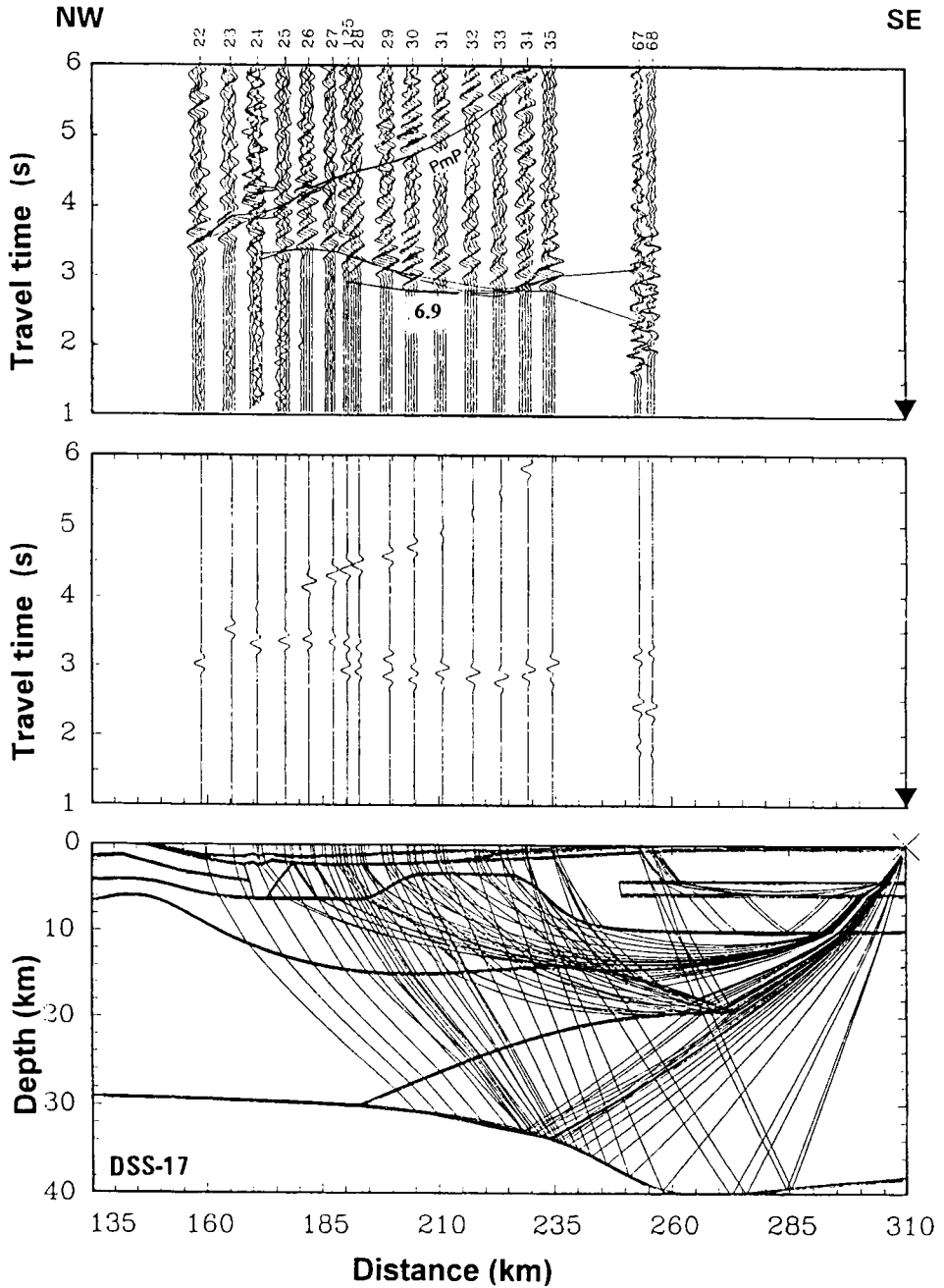


Fig. 25. Variant of two-dimensional modelling of the crustal structure along profile DSS-17. Seismic record section with theoretical traveltimes of the main waves (upper diagram), synthetic seismograms (middle diagram) and model of the structure with selected rays (floor) for Hope Bay station. Reduction velocity 7.0 km/s. See model from Fig. 27A.

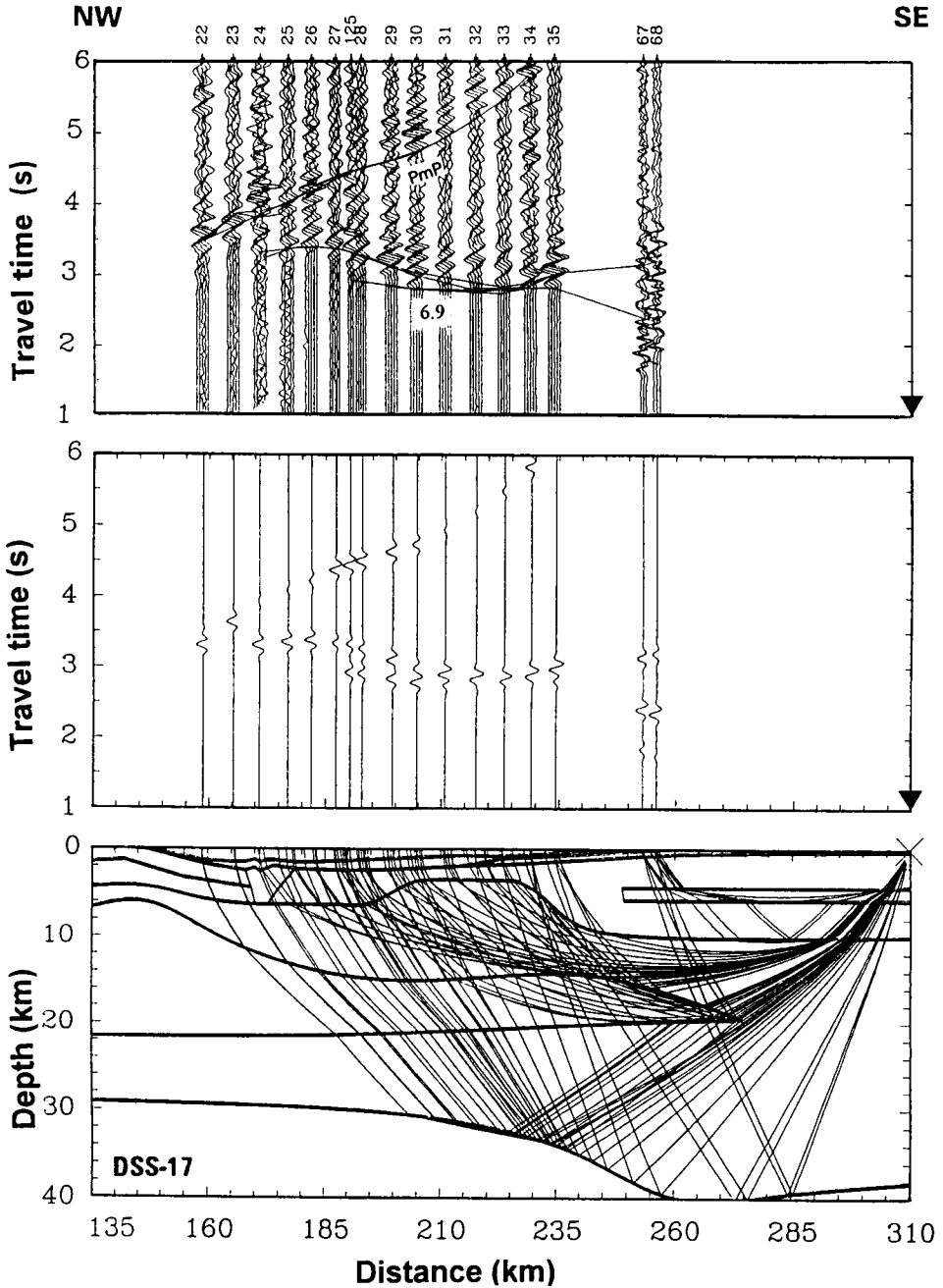


Fig. 26. Variant of two-dimensional modelling of the crustal structure along profile DSS-17. Seismic record section with theoretical travel times of the main waves (upper diagram), synthetic seismograms (middle diagram) and model of the structure with selected rays (floor) for Hope Bay station. Reduction velocity 7.0 km/s. See model from Fig. 27B.

advanced ones (2-D) but still multi-variant. Results of modelling at profile DDS-1 indicate how many factors influence a final effect. Among them, there is very complex geometry of a model including largely varied water depth, numerous inclined discontinuities, intrusions of high velocity bodies, lower velocity zones, shot-recording scheme that does not ensure a complete set of required information in such complex geologic structure, recording stations at large distances from one another, recording that covers the whole section, no reciprocal points for correlated waves. Finally, there is also a wave field itself, reflecting complex geologic structure and effects connected with shots in a sea (bubble effect and reverberations), frequently making other correlation of waves impossible except for their first arrivals. At such considerable discrepancy between real and ideal state, there is a very large group of models that, after accepting many necessary assumptions, perform a kinematic task. There is also a more limited group of models that fit also dynamic requirements. In such situation, every information that can enrich our knowledge about a model is extremely valuable as it delimits number of possible model solutions.

Modelling along profile DDS-17. — Model for profile DDS-17 (Fig. 11) was presented by Grad *et al.* (1993a, b). After supplementing the seismic sections with several records and receiving data from a junction with profile DDS-20, profile DSS-17 was remodelled in its Bransfield part. Results of modelling (Figs 25–26) and models are presented (Fig. 27A–B). Part of the model of a sedimentary cover with a high velocity intrusion from the South Shetland Islands was preserved. Sedimentary cover in the southeastern part of the model (antarctic shelf) has changed, its depth increased to 10 km, with intrusion of a body with velocity $V_p = 6.4$ km/s at depth about 4–6 km, similarly as along profile DDS-1. Beneath metamorphosed sediments(?), there is a crystalline bedrock with velocity $V_p = 6.5$ – 6.7 km/s at depths from 4 to 10 km. The HVB as the main element of the model, was discovered between 140 and 275 km of the profile, slightly more deep (6 to 18 km) than in the previous model, and also greater velocity V_p (7.1 and 7.6 km/s respectively) for these depths. Distinct reflected wave at the station HB is the evidence for a fragment of the Moho discontinuity between 205 and 275 km of the profile, increasing its depth from 30 to 40 km when moving from the axis of the strait towards the Antarctic Peninsula. Our data do not enable detailed determination of the depth of the HVB. Presented (Fig. 27A–B) alternative solutions indicate different thickness of the HVB. In one of the models (Fig. 27B), the HVB reaches maximum depth 22 km and is separated from the Moho discontinuity by a bed with velocity $V_p = 7.1$ – 7.3 km/s. In another case (Fig. 27A), the HVB reaches the Moho discontinuity directly, as far as 190 km of the profile. Both solutions seem to be similarly good.

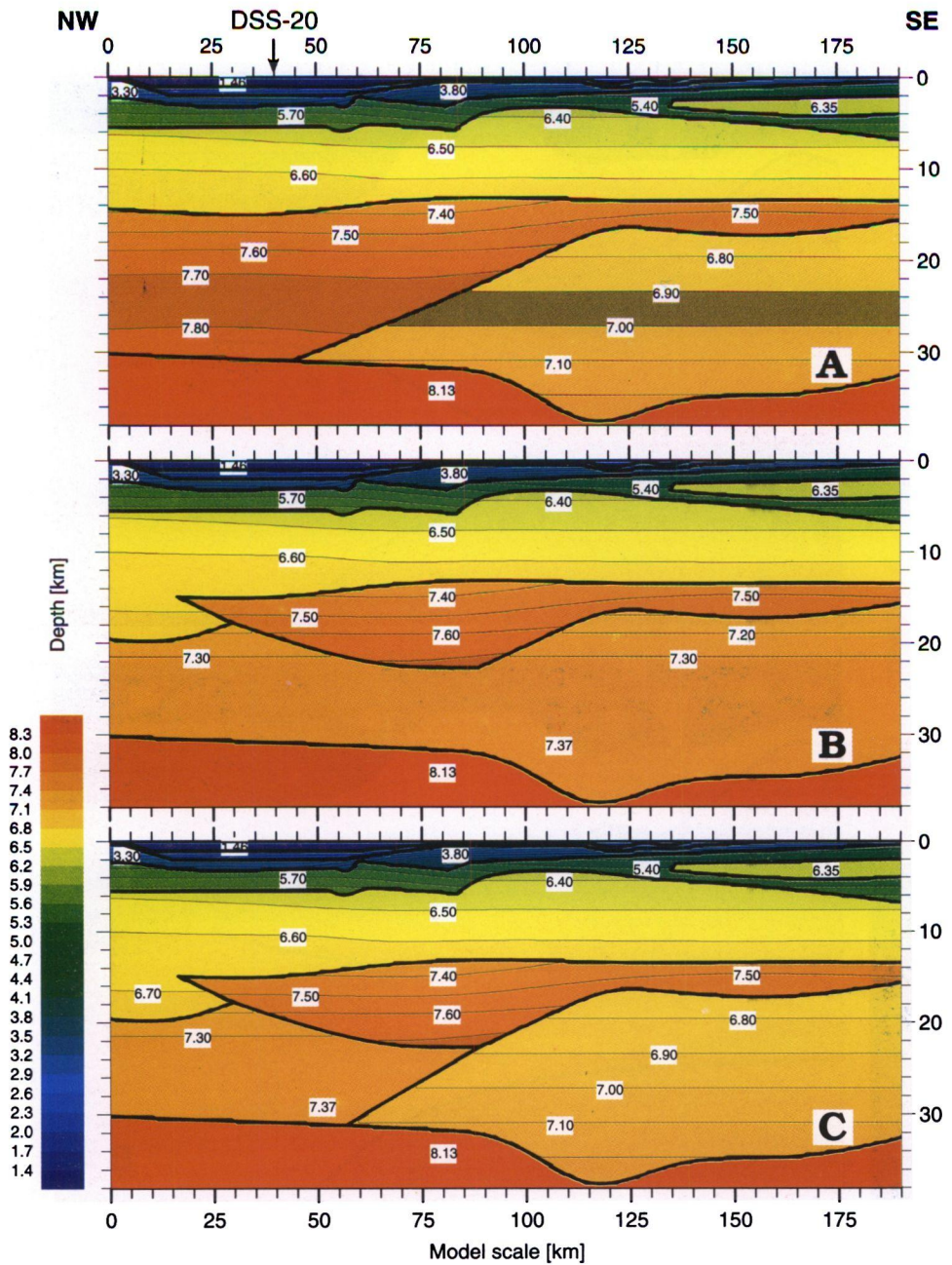


Fig. 28A–C. Variants of crustal velocity model across the Bransfield Rift, profile DSS-3. Thick lines: first order discontinuities; thin lines: P – wave velocity contours (in km/s), arrows indicate junction places with other profiles.

Modelling along profile DDS-3. — For profile DDS-3, only 1-D models were calculated previously (Guterch *et al.* 1985, 1987, 1990, 1991). 2-D modelling resulted in two variants of the lower crust structure (Fig. 28A, C). Sedimentary cover with a subdivision similar as along profile DDS-20, reaches depth to about 6 km and contains typical high velocity intrusion at the side of the Antarctic Peninsula ($V_p = 6.4$ km/s). The bed with velocity 6.4–6.6 km/s spreads almost horizontally, under the bed with $V_p = 5.8$ km/s at depth 6–15 km. In the central part, main element of the model (HVB) is located at depth about 15 km, with $V_p = 7.3$ km/s increasing to 7.75 km/s at depth 25 km. A distinct reflected wave and fragment of a refracted one at the station HB, are the evidence for a fragment of the Moho discontinuity between 55–140 km of the profile at depth 30 to 37 km, increasing from the strait axis towards the Antarctic Peninsula. Similarly as along profile DDS-17, detailed determination of the depth of the HVB does not seem possible for this part of the profile which is close to the South Shetland Islands. On the other hand, the HVB is known to be only several kilometers thick at the side of the Antarctic Peninsula. Associated refracted wave of high apparent velocity ($V_p = 7.0$ km/s), noted at first arrivals at distance from 60 km, rapidly disappears at distance about 100 km. It can be connected with seismic rays in a bed where velocity is lower than in the HVB. As it is the lower velocity bed, shielded from the top' and without representation of arrivals at a seismic section, its velocities cannot be directly determined. Depth of the Moho discontinuity at junction with profile DDS-20 is well known, the same as velocity in the bed between this discontinuity and the HVB ($V_p = 7.2$ –7.35 km/s). There is however a question if a bed with such velocity can be extended to the whole area of the section under the HVB (Fig. 28B). Negative answer is given by a model, formed with such assumption (Fig. 29). It indicates that the velocity, accepted for this bed, is too high at the right side of the model, and the waves PmP and Pn arrive about 0.5 s too early. The next calculated model (Fig. 28C) assumed varying velocities for this depth in two areas in the northwestern part of the profile with a previous velocity 7.2–7.35 km/s and in the northeastern part of the profile where the bed above the HVB continued, with velocities suitable for it at these depths (6.7–7.2 km/s at 16–34 km, respectively). Inconsistency of theoretical and experimental hodographs did not exceed 0.1 s in this model. The model from profile DDS-20 leaves much for interpretation at the junction with profile DDS-3 if a lower boundary of the HVB is concerned. Question is to be put therefore, how much the other model (Fig. 28C) is insensible in this fragment to changing velocities. However, the HVB is delimited from the bottom at its northwestern side to minimum dimensions that enable a correct solution (Fig. 28B–C). Successive model was tested (Fig. 28A), in which the HVB spreads already from a beginning of the model and replaces a previous transitional bed as far as the Moho discontinuity. This model ensures also a satisfactory solution. It confirms the opinion on unclear transition from the HVB to the Moho discontinuity in this part of the profile.

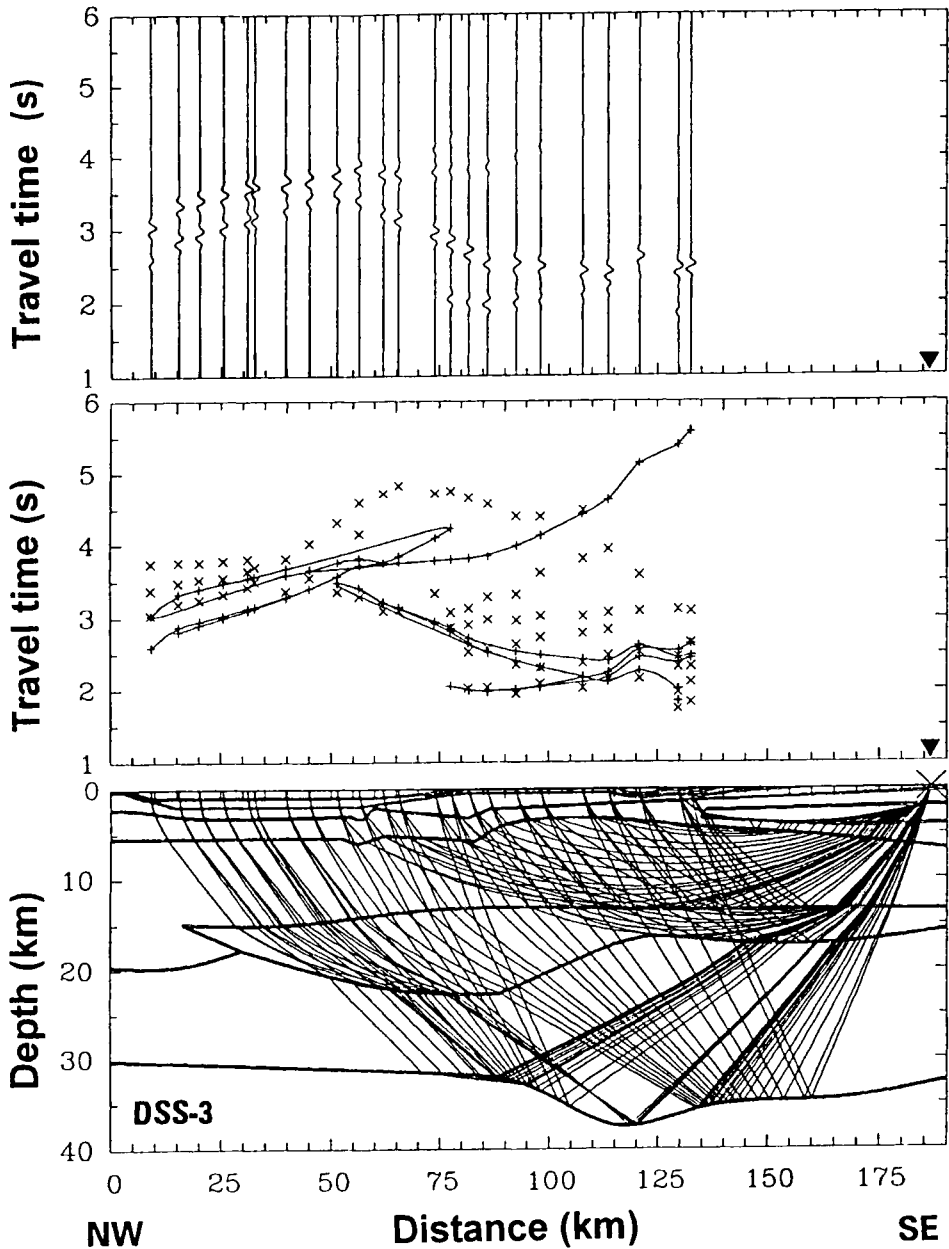


Fig. 29. Variant of two-dimensional modelling of the crustal structure along profile DSS-3. Seismic record section with synthetic seismograms of main waves (upper diagram), comparison of experimental (x) and theoretical (+) travel times (middle diagram) and model of the structure with selected rays (bottom) for Hope Bay station. Reduction velocity 7.0 km/s. Too early arrivals of wave Pn is noted. See model from Fig. 28B.

Modelling along profile DDS-4. — 2-D modelling along profile DDS-4 created two model variants (Fig. 30A–B). One of them was formed in result of calculations for data at both land stations (DC and PV) and the previously mentioned profile DDS-19 (Fig. 30A). Relatively little information from seismic record sections result in high free choice during model construction. The one presented (Fig. 30A) is selected among many others. The other model was created, after information from junction with profile DDS-20 was introduced and considerably smoothed a previous model (Fig. 30B). Branches of travel time recorded at the station DC control a model to maximum depth 6 km and distance 50 km to the north of the station and 25 km to the south of it only. They enabled to discover a sedimentary basin between 70 and 100 km of the profile, and to determine depth of the bed with velocity $V_p = 6.4$ km/s at depth 2–4 km near the station. Records at the station PV enabled to reach considerably deeper and further but unfortunately, without possible detailed recognition of shallow structure of the peninsula, because there is no record as far as 75 km from the station. After extrapolation of a shallower structure of a northern side onto a southern side of the model, a bed with lower velocity had to be introduced between 125 and 150 km of the profile at depth from 7 to 17 km (for the assumed velocity $V_p = 5.9$ km/s). It is responsible for 0.5 s delay of the first arrivals at distance about 90 km. The bed with velocities $V_p = 7.3$ – 7.35 km/s is located at depth 20 to 30–33 km (wave at seismic record section with apparent velocity 7.0 km/s). The Moho discontinuity with velocity $V_p > 8.1$ km/s for the upper mantle is directly underneath. These two last boundaries are controlled by seismic rays from the station PV, at distances about 80–140 km along profile. Unfortunately, present data are insufficient to describe structure of the crust beneath a depth 6 km under the Deception Island and the whole southern part of the model, as far as to distance of about 80 km. Lack of the HVB in a southern part of the model is an important information.

Seismic-geologic model of the Bransfield Strait

Structure of the Earth's crust in the Bransfield Strait is strongly anomalous. Final seismic-geologic interpretation of calculated variants of 2-D models is presented (Fig. 31). Beneath a water body there are recent poorly consolidated sediments with seismic wave velocities equal to 1.9–2.9 km/s. The next two beds with velocities 3.5 km/s and 4.0 km/s comprise presumably older and more consolidated sediments and pillow lavas. Beneath a sedimentary cover there is a bed with velocities 5.2–5.8 km/s, typical for metamorphic and acid crystalline rocks. It is underlain by crystalline bedrock itself, with velocities 6.4–6.9 km/s. Beneath a body with velocity 6.4 km/s at depth 2–4 km close to the station HB, there is a bed with lower velocities, being presumably a continuation of the

previously mentioned bed (with $V_p > 5.2$ km/s). In the mentioned models of the Earth's crust, the HVB is the main element with $V_p = 7.1\text{--}7.4$ km/s in the upper part of the body and high vertical velocity gradient, discovered at depth from about 10–15 km to about 25 km on all examined profiles, with the only exception of profile DDS-4. The area with anomalous the HVB, detected from a common analysis of 2-D models for a network of 5 profiles in the Bransfield Strait, is presented (Fig. 32). Thickness of the HVB increases from several kilometres in southeastern parts of profiles DDS-3 and DSS-17, as far as the depth 30 km along profile DDS-20 in central part of the Bransfield Strait. Beneath the HVB, to depth 30–35 km in southeastern parts of profiles DDS-17 and DSS-3, crustal velocities from 6.8 km/s to 7.2 km/s were detected. In southwestern parts of profiles DDS-20 and DSS-4, and in the northwestern part of profile DDS-3, the second bed of crystalline bedrock was detected with velocities 7.3–7.4 km/s at depth from 20 to 30 km, corresponding to the lower crust. Our data make detailed determination of seismic wave velocities distribution beneath the HVB in its northwestern part impossible. The velocity is known to must be over 7.0 km/s or presumably the same as in the HVB. Location of the lower boundary of 'a body' cannot be easily determined (dashed lines at Fig. 31), as distinctly masks observations of the lower crust. Structure of the Earth's crust under the Deception Island below a depth 6 km still remains unknown if our data are concerned. On the other hand, the HVB does not occur in a southern part of profile DDS-4, close to the station PV. Along profile DDS-4 in a southeastern part of the Bransfield Strait, a zone with lower velocities (assumed $V_p = 6.1$ km/s) was found beneath a bed with velocity $V_p > 6.4$ km/s at depth 7–17 km. Along profile DDS-20 two fracture zones were noted, one at distance 100–120 km and the other at about 250 km of the profile. They can be presumably connected with fractures that transect the Bransfield Strait. Location of the second zone coincides with a fracture that is postulated at this very place by Gambôa and Maldonado (1990).

Accepted velocities of seismic waves for individual beds and depths of discontinuities in the described models are practically the same along profile junctions (see arrows at Fig. 31) as distinct change occurs below 0.1 km/s (velocity) and 100–200 m (depth).

Fragment of the HVB was detected by modelling along profile DDS-10 to the south-west of the Deception Island (Środa *et al.* 1997). This body appears along profile DDS-10 after passing the area which is ascribed to HFZ. It supports the opinion of Barker *et al.* (1982) that HFZ cuts the western coast of the Antarctic Peninsula into a southwestern part (with continental crust after collision of a ridge with a rift) and a northeastern part (where no collision occurred but the Bransfield Rift was opened). At the seismic record sections of a very good quality, received from shots along profile DDS-20 and recorded at the station HM, apart from the profile (the so-called non-longitudinal records) (Fig. 12F), apparent velocity is

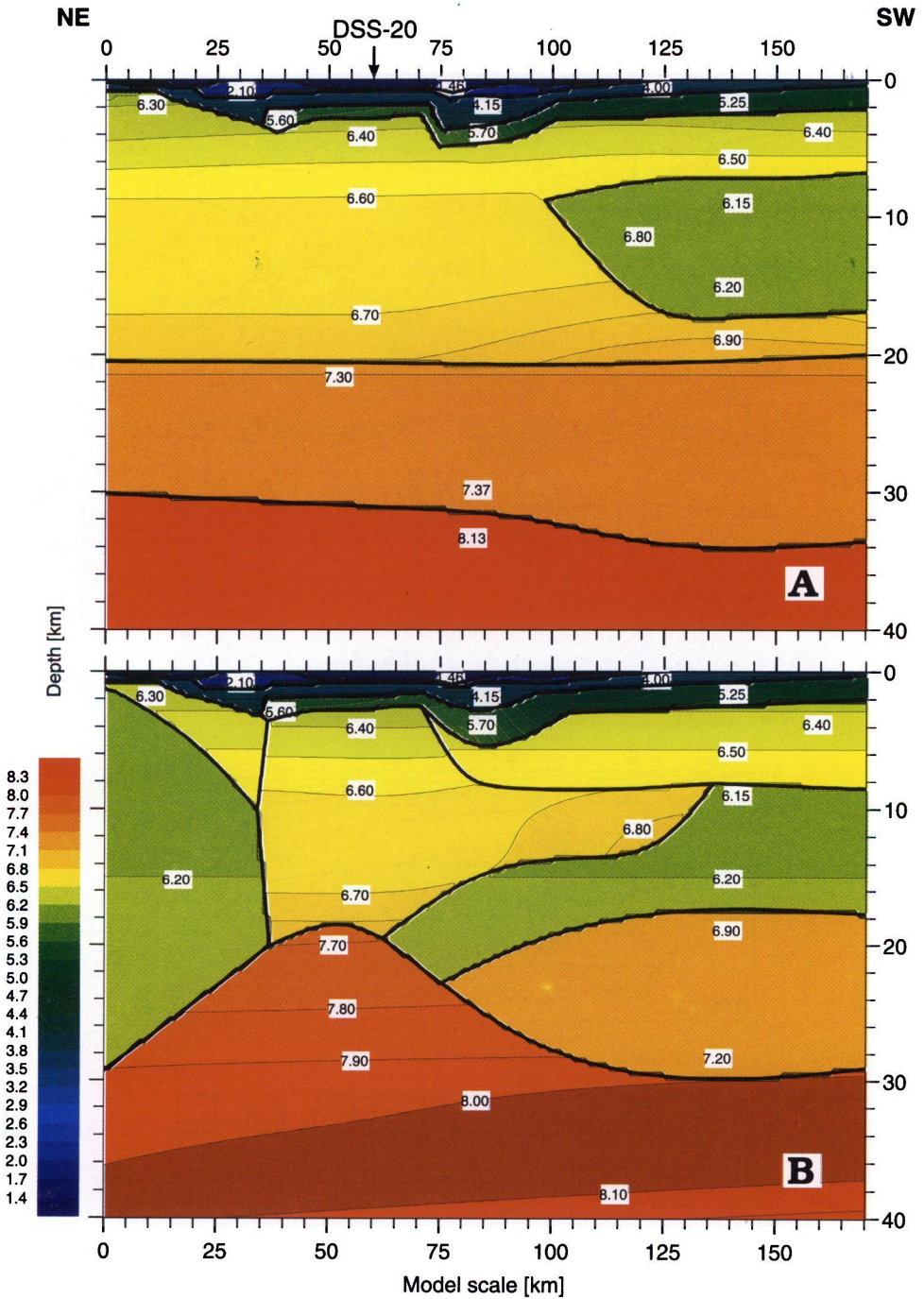


Fig. 30A–B. Variants of crustal velocity model across the Bransfield Rift, profile DSS-4. Thick lines: first order discontinuities; thin lines: P – wave velocity contours (in km/s), arrows indicate junction places with other profiles.

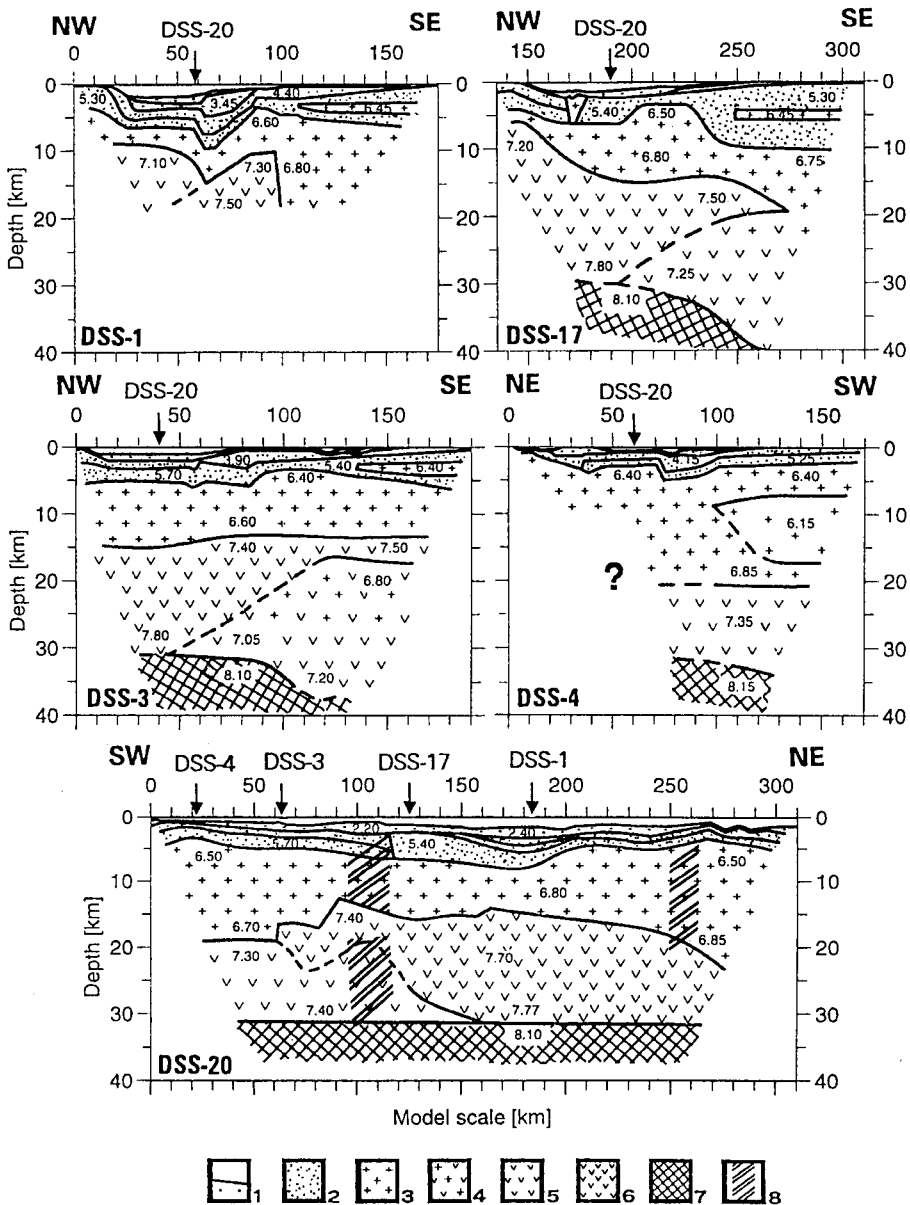


Fig. 31. Final geological/seismic model of the Bransfield Strait structure beneath profiles: DSS-1, DSS-17, DSS-3, DSS-4 and DSS-20. (1) water column and post- or syn-rift young sediments, $V_p = 1.9\text{--}2.2$ km/s; (2) layer corresponding to sedimentary sequence and intercalated syn-rift volcanic sequence, $V_p = 4.0\text{--}5.7$ km/s; (3) layer corresponding to the pre-rift upper crust, and likely intercalated syn-rift sequence, $V_p = 6.4\text{--}6.9$ km/s; (4) layer corresponding to the pre-rift lower (mafic) crust, $V_p = 6.9\text{--}7.2$ km/s; (5) layer corresponding to the pre-rift lower (mafic) crust, $V_p = 7.0\text{--}7.4$ km/s; (6) anomalous high-velocity body, mafic crust beneath the central subs basin in the Bransfield Strait, $V_p = 7.4\text{--}7.8$ km/s; (7) ultramafic upper mantle, $V_p > 8.1$ km/s; (8) transitional zones between crustal blocks; dashed lines – uncertain boundaries.

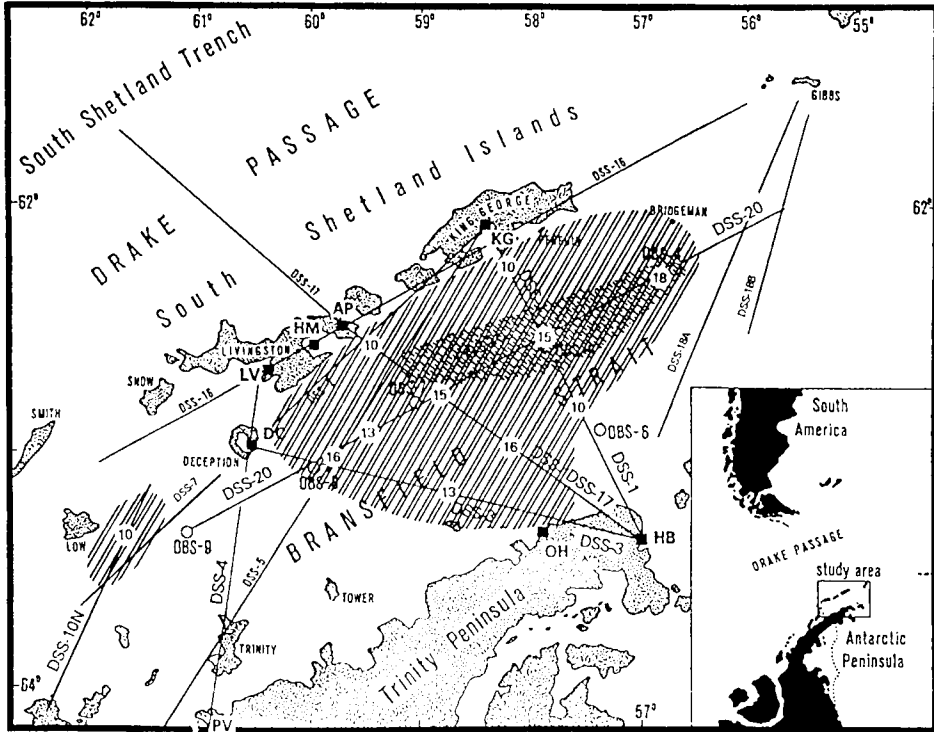


Fig. 32. Range of the existing high velocities body with $V_p > 7.4$ km/s in the Bransfield Strait, detected at a depth of 10–14 km, deduced from 2-D modelling of five intersecting deep seismic profiles. A more intense hatching in the centre indicates the very place where a high velocity body reaches depth 30 km. At other places, the thickness of the body is relatively small (southern part) or unknown (northwestern part), see Janik 1997.

equal about 7.0 km/s at a hodograph branch directed to the south-west. Seismic rays that correspond to this part of the hodograph ‘throw some light’ on structures beneath the Deception Island. It seems therefore probable that the HVB continues also beneath the island and suggests to undertake the 3-D modelling.

The Moho discontinuity with velocity $V_p = 8.1$ km/s below, was detected at depth 30–32 km along profile DDS-20. Fragments of the Moho discontinuity were also discovered on along profiles DDS-17 and DSS-3, and presumably also profile DDS-4 at depth 30–37 km.

Final remarks

Received results of 2-D modelling for 5 profiles in the Bransfield Strait and particularly, delimiting the HVB of anomalously high velocity ($V_p = 7.3$ – 7.8 km/s) in its centre at depth 10–30 km, enable to refer it to the opinions on structure of

the Bransfield Strait and through them, to opinions on tectonic structure of the region, presented at the beginning of this paper.

The Bransfield Strait seems to have been opened (Barker 1982) after cessation of spreading at the Aluk Ridge when sinking of the subducted plate continued and the rift moved apart (roll-back effect) from the peninsula, taking along (trench suction) its fragment *i.e.* the South Shetland Islands. Simultaneously with this process, there was active extension of the Bransfield Strait. The crust subjected to slow extension was cut by numerous fractures what enabled intrusion of the upper mantle material and resulted in opening of the Bransfield Rift.

Opinions on age of initial rifting in the Bransfield Strait and opening of the Bransfield Basin are varying. Birkenmajer (1989, 1992) finds rifting to have been initiated at the turn of the Oligocene and Miocene (isotopic datings). Opening of the rift itself could occur about 14 mln years ago. Trouw (1991) suggests that opening of the basin could occur earlier. Some normal faults and subsidence at margins of the basin ascribe it to the Late Pliocene (Barton 1965, Weaver *et al.* 1979). Chronology of the Bransfield Strait extension seems to have been connected with collision of the ridge crest – graben type. According to Jeffers *et al.* (1991), rifting could be started in the Early Pliocene, before opening of the basin occurred about 2 mln years ago (Weaver *et al.* 1982, González-Ferrán 1991). In his analysis of magnetic anomalies (Roach 1978) speculates that spreading of sea floor occurred during the last ~1.3 mln years. Parra *et al.* (1988) estimated age of the rift at 1.8 mln years.

Present volcanism (Saunders and Tarney 1982) and seismicity (Forsyth 1975, Pelayo and Wines 1989) in the Bransfield Strait region indicate that slow subduction and extension occur also at present. Slow convergence rate can be similar to the extension rate in the Bransfield Strait (Pelayo and Wines 1989). Extension is observed in volcanic domes of the central basin (Gràcia *et al.* 1996). Several neovolcanic strips at the central basin floor (González-Ferrán 1985, Birkenmajer 1992, Gràcia *et al.* 1996, Lawver 1995) indicate its diffused extension. All volcanic rows are grouped between the South Shetland Islands and the basin axis, generally defined as line that connects the islands Deception and Bridgeman, and they are parallel to it. Geochemical and isotopic composition of volcanic products in the strip Deception-Bridgeman change along its axis (Keller *et al.* 1991), and are transitional between magmas coming from an ocean ridge and calcareous-alkaline ones (Weaver *et al.* 1979) – such as occurs in areas of the early stage of back-arc spreading. In the central basin there are also higher values of heat outflow (Lawver and Nagihara 1991, Lawver *et al.* 1995) and hydrothermal activity (Han and Suess 1987, Suess *et al.* 1987), and also minimum values of negative magnetic anomalies (Parra *et al.* 1988, Garrett 1990, Maslanyj *et al.* 1991, Kim *et al.* 1992, Bochu *et al.* 1995, Gràcia *et al.* 1996). Also gravimetric measurements detect maximum positive anomalies over the Bransfield Strait (Garrett 1990, Sandwell 1992, Bochu *et al.* 1995). Unfortunate-

ly, all hitherto presented model solutions for the collected magnetic and gravimetric measurements (Garrett 1990, Johnson and Smith 1992, Kim *et al.* 1992) deal either with shallow solutions of limited extent or base on models of Earth's crust of structure, presented still by Ascroft (1972).

Results of seismic 2-D modelling presented in the preceding chapter, seem to support thesis on strong activity of the processes which were connected with intrusion of the upper mantle material into crystalline bedrock of a central part of the central basin. However, transition between the HVB and the upper mantle is not univocal along profile DDS-20. The Moho discontinuity, modelled between them, indicates relatively weak reflection (Grad *et al.* 1997a, b). It is probably connected with intrusion of the upper mantle material above the Moho discontinuity. There are however no data that could confirm depth of the HVB in the northwestern part of the Bransfield Strait (particularly the area close to the King George Island) and whether the Moho discontinuity with $V_p = 8.1$ km/s is to be found there, but alimentary zones with the upper mantle material seem to occur there too.

Interpreted material has not been sufficient yet to find and prove breaks in the Moho discontinuity that could enable intensive intrusion of the upper mantle material. It can occur between profile DDS-20 and the South Shetland Islands or this passage is rather a discrete and diffusive one – suggested by many cited authors – and the material enters through many, relatively narrow fractures that cannot be discovered by seismic waves. The HVB spreads far southeastwards from the main axis of the rift (profiles DDS-3 and DSS-17). It becomes thinner at larger and larger distances, and continued horizontal intrusion into a continental crust of the Antarctic Peninsula. Maximum distance from a rift axis is equal to about 80 km. Also the beds which are underlain by the HVB, contain numerous sills and dikes (Barker *et al.* 1988). Dimensions, thickness and extents exclude existence of a single huge magmatic chamber. Question is put how a part of the HVB which spreads towards the Deception Island, is fed. Acting of a complex stress field, 'unstable balance' between subduction of the Drake microplate and dispersed extension in the Bransfield Rift resulted however in slight predominance of extension, with participation of left-hand strike-slip movements in the South Scotia Ridge, discovered at the King George Island (Tokarski 1991). Finally, very slow extension of the Bransfield Strait was discovered what made presumably possible that very far-distant horizontal injections of magmatic material occurred, similar to the ones in the Yamato Basin of the Japan Sea (Hirata *et al.* 1989).

Except for the stresses, connected with subduction and extension, propagation of stresses from the Scotia Sea to the Bransfield Strait also exists (Jeffers *et al.* 1991). Their activity is reflected mainly in the eastern basin (Gràcia *et al.* 1996, Lawver *et al.* 1995) as the pull-apart basins.

Still active tectonic extension-indicative movements appear in numerous active normal fractures that cut the present marine sediments across the basin

(Barker and Austin 1994). Segmentation seems to be of tectonic origin, eastern and western subbasins have relatively frequent seismic events whereas the central basin is distinctly non-seismic (Pelayo and Wiens 1989). The present tectonic situation is considerably unclear. There are no deep earthquakes associated with the South Shetland trench (Barker 1982).

Finally, basing on the presented data, the HVB detected in large area beneath central part of the Bransfield Strait can be interpreted as intrusion of the upper mantle (?asthenospheric) material in the extension stage of the Earth's crust. Davey (1972), Ashcroft (1972) and others suggest that ocean crust exists beneath the Bransfield Strait. Our experiment did not supply us with evidence on a well-developed ocean crust, and the other data suggest that a very early development stage of diffused back-arc spreading only occurs in this area.

Acknowledgements. — This paper is based on the author's PhD thesis completed at the Institute of Geophysics of Polish Academy of Sciences, Warszawa. I wish to express my sincere thanks to Professors Aleksander Guterch and Marek Grad for valuable remarks during preparation of the paper. Preparation of this paper has been supported by Committee for Scientific Research (KBN).

References

- ACOSTA J., HERRANZ P., SANZ J.L. and UCHUPI E. 1992. Antarctic continental margin: geologic image of the Bransfield Trough, an incipient ocean basin. — *In*: Poag C.W. and de Graciansky P.C. (eds), *Geologic Evolution of the Atlantic Continental Rises* Van Nostrand Reinh., New York: 49–61.
- ARCTOWSKI H. 1895. Observations sur l'intérêt que présente l'exploration géologique des terres australes. — *Bulletin de la Société de Géologie de France*, 3, 23: 589–591.
- ARCTOWSKI H. 1896. Quelques remarques sur l'intérêt qu'offre pour la géologie l'exploration des régions antarctiques. — *Bulletin de la Société Belge de Géologie*, 10: 61.
- ARCTOWSKI H. 1897. Antarktyka. — *Wszecławiat*, 16: 17.
- ASHCROFT W.A. 1972. Crustal structure of the South Shetland Islands and the Bransfield Strait. — *British Antarctic Survey Scientific Reports*, 66: 1–43.
- BANFIELD L.A. and ANDERSON J.B. 1994. Seismic Facies Investigation of the Late Cenozoic Glacial History of the Bransfield Basin, Antarctica. — *Terra Antarctica*, spec. iss., 1: 285–286.
- BARKER D.H.N. and AUSTIN J.A. 1994. Tectonic evolution of the Bransfield Strait, Antarctica: intracrustal diapirism, distributed extension and stratigraphic response to marginal basin rifting. — *Terra Antarctica*, 1: 287–288.
- BARKER P.F. 1970. Plate tectonics of the Scotia Sea region. — *Nature*, 228: 1293–1297.
- BARKER P.F. 1976. The tectonic framework of Cenozoic volcanism in the Scotia Sea region, a review. — *In*: González-Ferrán O. (ed.), *Andean Antarctic Volcanology Problems*. Int. Ass. Volc., Chem., Earth's Inter., Rome: 330–346.
- BARKER P.F. 1982. The Cenozoic subduction history of the Pacific margin of the Antarctic Peninsula: ridge-crest interactions. — *Journal of the Geological Society, London*, 139: 787–802.
- BARKER P.F. 1995. Tectonic framework of the East Scotia Sea. — *In*: Taylor B. (ed.), *Back-Arc basins. Tectonics and magmatism*. Plenum Publ. Corp., New York: 281–312.
- BARKER P.F. and BURRELL J. 1977. The opening of Drake Passage. — *Marine Geology*, 25: 15–34.

- BARKER P.F. and DALZIEL I.W.D. 1983. Progress in geodynamics in the Scotia Arc region. — *In*: Cabre R.(ed.), *Geodynamics of the Eastern Pacific region, Caribbean and Scotia Arcs*. Geodyn. Ser. American Geophysical Union, Washington, D.C., 9: 137–170.
- BARKER P.F. and GRIFFITHS D.H. 1977. The evolution of the Scotia Ridge and Scotia Sea. — *Philosophical Transactions of the Royal Society of London*, A271: 151–183.
- BARKER P.F. and HILL I.A. 1981. Back-arc extension in the Scotia Sea. — *Philosophical Transactions of the Royal Society of London*, A300: 249–262.
- BARKER P.F. and LAWVER L.A. 1988. South American–Antarctic plate motion over the past 50 Myr, and the evolution of the South American–Antarctic Ridge. — *Geophysical Journal*, 94: 377–386.
- BARTON C.M. 1965. The geology of the South Shetland Islands. III. The stratigraphy of King George Island. — *British Antarctic Survey Scientific Reports*, 44: 33 pp.
- BEHRENDT J.B. 1990. Multichannel seismic reflection surveys over the Antarctic continental margin relevant to petroleum resource studies. — *In*: St. John B. (ed.), *Antarctica as an Exploration Frontier*. American Association of Petroleum Geologists, Tulsa, Oklahoma, 31: 69–75.
- BIRKENMAJER K. 1983. Late Cenozoic phases of block-faulting on King George Island (South Shetland Islands, West Antarctica). — *Bulletin of Polish Academy of Sciences, Earth Sciences*, 30: 21–32.
- BIRKENMAJER K. 1989. A guide to Tertiary geochronology of King Gorge Island, West Antarctica. — *Polish Polar Research*, 10: 555–579.
- BIRKENMAJER K., 1992. Evolution of the Bransfield Basin and Rift West Antarctica. — *In*: Yoshida Y. et al. (eds), *Recent progress in Antarctic Earth science*. Proceedings of Sixth International Symposium on Antarctic Sciences, 9–13 September 1991, Tokyo, Terra Scientific Publishing Company, Tokyo: 405–410.
- BIRKENMAJER K., GUTERCH A., GRAD M., JANIK T. and PERCHUĆ E. 1990. Lithospheric transect South Shetland Islands – Antarctic Peninsula, West Antarctica. — *Polish Polar Research*, 11: 241–258.
- BIRKENMAJER K. and KELLER R.A. 1990. Pleistocene age of the Melville Peak volcano, King George Island, West Antarctica, by K-Ar dating. — *Bulletin of Polish Academy of Sciences, Earth Sciences*, 38: 17–24.
- BOCHU Y., GUANGYU W., BANGYAN CH. and SHENGYUAN CH. 1995. The characteristics of geophysical field and tectonic evolution in the Bransfield Strait. — *Antarctic Research*, 6: 12–23.
- BRITISH ANTARCTIC SURVEY 1985. Tectonic Map of the Scotia Arc, 1 : 3,000,000. — BAS (Misc), 3. British Antarctic Survey, Cambridge.
- BROCHER T.M., KEMPNER W.C. and GETTRUST J.F. 1982. Comparison of synthetic P-tau sections for proposed models of two ophiolites. — *Journal of Geophysical Research*, 87 (B11): 9355–9364.
- CANALS M., DE BATIST M., BARAZA J., ACOSTA J. and THE GEBRA TEAM 1994. New reflection seismic data from the Bransfield Strait: preliminary results of the GEBRA-93 survey. — *Terra Antarctica, spec. iss.*, 1: 291–292.
- CANDE S.C., HERRON E.M. and HALL B.R. 1982. The early Cenozoic history of the south-east Pacific. — *Earth and Planetary Science Letters*, 57: 63–74.
- CAMERLENGHI A., BOHEM G., DELLA VEDOVA B., LODOLO E., PELLIS G. and VESNAVER A. 1994. Seismic reflection tomography and thermal implications of a gas hydrate floor simulating reflector on the South Shetlands margin (Antarctic Peninsula). — *Terra Antarctica*, 1: 295–296.
- ČERVENÝ V. and PŠENČÍK I. 1983. Program SEIS83, numerical modeling of seismic wave fields in 2-D laterally varying bedded structures by ray method. — Charles University, Praha.
- CUNNINGHAM A.P., VANNESTE L.E. and ANTOSTRAT Antarctic Peninsula regional Working Group 1995. The ANTOSTRAT Antarctic Peninsula regional Working Group digital navigation compilation. — *Geology and Seismic Stratigraphy of the Antarctic Margin, Research Series*, 68: A297–301.
- DADLEZ R. and JAROSZEWSKI W. 1994. *Tektonika*. — PWN, Warszawa.

- DALZIEL I.W.D. 1972. Large-scale folding in the Scotia arc. — In: Adie R.J. (ed.), *Antarctic Geology and Geophysics*. Universitetsforl., Oslo: 47–55.
- DALZIEL I.W.D. 1983. The evolution of the Scotia Arc, a review. — In: Olivier R.L. (ed.), *Antarctic Earth Sciences*. Australian Ac. Sci., Cambridge University Press, Cambridge: 283–288.
- DALZIEL I.W.D. 1984. Tectonic Evolution of a Forearc Terrane, Southern Scotia Ridge, Antarctica. — *Geol. Soc. Am.*, spec. paper, 200: 32.
- DALZIEL I.W.D. and ELLIOT D.H. 1973. The Scotia arc and Antarctic margin. — In: Nairn A.E.M. and Stehli F.G. (eds), *The Ocean Basins and Margins, 1. The South Atlantic*. Plenum Press, New York – London: 171–246.
- DAVEY F.J. 1972. Marine gravity measurements in the Bransfield Strait adjacent areas. — In: Adie R.J. (ed.), *Antarctic Geology and Geophysics*. Universitetsforl., Oslo: 39–46.
- DE WIT M.J. 1977. The evolution of the Scotia arc as a key to the reconstruction of southwestern Gondwanaland. — *Tectonophysics*, 37: 53–81.
- DOTT R.H. jr. 1976. Contrast in tectonic history along the Eastern Pacific Rim. — In: Sutton G.H. (ed.), *The Geophysics of the Pacific Ocean Basin and its Margin*. Washington.
- DOTT R.H. jr., WINN R.D. and SMITH C.H.L. 1982. Relationship of late Mesozoic and early Cenozoic sedimentation to the tectonic evolution of southernmost Andes and Scotia Arc. — In: Craddock C. (ed.), *IUGS Antarctic Geoscience, B (4)*, University of Wisconsin Press, Madison: 193–202.
- ELLIOT D.H. 1991. Triassic–Early Cretaceous evolution of Antarctica. — In: Thomson M.R.A., Crame J.A. and Thomson J.W. (eds), *Geological Evolution of Antarctica*. Fifth International Symposium on Antarctic Earth Sciences, Cambridge, 1987, Cambridge University Press: 541–547.
- FORSYTH D.W. 1975. Fault plane solutions and tectonics of the South Atlantic and Scotia area. — *Journal of Geophysical Research*, 80: 1429–1443.
- GAMBÔA L.A.P., CUNNINGHAM A.P., BOCHU Y., CAMERLENGHI A., NAKADO S. and RUDOWSKI S. 1994. Origin and evolution of the Bransfield Basin Based on Integrated MCS data. — *Terra Antarctica*, spec. iss., 1: 293–294.
- GAMBÔA L.A.P. and MALDONADO P.R. 1990. Geophysical investigation in the Bransfield Strait and Bellingshausen Sea. Antarctica. — In: St. John B. (ed.), *Antarctica as an Exploration Frontier*. American Association of Petroleum Geologists, Tulsa, Oklahoma, 31: 127–141.
- GARRETT S.W. 1990. Interpretation of reconnaissance gravity and aeromagnetic surveys of the Antarctic Peninsula. — *Journal of Geophysical Research*, 95 (B5): 6759–6777.
- GARRETT S.W., RENNER R.G.B., JONES J.A. and MCGIBBON K.J. 1986/87. Continental magnetic anomalies and the evolution of the Scotia arc. — *Earth and Planetary Science Letters*, 81: 273–281.
- GARRETT S.W. and STOREY B.C. 1987. Lithospheric extension on the Antarctic Peninsula during Cenozoic subduction. — In: Coward Devey M.P. and Hancock P.L. (eds) *Continental Extension Tectonics*. Special Publication of the Geological Society, London, 28: 419–431.
- GIZEJEWSKI J. 1995. Young sedimentary cover of the Bransfield Strait and South Shetland Trench. — VII International Symposium on Antarctic Earth Sciences, Siena (Italy), Abstr.: 155.
- GONZÁLEZ-FERRÁN O. 1983. The Larsen Rift: an active extension fracture in West Antarctica. — In: Oliver R.I. (ed.) *Antarctic Earth Science*. Canberra–Cambridge University Press, Cambridge: 344–346.
- GONZÁLEZ-FERRÁN O. 1985. Volcanic and tectonic evolution of the northern Antarctic Peninsula – Late Cenozoic to Recent. — *Tectonophysics*, 114: 389–409.
- GONZÁLEZ-FERRÁN O. 1991. The Bransfield Rift and its active volcanism. — In: Thomson M.R.A., Crame J.A. and Thomson J.W. (eds), *Geological Evolution of Antarctica*. Fifth International Symposium on Antarctic Earth Sciences, Cambridge, 1987, Cambridge University Press: 505–509.
- GONZÁLEZ-FERRÁN O. and KATSUI Y. 1970. Estudio integral del volcanismo cenozoico superior de las Islas Shetland del Sur, Antártica. — *Serie Científica Instituto Antártico Chileno*, 1: 123–174.

- GRÀCIA E., CANALS M., FARRÀN M., PRIETO M.J., SORRIBAS J. and GEBRA TEAM. 1996. Morpho-structure and evolution of the Central and Eastern the Bransfield (NW Antarctic Peninsula). — *Marine Geophysical Research*, 18: 429–448.
- GRAD M., GUTERCH A. and JANIK T. 1993a. Seismic structure of the lithosphere across the zone of subducted Drake plate under the Antarctic plate, West Antarctica. *Geophysical Journal International*, 115: 586–600.
- GRAD M., GUTERCH A., JANIK T. and ŚRODA P. 1993b. 2-D seismic models of the lithosphere in the area of the Bransfield Strait, West Antarctica. — *Polish Polar Research*, 14: 123–151.
- GRAD M., GUTERCH A. and ŚRODA P. 1992. Upper crustal structure of Deception Island, the Bransfield Strait, West Antarctica. — *Antarctic Science*, 1: 460–476.
- GRAD M., SHIOBARA H., JANIK T., GUTERCH A. and SHIMAMURA H. 1997a. Crustal Model of the Bransfield Rift, West Antarctica, from Detailed OBS Refraction Experiment. — *In: Ricci C.A. (ed.), The Antarctic Region: Geological Evolution and Processes*, Proceedings of the VII International Symposium on Antarctic Earth Sciences, Siena 1995, Terra Antarctica Publication, Siena: 675–678.
- GRAD M., SHIOBARA H., JANIK T., GUTERCH A. and SHIMAMURA H. 1997b. New seismic crustal model of the Bransfield Rift, West Antarctica from OBS refraction and wide – angle reflection data. — *Geophysical Journal International*, 130: 506–518.
- GRAPE (THE) TEAM 1990. Preliminary results of seismic reflection investigations and associated geophysical studies in the area of the Antarctic Peninsula. — *Antarctic Science*, 2: 223–234.
- GUTERCH A., GRAD M., JANIK T. and PERCHUĆ E. 1990. Deep crustal structure in the region of the Antarctic Peninsula from seismic refraction modelling (next step of data discussion). — *Polish Polar Research*, 11: 215–239.
- GUTERCH A., GRAD M., JANIK T. and PERCHUĆ E. 1991. Tectonophysical models of the crust between the Antarctic Peninsula and the South Shetland Trench. — *In: Thomson M.R.A., Crame J.A. and Thomson J.W. (eds), Geological Evolution of Antarctica*. . Fifth International Symposium on Antarctic Earth Sciences, Cambridge, 1987, Cambridge University Press, Cambridge: 499–504.
- GUTERCH A., GRAD M., JANIK T., PERCHUĆ E. and PAJCHEL J. 1985. Seismic studies of the crustal structure in West Antarctica 1979–1980 – preliminary results. — *Tectonophysics*, 114: 411–429.
- HAN M.W. and SUESS E. 1987. Lateral migration of pore fluids through sediments of an active back-arc basin, the Bransfield Strait, Antarctica. — *American Geophysical Union EOS Trans.*, 24: 1769.
- HENRIET J.P., MILLER H., MEISSNER R., MOONS A., HUWS D., JOKAT W., KAUL N., VAN HEUVER-SWYN E. and VERSTEEG W. 1990. Reflection seismic investigations in the Weddell Sea and long the Antarctic Peninsula. — *Belgian Scientific Research Programme on Antarctic Science Results of Phase One. vol. 2 (B): marine geophysics*, 53–82.
- HENRIET, J.P., MEISSNER, R., MILLER, H. and THE GRAPE TEAM 1992. Active margin along the Antarctic Peninsula. — *In: Shimamura H., Hirn A. and Makris J. (eds), Detailed Structure and Processes of Active Margins. Tectonophysics*, 201: 229–253.
- HERRON E.M. and TUCHOLKE B.E. 1976. Sea-floor magnetic patterns and basement structure in the southeastern Pacific. — *In: Hollister C.D., Craddock C. et al. (eds), Initial Reports of Deep Sea Drilling Project*, 35. (U.S. Government Printing Office), Washington: 263–278.
- HERRON E.M., CANDE S.C. and HALL B.R. 1981. An active spreading center collides with a subduction zone, a geophysical survey of the Chile Margin triple junction. — *GSA Mem.*, 154: 683–701.
- HIRATA N. and SHINJO N. 1986. SEISOBS: modified version of SEIS83 for ocean floor seismographs. — *Zisin*, 39: 317–320.
- HIRATA N., TOKUYAMA H. and CHUNG T.W. 1989. An anomalously thick beding of the crust of the Yamato Basin, southeastern Sea of Japan: the final stage of back-arc spreading. — *Tectonophysics*, 165: 303–314.

- JANIK T. 1994. 2-D seismic models of the lithosphere in the young rift zone. — the Bransfield Strait, West Antarctica. — XXIV General Assembly, Europ. Seism. Comm., Athens (Greece), Proc., Activity Report 1992–1994, 2: 1007–1016.
- JANIK T. 1996. Seismiczny i tektoniczny model skorupy ziemskiej Cieśniny Bransfielda – PhD thesis, Institute of Geophysics of Polish Academy of Sciences, Warszawa.
- JANIK T. 1997. Seismic Crustal Structure in the Transition Zone between Antarctic Peninsula and South Shetland Islands. — In: Ricci C.A. (ed.), *The Antarctic Region: Geological Evolution and Processes*, Proceedings of the VII International Symposium on Antarctic Earth Sciences, Siena 1995, Terra Antarctica Publication, Siena: 679–684.
- JEFFERS J.D. 1987. Preliminary results of marine geological and geophysical investigations in the Bransfield Strait, Antarctic Peninsula. — U.S. Antarctic Journal, 22: 131–133.
- JEFFERS J.D. and ANDERSON J.B. 1986. Sedimentation and tectonics in the Bransfield Strait. — A preliminary report. — U.S. Antarctic Journal, 21: 141–143.
- JEFFERS J.D. and ANDERSON J.B. 1990. Sequence stratigraphy of the Bransfield Basin, Antarctica: implications for tectonic history and hydrocarbon potential. — In: St. John B. (ed.), *Antarctica as an Exploration Frontier. — Hydrocarbon Potential, Geology and Hazards*, American Association of Petroleum Geologists, Tulsa, Oklahoma, 31: 13–29.
- JEFFERS J.D., ANDERSON J.B. and LAWVER L.A. 1991. Evolution of the Bransfield Basin, Antarctic Peninsula. — In: Thomson M.R.A., Crame J.A. and Thomson J.W. (eds), *Geological Evolution of Antarctica*. Fifth International Symposium on Antarctic Earth Sciences, Cambridge, 1987, Cambridge University Press, Cambridge: 481–485.
- JOHNSON A.C. and SMITH A.M. 1992. New aeromagnetic map of West Antarctica (Weddell Sea sector): introduction to important features. — In: Yoshida Y. et al. (eds), *Recent progress in Antarctic Earth science*. Proceedings of Sixth International Symposium on Antarctic Sciences, 9–13 September 1991, Tokyo, Terra Scientific Publishing Company, Tokyo: 555–562.
- KELLER L.A. and FISK M.R. 1987. Magmatism associated with the initial stages of backarc rifting, the Bransfield Strait, Antarctica. — U.S. Antarctic Journal, 21: 102–104.
- KELLER L.A., FISK M.R., WHITE W.M. and BIRKENMAJER K. 1988. Late Tertiary Quaternary transition from arc to back-arc volcanism, South Shetland Islands and the Bransfield Strait, Antarctica. — American Geophysical Union EOS Trans., Abstract 69: 1471.
- KELLER L.A., FISK M.R., WHITE W.M. and BIRKENMAJER K. 1991. Isotopic and trace element constraints on mixing and melting models of marginal basin volcanism, the Bransfield Strait, Antarctica. — Earth and Planetary Science Letters, 111: 287–303.
- KIM Y., CHOUNG T.W. and NAM S.H. 1992. Marine magnetic anomalies in the Bransfield Strait, Antarctica. — In: Yoshida Y. et al. (eds), *Recent Progress in Antarctic Science*. Proceedings of Sixth International Symposium on Antarctic Sciences, 9–13 September 1991, Tokyo, Terra Scientific Publishing Company, Tokyo: 431–437.
- KING E.C. and BARKER P.F. 1988. The margins of the South Orkney microcontinent. — Journal of the Geological Society, London, 145: 317–332.
- KOMMINAHO K. 1993. Software manual for programs MODEL and XRAY5 – a graphical interface for SEIS83 program package. University of Oulu, Department of Geophysics, Report No. 20: 31.
- LABREQUE J.L. and BARKER P.F. 1981. The age of the Weddell Basin. — Nature, 290: 489–492.
- LARTER R.D. 1991. Debate. Preliminary results of seismic reflection investigations and associated geophysical studies in the area of the Antarctic Peninsula, discussion. — Antarctic Science, 3: 217–220.
- LARTER R.D. and BARKER P.F. 1991. Neogene interaction of tectonic and glacial processes at the Pacific margin of the Antarctic Peninsula. — Int. Ass. Sed. Spec. Publ., 12: 165–186.
- LAWVER L.A. and HAWKINS J.W. 1978. Diffuse magnetic anomalies in marginal basins: their possible tectonic and petrologic significance. — Tectonophysics, 45: 323–339.
- LAWVER L.A. and GAHAGAN L.M. 1991. Constraints on Mesozoic transection in Antarctica. — Sixth International Symposium on Antarctic Earth Sciences, 9–13 September 1991, Tokyo. Abstr.: 343.

- LAWVER L.A. and NAGIHARA S. 1991. Heat flow measurements in the King George, the Bransfield Strait. — Sixth International Symposium on Antarctic Earth Sciences, 9–13 September 1991, Tokyo, Abstr.: 345.
- LAWVER L.A., KELLER R.A., FISK M.R. and STRELIN J. 1995. the Bransfield Strait, Antarctic peninsula: active extension behind a dead arc. — In: Taylor B. (ed.), *Back-arc basins, tectonics and magmatism*, Plenum Publ. Corp., New York: 315–342.
- LAWVER L.A., SCLATER J.G. and MEINKE L. 1985. Mesozoic and cenozoic reconstruction of the South Atlantic. — *Tectonophysics*, 114: 233–254.
- LAWVER L.A. and SCOTese C.R. 1988. A revised reconstruction of Gondwana. — In: McKenzie G.D. (ed.), *Gondwana Six: Structure, tectonics and geophysics*. American Geophysical Union, Washington: 17–23.
- MACDONALD D.I.M., BARKER P.F., GARRETT S.W., INESON J.R., PIRRIE D., STOREY B.C., WHITHAM A.G., KINGHORN R.R.F. and MARSHALL J.E.A. 1988. A preliminary assessment of the hydrocarbon potential of the Larsen Basin, Antarctica. — *Marine and Petroleum Geology*, 5: 34–53.
- MACDONALD D.I.M., BUTTERWORTH P.J. 1990. The stratigraphy setting and hydrocarbon potential of the Mesozoic sedimentary basins of the Antarctic Peninsula. — In: St. John B. (ed.), *Antarctica as an Exploration Frontier. — Hydrocarbon Potential, Geology and Hazard*, American Association of Petroleum Geologists, Tulsa, Oklahoma, 31:101- 125.
- MASLANYJ S.W., GARRETT S.W., JOHNSON A.C, RENNER R.G.B. and SMITH A.M. 1991. Aeromagnetic anomaly map of West Antarctica (Weddell Sea sector), sheet 2. — BAS GEOMAP Series., British Antarctic Survey, Cambridge.
- MEISSNER R., HENRIET J.P. and THE GRAPE TEAM 1988. Tectonic features northwest of the Antarctic Peninsula: new evidence from magnetic and seismic studies. — *Serie Cientifica Instituto Antártico Chilieno*, 38: 89–105.
- OKAL E.A. 1981. Interplate seismicity of Antarctica and tectonic implications. — *Earth and Planetary Science Letters*, 52: 397–409.
- PARRA J.C., GONZÁLEZ-FERRÁN O., BANISTER J. 1984 Aeromagnetic survey over the South Shetland Islands, the Bransfield Strait and part of the Antarctic Peninsula.. — *Revista de Geología, Chile*, 23: 3–20.
- PARRA J.C., YAÑEZ G. and GRUPO DE TRABAJO USAC 1988. Aeromagnetic survey on the Antarctic Peninsula and surrounding seas: integration of data obtained at different altitudes. — *Serie Cientifica Instituto Antártico Chilieno*, 38: 117–131.
- PELAYO A.M. and WIENS D.A. 1989. Seismotectonics and relative plate motions in the Scotia Sea region. — *Journal of Geophysical Research*, 94: 7293–7320.
- RENNER R.G.B., DIKSTRA B.J. and MARTIN J.L. 1982. Aeromagnetic surveys over the Antarctic Peninsula. — In: C. Craddock (ed.), *Antarctic Geoscience*, University of Wisconsin Press, Madison:363–367.
- RENNER R.G.B., STURGEON L.J.S. and GARRET S.W. 1985. Reconnaissance Gravity and Aeromagnetic Surveys of the Antarctic Peninsula. — *British Antarctic Survey Scientific Reports*, 110: 1–54.
- ROACH P.J. 1978. The nature of back-arc extension in the Bransfield Strait. — *Geophysical Journal of Research, Royal Astronomical Society*, (Abstr.), 53: 165.
- ROYER J.-Y., GAHAGAN L.M., LAWVER L.A., MAYES G.L., NURBERG D., SANDWELL D.T. and SCOTese CH.R. 1990. A tectonic chart for the Southern Ocean derived from Geosat altimetry data.. — In: St. John B. (ed.), *Antarctica as an Exploration Frontier – hydrocarbon potential, geology and hazard*. American Association of Petroleum Geologists, Tulsa, Oklahoma, 31: 89–99.
- SAUNDERS A.D. and TARNEY J. 1982. Igneous activity in the southern Andes and northern Antarctic Peninsula, a review. — *Journal of the Geological Society, London*, 139: 691–700.
- SAUNDERS A.D. and TARNEY J. 1984. Geochemical characteristics of basaltic volcanism within back-arc basins. — In: Kokelaar B.P. and Howells M.F. (eds), *Marginal basin geology*:

- Volcanic and associated sedimentary and tectonic processes in modern and ancient basins*, Special Publication of the Geological Society, London, 16: 59–76.
- SANDWELI D.T. 1992. Antarctic marine gravity field from high-density satellite altimetry. — *Geophysical Journal International*, 109: 437–448.
- SIBUET J.C., LETOUZEY J., CHARVET J., FOUCHER J.P., HILDE T.W.C., KIMURA M., LING-YUN C., MARSSET B. and STEPHAN J.F., 1987. Back-arc extension in the Okinawa Trough. — *Journal of Geophysical Research*, 92: 14041–14063.
- SHIMAMURA H. 1990. Ocean Floor Seismographs as a tool to Study the Interior of the Earth. — *Progres in Acoustic Emission V. The 10th Int. Acoustic Emission Symposium*, Sendai (Japan), The Japanese Society for Non-destructive Inspection: 11–19.
- SMELLIE J.L. and CLARKSON P.D. 1975. Evidence for pre-Jurassic subduction in Western Antarctica. — *Nature*, 258: 701–702.
- STOREY B.C. and GARRETT S.W. 1985. Crustal growth of the Antarctic Peninsula by accretion, magmatism and extension. — *Geological Magazine*, 122: 5–14.
- SUESS E., FISK M and KADKO D. 1987. Thermal interaction between back arc volcanism and basin sediments in the Bransfield Strait, Antarctica. — *Antarctic Journal U.S.*, 22: 47–49.
- SZELIGA J. and RAKUSA-SUSZCZEWSKI S. 1994. Morphometry of the Bransfield Strait, West Antarctica. — *Polish Polar Research*, 15: 21–29.
- ŚRODA P. 1994. Seismic modelling of the Earth's crust structure in the area of the Adelaide Island and Palmer Archipelago, West Antarctica. — XXI Polar Symp., Warszawa. Abstr.: 67–77.
- ŚRODA P., GRAD M. and GUTERCH A. 1997. Seismic models of the Earth's crust structure between South Pacific and Antarctic Peninsula. — In: Ricci C.A. (ed.), *The Antarctic Region: Geological Evolution and Processes*, Proceedings of the VII International Symposium on Antarctic Earth Sciences, Siena 1995, Terra Antarctica Publication, Siena: 685–689.
- TATSUMI Y., OTOFUJI Y., MATSUDA T. and NOHDA S. 1989. Opening of the Japan back-arc basin by asthenospheric injection. — *Tectonophysics*, 166: 317–329.
- THOMSON M.R.A., PANKHURST R.J. and CLARKSON P.D. 1983. The Antarctic Peninsula – a late Mesozoic-Cenozoic arc (review). — In: Olivier R.L., James P.R. and Jago J.B. (eds), *Antarctic Earth Science*. Cambridge University Press, London: 289–294.
- TOKARSKI A.K. 1991. The Late Cretaceous–Cenozoic structural history of King George Island, South Shetland Islands, and its plate-tectonic setting. — In: Thomson M.R.A., Crame J.A. and Thomson J.W. (eds), *Geological Evolution of Antarctica*. Fifth International Symposium on Antarctic Earth Sciences, Cambridge, 1987, Cambridge University Press: 493–497.
- TROUW R.A.J. and GAMBÓA L.A.P. 1992. Geotranssect Drake Passage – Weddell Sea, Antarctica. — In: Yoshida Y. *et al.* (eds), *Recent progress in Antarctic Earth science*. Proceedings of Sixth International Symposium on Antarctic Sciences, 9–13 September 1991, Tokyo, Terra Scientific Publishing Company, Tokyo: 417–422.
- WEAVER S.D., SAUNDERS A.D., PANKHURST R.J. and TARNEY J. 1979. A geochemical study of magmatism associated with the initial stages of back-arc spreading: the Quaternary volcanics of the Bransfield Strait from South Shetland Islands. — *Contributions for Mineralogy and Petrology*, 68: 151–169.
- WEAVER S.D., SAUNDERS A.D. and TARNEY J. 1982. Mesozoic–Cenozoic volcanism in the South Shetland Islands and the Antarctic Peninsula: geochemical nature and plate tectonic significance. — In: Craddock C. (ed.), *Antarctic Geoscience*, University of Wisconsin Press, Madison: 263–273.
- VILLA J., ORTIZ R., CORREIG A.M. and GARCIA A. 1992. Seismic Activity on Deception Island. — In: Yoshida Y. *et al.* (eds), *Recent Progress in Antarctic Sciences*. Proceedings of Sixth International Symposium on Antarctic Sciences, 9–13 September 1991, Tokyo, Terra Scientific Publishing Company, Tokyo: 449–456.

Streszczenie

Określenie geotektonicznej roli Antarktyki Zachodniej w rozpadzie superkontynentu Gondwany ma istotne znaczenie dla zdefiniowania fizycznych i geologicznych procesów zarówno w skali regionalnej jak i globalnej. Powstało kilkanaście takich rekonstrukcji. Dwie z nich prezentowane są na fig. 1–2. Określenie tej roli uzależnione jest od postępu badań geodynamicznych dotyczących wzajemnej relacji mikropłyty Szetlandów Południowych i subdukującej pod nią płyty antarktycznej, a ściślej, jej części zwanej mikropłytą Drake'a (Aluk lub Phoenix). Ryft Bransfielda wraz z platformą Bransfielda tworzą basen marginalny w odniesieniu do wulkanicznego łuku wyspowego, jakim są Szetlandy Południowe. Półwysp Antarktyczny, jeden z pięciu bloków kontynentalnych tworzących Antarktykę Zachodnią, jest wąską, długą na ponad 1500 km drzazgą skorupy kontynentalnej otoczonej skorupą oceaniczną Cieśniny Drake'a, południowego Pacyfiku, Morza Scotia i Morza Weddella. Aktualny, mocno skomplikowany układ tektoniczny dla tego regionu prezentuje fig. 3. Wyspy Deception, Penguin i Bridgeman określane są jako stratowulkany powstałe pomiędzy plejstocenem, a współczesnością w związku z otwarciem Cieśniny Bransfielda. Reprezentują one tylko widoczną część z serii kilku (kilkunastu?) wulkanów dużego podmorskiego grzbietu, o długości około 300 km, który przebiega między wyspami Deception i Bridgeman w Cieśninie Bransfielda (fig. 4–6).

Złożoność budowy geologicznej Antarktyki Zachodniej w rejonie Cieśniny Bransfielda znajduje odzwierciedlenie w obserwowanych anomaliach grawimetrycznych i magnetycznych (fig. 7–8). W Antarktyce Zachodniej, a w szczególności w Cieśninie Bransfielda przeprowadzono wiele morskich, sejsmicznych badań refleksyjnych. Zebrane dane są gromadzone we wspólnym banku w ramach projektu ANTOSTRAT (fig. 9). Przykłady rejestracji z profili refleksyjnych możemy zobaczyć na fig. 10A–B.

Cztery Ekspedycje Geodynamiczne Polskiej Akademii Nauk, które w latach 1979–1991 prowadziły prace badawcze w Antarktyce Zachodniej, wykonały obszerny program badań sejsmicznych, geologicznych, sedimentologicznych i paleontologicznych. Obszarem działania dla trzech spośród nich był rejon Cieśniny Bransfielda (fig. 11). Głównym celem badań geodynamicznych Antarktyki Zachodniej było rozpoznanie głębokiej struktury litosfery, a przede wszystkim skorupy ziemskiej, metodami głębokich sondowań sejsmicznych (GSS). W Cieśninie Bransfielda wykonano sieć profili GSS (fig. 11). Pięć stacji lądowych na Szetlandach Południowych, trzy stacje na Półwyspie Antarktycznym oraz dziewięć sejsmografów dennych rejestrowało fale sejsmiczne od eksplozji wykonywanych w morzu. Otrzymano bardzo obszerny materiał badawczy. Był on przedmiotem wielu wcześniejszych opracowań z zastosowaniem głównie modelowania jednowymiarowego i dla kilku profili, modelowania dwuwymiarowego (fig. 18–20). W niniejszej pracy prezentowane są dwuwymiarowe modele sejsmiczne dla sieci pięciu wybranych profili. Cztery z nich, o długościach od 150 do 190 km, przecinały główne struktury Cieśniny Bransfielda, a piąty, wiążący wszystkie poprzednie, o długości 310 km, przebiegał wzdłuż ryftu Bransfielda.

Pole falowe na sekcjach sejsmicznych z Cieśniny Bransfielda (fig. 12–17, 20) jest szczególnie skomplikowane, gdyż nakładają się tu na siebie różne, niekorzystne dla pomiarów uwarunkowania. Dla każdego z profili zostały przedstawione po dwa lub trzy rozwiązania modelowe. Przy czym prezentowane są zarówno przykłady wariantów modelowania (eksperymentalna sekcja sejsmiczna, sekcja sejsmogramów syntetycznych lub hodograf teoretyczny wraz z sekcją eksperymetalną oraz model z przebiegiem promieni sejsmicznych) (fig. 19, 22–23, 25–26, 29), jak też warianty modeli prędkościowych dla danych profili (fig. 21, 24, 27–28, 30). Jako wynik końcowy otrzymano, wzajemnie korygowane i kontrolowane modele dwuwymiarowe omawianych profili (fig. 31). Wspólnie, dają one wyobrażenie o przestrzennej komplikacji budowy skorupy ziemskiej młodego ryftu Cieśniny Bransfielda, w tym o zasięgu jego głównego elementu – ciała o anomalnie wysokiej prędkości fali P ($V_p = 7.4$ km/s) zlokalizowanego na głębokości około 15 km (fig. 32). Niejednorodność ta jest interpretowana jako intruzja materiału górnopłaszczowego (astenosferycznego?) w fazie rozciągania skorupy ziemskiej. Na głębokości 30–35 km zlokalizowano granicę Moho o prędkości około 8.1 km/s.